

**SPECTROSCOPIC INVESTIGATIONS ON POLYMER  
BLENDS/COMPOSITES**

**A THESIS SUBMITTED TO  
THE MAHARAJA SAYAJIRAO UNIVERSITY OF BARODA  
FOR THE DEGREE OF  
DOCTOR OF PHILOSOPHY  
IN PHYSICS**



**BY  
GAURANG PATEL**

**UNDER THE GUIDANCE OF  
DR. M. B. SURESHKUMAR  
DEPARTMENT OF PHYSICS  
FACULTY OF SCIENCE  
THE MAHARAJA SAYAJIRAO UNIVERSITY OF BARODA  
VADODARA-390 002**

**March 2014**

# THE MAHARAJA SAYAJIRAO UNIVERSITY OF BARODA

**Dr. M. B. Sureshkumar**

Associated Professor

**E-mail:-** mbsklereja8@yahoo.com

sureshkumar.msu@gmail.com

**Tel.** 0265-2795339(O); 09427301163(M)



Department of Physics

Faculty of Science

The M. S. University of Baroda

Vadodara – 390 002

Gujarat, India.

## CERTIFICATE

This is to certify that the thesis entitled “**Spectroscopic Investigation on Polymer Blends/Composites**” is an authentic record of the research work carried out by **Mr. Gaurang Patel** under my supervision and guidance during the period from **December 2008 to March 2014** in partial fulfillment of the degree of **Doctor of Philosophy** under the **Department of Physics, Faculty of Science, The Maharaja Sayajirao University.**

To the best of my knowledge and belief the thesis

1. embodies the work of the candidate him self
2. has duly been completed
3. fulfills the requirement of the ordinance relating to Ph.D. degree of the university
4. is up to the standard both in respect to the content and language for being referred to examiner.
5. and the work presented in this thesis has not been submitted for any other degree earlier and it has duly been completed.

Dr. M. B. Sureshkumar

Thesis Supervisor

Department of Physics

Faculty of Science

The M. S. University of Baroda, India.

## **DECLARATION**

I hereby declared that the work presented here in this thesis entitled “**Spectroscopic Investigation on Polymer Blends/Composites**” is the result of investigations carried out under the supervision of **Dr. M. B. Sureshkumar** at the Department of physics, Faculty of Science, The M. S. University of Baroda, Vadodara, India. Also it was approved by Council of Post-Graduate Studies and Research. Further in the best of my knowledge, it has not been submitted elsewhere for the award of any degree either in this university or in any other universities /Institutes.

**Gaurang Patel**

**DEDICATED TO MY BELOVED  
FAMILY.....!!!!**

## **ACKNOWLEDGEMENTS**

My deepest appreciation goes to my advisor, **Dr. M. B. Sureshkumar**. I thank him for his constant supervisions, recommendations and suggestions during all years involved in my research work. I could not have imagined having a better advisor and mentor for my Ph.D., and without his excellent guidance and continuous support, knowledge and perceptiveness I would never have finished. I would like to thank him for providing me with a lot of opportunities and independence by giving me the freedom to develop myself as a truly independent researcher with creativity, by developing my ideas. His professional and personnel attitude has made my stay in the University a very rewarding and memorable experience. It is my great pleasure and honor to be his student.

I would like to express my sincere gratitude to **Prof. N. L. Singh**, Department of Physics, The M. S. University of baroda, Vadodara, for the continuous support to my Ph.D. and research work, for his motivation and immense knowledge. His guidance helped me in all the time of research.

I take this opportunity to show my regards for **Dr. K. R. Jotania** and **Prof. R. B. Jotania**, who gave me the path and guide me for the same. Without their guidance, I may not be here. I am also thankful to **Prof. C. F. Desai**, Department of Physics, The M. S. University for providing experimental facilities and also guide me whenever I needed.

I specially want to thank, **Dr. Anita Gharekhan**, my senior fellow. Her perpetual energy and enthusiasm in research had always motivated me. In addition, she is always accessible and willing to help me.

I take this opportunity to show my regards for **Prof. Bhattacharya**, Department of Textile Engineering, The M. S. University of Baroda, Vadodara, who provide me mechanical testing facilities. I am very much thankful to **The Department of Zoology** and **The Department of Geology** for providing research facility, UV-Vis spectrophotometer and Thermal Gravimetric Analysis for my research work.

I am very much thankful to **Head of the department** and **all teaching staff** of the department for giving me space, encouragement and all possible help to complete my research.

I specially acknowledge my **University** for giving me an opportunity to work over here and also **UGC-New Delhi** for providing me research fellowship for meritorious student (UGC-RFSMS) for the year of 2009-2013.

I am thankful to my laboratory colleagues and friends **Dr. Maunik Jani, Dr. Devang Shah, Dr. Nikit Deshmukh, Ms. Chaitali Gavade, Ms. Purvi Patel, Ms. Dipika Patel, MR. Dhaval Modi, Ms. Sangeeta, Mr. Naveen Agrawal** for holding scientific discussion as well as relaxing conversations during lunch breaks. I also wish to thank the whole **non-teaching staff** of the department for helping me in all kinds of administrative work.

I would like to thank to my entire fellow **Dolly, Poonam Sharma, Manish Jayswal, Dr. Sagar Ambavale, Aditya, Akshay, Nishant, Rakeshbhai, Ketan, Abhisek** for their valuable support.

I would like to wish “Good Luck” to my all research fellow working in the Department of Physics, The M. S. University of Baroda.

I acknowledge Maheshbhai and family for their valuable support. Thanks to all my friends, **Babu, Rahul, Kalu, Nirav** without their support it might have tougher to complete my work.

Also thankful to my junior M.Sc. Students **Sarthak, Nilesh, Jaydeep, Aditya, Tejas, Namrata,**

**Zarna** etc. and all the **student of 2014<sup>th</sup> batch**. Specially thanks to **Hitesh Yadav** for helping me for the thesis writing and give company to complete my work.

I thank my family: **My father**, my mentor without his support I couldn't achieve my dream. **My Mother**, my strong supporter, who give me courage and support when it was most required and of course without her love I am not able to reach here. **My Bhai** and **Bhabhi** who continuously boost my dream and who always ready to help me by any means, without their support it was not possible.

Special heartily thanks to my beloved wife **Purvi** for her understanding, unconditional support, and encouragement to pursue my interests and endless love with great patience when it was really required. She always gives me inspiration and energy to my life. Without her it was not possible. Thank you dear for your endless support.

I also thank to my **Father in Law** and **Mother in law** for their never ending support and trust in me and also giving me a new way of thinking.

Last but not the least, the three Gurus who changed my life, giving me the essence of life and at this moment I would like to thank them from the bottom of my heart. **Mr. P. N. Patel sir, My parents** and **Mr. Magan sir**. Due to their efforts, I have been able to reach here. With their knowledge and education, I dreamed this and able to achieve my goal.

Date:

Vadodara

## Summary

The introduction of new polymer needs many efforts in terms of production cost and marketing. So now a days improved polymer can be produced by blending and alloying the existing polymers. Combining polymers by blending or alloying can reduce the cost as well as development time. Blending and alloying of polymer is a powerful way to produce materials with desirable combination of properties which is not available with single polymer.

Mixing of two or more miscible polymers at their matrix level is termed as *Polymer Blends*, while composite can be defined as the combination of two or more different materials. A subclass of the composites consists of a polymer matrix and inorganic filler with dimension either micro or nano scale which is known as *Polymer composite*.

Benefits from blending and alloying include improvement in mechanical, electrical and thermal properties. Because the creation of blends and composites relies upon the use of existing polymers with well known characteristics, their development is considerably less costly than new-polymer synthesis. Applications of polymer blends are myriad, including automotive, aerospace, electronics, medical equipments, etc. Furthermore, thermoplastic polymer types and a range of composites based on them continue to replace metals, wood and ceramics. Polymer composites are used in a wide variety of products. Polymer composites have also been used for different kind of sensing applications.

Once the polymer blends and composites have been made, several analytical techniques are used to identify various characteristics like optical, thermal, mechanical, structural etc. of polymer blends and composites. The most important of these techniques include the common

spectroscopic methods such as Infrared, Raman, UV-Vis spectroscopy and others like Mechanical testing, Thermo gravimetric analysis (TGA).

The motivation behind this work is to study the influence of different blend and composite concentration on different properties of pure, blend and composite polymer films. And also study the spectroscopic correlation of different properties with spectroscopic results.

In the present work, we have made three different blends system and a composites system in different weight percentage as shown below.

- Polyvinyl Chloride (PVC) and Polymethyl methacrylate (PMMA) blends
- Poly Acrylamide (PAM) and Polyvinyl Alcohol (PVA) blends
- Poly Acrylamide (PAM) and Polyethylene Oxide (PEO) blends
- Polymethyl methacrylate (PMMA) and Titanium Dioxide (TiO<sub>2</sub>) composites

Polyvinyl chloride (PVC) is one of the most important and widely used thermoplastic due to its valuable properties. But its main drawback is low thermal stability. Several polymers are mixed with PVC to overcome this deficiency. We here add poly methyl methacrylate (PMMA) as processing aids for PVC. Many researchers have been worked and reported on PVC/PMMA blend system. The present study involves the blending of PVC with amorphous and a rigid polymer, PMMA. PMMA might be expected to counter balance the fall in mechanical properties of PVC is attributed to the disruption in molecular packing of stiff and rigid chains of PVC. PMMA influences the matrix structure of PVC which in turn affects properties of PVC. We have studied here the change in different properties due to the intermolecular interaction between PVC

and PMMA polymers. We have correlated the change in the properties by different spectroscopic techniques results.

Poly acrylamide (PAM) is well-known hydrophilic polymer and has been greatly used in the field of agriculture and biomedical. Poly vinyl alcohol (PVA) is widely used as a basic material for a variety of biomedical applications. Blends of polyvinyl alcohol (PVA) with other polymers have been mechanically characterized by many researchers. Preparing Semi-interpenetrating polymer networks (semi-IPNs) of PAM and cross linked PVA to achieve strong and desired mechanical property are also studied. Thus, realizing the vital role of PAM and PVA in biomedical engineering, the present investigation aims to study the intermolecular interaction between two polymer networks and its effect on other properties of blends.

In recent years, studies on the electrical and optical properties of polymers have attracted much attention due to their applications in optical devices. The optical properties of polymers can be suitably modified by addition of dopants or other polymer with the host matrix. Polyacrylamide (PAM) is highly water-absorbent, forming a soft gel when hydrated. It is used in manufacturing of soft contact lenses, in potable water treatment industry etc. Polyethylene oxide (PEO) is becoming increasingly important in a variety of fields as the most suitable material for optical and electrical applications, because of its advantages such as water solubility, low glass transition temperature, large dipole moment, low cost, easy processability. Blend of PAM and PEO may be utilized in many applications established industrially due to their useful physical properties.

In recent years, studies on optical and electrical characteristics of polymers have fascinated much consideration in their application in optical and electronic devices. The optical properties of the

polymers can be correctly customized by the addition of dopant depending on their reactivity with host matrix. Incorporating inorganic particles into polymer matrix is a practicable way to obtain advanced materials of composites. Organic/inorganic composites materials have great consideration, because of their attractive potential application of traditional polymeric materials. Optical parameters (e.g. optical band gap, etc.) of poly methyl methacrylate (PMMA) depend on its molecular structure and they can be modified. Titanium dioxide or Titania ( $\text{TiO}_2$ ) is a harmless white material widely used as an inorganic material, in photo electrochemical solar energy conversion and environmental photo catalysis (treatment of polluted water and air) including self cleaning and anti fogging surfaces. It is also commonly used as a high refractive index material in optical filter applications and sensors. In order to improve the performance of PMMA,  $\text{TiO}_2$  particle was used to enhance different PMMA properties.

All blends and composite films were prepared by solution cast techniques. Mechanical, optical, structural, thermal properties and surface morphology of pure, blends and composites were studied. Effects of different concentrations on properties of blend and composites polymer films were also studied. Blend and composite films were characterized by TGA, SEM, FTIR, UV- Vis, Raman spectroscopy.

To identify the chemical nature of the polymer or to determine its composition, IR is a highly useful specific tool. For quantitative analysis of microstructure, stereo regularity, branching, or crosslinking, IR analysis is the simplest and most sensitive method. FT-IR spectroscopy is a powerful and potentially very widely applicable method for obtaining the dominance of the chemical functional groups, miscibility of the two polymers in the blend specimens. It helps in understanding the structure – property relationship in variety of polymers and gives quantitative approach, which can interpret the resulting data.

Raman spectroscopy of polymers also measures the vibrational energy levels. Raman spectroscopy has become the most important tool for the characterization of polymers. It may provide evidence of molecular interactions among polymer/ polymer or polymer/filler in addition to the functional groups.

UV- Vis Spectrophotometer studies will provide detailed information about the optical properties of polymer and polymer blends. Various optical parameters like optical band energy gap, absorption coefficient, absorption edge etc were calculated.

TGA is considered as the most important method for studying thermal stability of polymers. Moreover, the kinetics of the accompanied decomposition reaction has been reviewed. The weight of the sample decreases slowly as the reaction begins, then decreases rapidly over a comparatively narrow temperature range and finally levels off as the reactants are used up.

SEM is an important tool for polymer analysis, since it is extensively used to study fracture and failure mechanics, particles size and shape, filler orientation and dispersion in polymer matrices.

Mechanical properties of polymer blends and composites were carried out to study the Young's modulus (YM), Ultimate Tensile Strength (UTS), Stress at Peak load and Elongation at Break (EB).

The spectroscopic investigations on polymer and polymer blends using FTIR , Raman, UV- Vis and DSC studies enables us to understand the issues related to the processing and structure-property relationship for pure polymer and polymer blends/composites.

1.	1
Chapter 1	1
1.1. Introduction to Polymeric age	2
1.2. Introduction of Polymer	3
1.2.1. Classification of Polymer	3
1.2.2. Properties	6
1.3. Polymer Blends	7
1.3.1. What is Polymer Blends?	7
1.3.2. Different kind of Polymer Blends	8
1.3.3. Properties of Polymer Blends	9
1.3.4. Methods for Blending	9
1.3.5. Application of Polymer Blends	11
1.4. Polymer Composites	12
1.4.1. What is Polymer Composites?	12
1.4.2. Different kind of Polymer composites	12
1.4.3. Properties of Polymer Composites	13
1.4.4. Methods to make Polymer Composites	14
1.4.5. Application of Polymer Composites	14
1.5. Selection of Polymer blends	14
1.5.1. Polyvinyl chloride (PVC) and Poly methyl methacrylate (PMMA) blend	14
1.5.2. Poly acrylamide (PAM) and Poly vinyl alcohol (PVA) blend	16
1.5.3. Poly acrylamide (PAM) and Poly ethylene oxide (PEO) blend	18
1.5.4. Poly methyl methacrylate (PMMA) and Titanium Dioxide (TiO <sub>2</sub> )	18
1.6. Spectroscopy in Polymer Science	19
1.7. Objective of the work	20
References	22
2.	30
Chapter 2	30
2.1. Introduction	31
2.2. Materials	31
2.2.1. Polyvinyl Chloride (PVC)	32
2.2.2. Poly (methyl methacrylate) (PMMA)	34

2.2.3.	Polyacrylamide (PAM)	36
2.2.4.	Polyvinyl Alcohol (PVA)	37
2.2.5.	Polyethylene Oxide (PEO)	39
2.2.6.	Titanium Dioxide (TiO <sub>2</sub> )	40
2.3.	Methods	41
2.3.1.	Blend preparation	41
2.3.2.	Composites Preparation	42
2.3.3.	Thickness Measurement	42
2.4.	Experimental Techniques and Instruments	44
2.4.1.	Fourier Transform Infrared (FTIR) Spectroscopy	44
2.4.2.	UV- Vis Spectroscopy	48
2.4.3.	RAMAN Spectroscopy	54
2.4.4.	Mechanical Testing Facility	59
2.4.5.	Differential Scanning Calorimeter (DSC)	62
2.4.6.	Thermal Gravimetric Analysis (TGA)	65
2.4.7.	Scanning Electron Microscopy (SEM)	68
2.5.	Experiment specification detail	70
2.5.1.	Fourier Transform Infrared Spectroscopy	70
2.5.2.	UV-Vis Spectroscopy	70
2.5.3.	FT-RAMAN Spectroscopy	70
2.5.4.	Mechanical Analysis	71
2.5.5.	Differential Scanning Calorimeter	71
2.5.6.	Thermal Gravimetric Analysis	71
2.5.7.	Scanning Electron Microscopy	71
2.6.	References	73
3.		77
Chapter 3		77
3.1.	Introduction	78
3.2.	Results and Discussion	81
3.2.1.	FTIR Analysis	81
3.2.2.	UV-Vis Analysis	84
3.2.3.	RAMAN Analysis	86

3.2.4.	Mechanical Analysis	87
3.2.5.	Thermal gravimetric Analysis	89
3.2.6.	Scanning Electron Microscopy	92
3.3.	Conclusions	93
3.4.	References	95
4.		98
Chapter 4		98
4.1.	Introduction	99
4.2.	Results and Discussion	101
4.2.1.	FTIR Analysis	101
4.2.2.	UV-Vis Analysis	105
4.2.3.	RAMAN Analysis	108
4.2.4.	Mechanical Analysis	110
4.2.5.	Thermal gravimetric Analysis	112
4.2.6.	Scanning Electron Microscopy	114
4.3.	Conclusions	115
4.4.	References	116
5.		120
Chapter 5		120
5.1.	Introduction	121
5.2.	Results and Discussion	122
5.2.1.	FTIR Analysis	122
5.2.2.	UV-Vis Analysis	126
5.2.3.	RAMAN Analysis	130
5.2.4.	Mechanical Analysis	133
5.2.5.	Thermo gravimetric Analysis	134
5.2.6.	DSC Analysis	137
5.2.7.	Scanning Electron Microscopy	140
5.3.	Conclusions	141
5.4.	References	143
6.		148
Chapter 6		148

---

6.1.	Introduction	149
6.2.	Results and Discussion	151
6.2.1.	FTIR Analysis	151
6.2.2.	UV-Vis Analysis	155
6.2.3.	Mechanical Analysis	157
6.2.4.	Differential Scanning Calorimeter Analysis	159
6.2.5.	Thermal gravimetric Analysis	160
6.2.6.	Scanning Electron Microscopy	162
6.3.	Conclusions	163
6.4.	References	164
7.		167
Chapter 7		167
7.1.	Conclusion	168
7.1.1.	PVC/PMMA Blends	168
7.1.2.	PAM/PVA Blends	169
7.1.3.	PAM/PEO Blends	170
7.1.4.	PMMA/TiO <sub>2</sub> Composites	171
7.2.	Future Work	173

Figure 1.1 Spectral Range of Spectroscopic methods used in spectroscopy. ....	20
Figure 2.1 Schematic Diagram of an Infrared Spectrophotometer .....	47
Figure 2.2 Analysis of IR spectroscopy data .....	47
Figure 2.3 Different molecular orbital transitions.....	49
Figure 2.4 Essential elements of UV-Vis Spectrophotometer .....	50
Figure 2.5 Schematic Diagram of UV-Vis Spectrophotometer .....	52
Figure 2.6 Tauc's plot of Indirect and Direct energy band gap .....	54
Figure 2.7 Energy level diagram of the states involved in Raman signal. ....	56
Figure 2.8 Scheme of Raman Spectrometer .....	58
Figure 2.9 A typical stress versus strain curve.....	60
Figure 2.10 Cross section of Power-compensation DSC .....	62
Figure 2.11 Cross section of main components of a typical heat-flux DSC cell. ....	63
Figure 2.12 A typical DSC curve for polymer.....	64
Figure 2.13 Scheme of Thermal gravimetric analysis .....	66
Figure 2.14 A typical thermal degradation TGA curve .....	67
Figure 2.15 Cross section and lab image of Scanning electron microscope .....	68
Figure 3.1 FTIR Spectra of pure PVC, pure PMMA and Their blends (a) in the range 600 – 2000 $\text{cm}^{-1}$ (b) in the range 2500 – 3300 $\text{cm}^{-1}$ .....	83
Figure 3.2 Plot of (a) Absorption coefficient ( $\alpha$ ) vs Wavelength ( $\lambda$ ), (b) Absorption coefficient ( $\alpha$ ) vs Photon Energy ( $h\nu$ ), (c) $(\alpha h\nu)^2$ vs $h\nu$ , (d) $(\alpha h\nu)^{1/2}$ vs $h\nu$ .....	85
Figure 3.3 Raman Spectra of Pure PVC, Pure PMMA and their blends (a) in the C-Cl stretching region of PVC (b) in the C=O stretching region of PMMA .....	86
Figure 3.4 Variation in Ultimate tensile strength, Stiffness, Young's Modulus, stress at peak, Elongation at break, as a function of PMMA content .....	88
Figure 3.5 (a) TG of pure PVC, pure PMMA and their blends (b) Derivative TG of pure PVC, pure PMMA and their blends .....	90
Figure 3.6 Scanning Electron Micrograph of (a) Pure PVC (b) Pure PMMA (c) 80/20 (d) 60/40 (e) 40/60 .....	93
Figure 4.1 FTIR Spectra of pure PAM, pure PVA, 70/30, 50/50 and 30/70 blend ratio (a) in the region of 600-1800 $\text{cm}^{-1}$ (b) in the region of 2500-3800 $\text{cm}^{-1}$ .....	103
Figure 4.2 Deconvolution spectra of pure PAM, pure PVA, 70/30, 50/50 and 30/70 blend ratio (a) band in the region of 1500-1800 $\text{cm}^{-1}$ (b) band in the region of 2600- 3700 $\text{cm}^{-1}$ .....	104
Figure 4.3 Plot of (a) Absorption coefficient ( $\alpha$ ) vs Wavelength ( $\lambda$ ), (b) Absorption coefficient ( $\alpha$ ) vs Photon Energy ( $h\nu$ ), (c) $(\alpha h\nu)^2$ vs $h\nu$ , (d) $(\alpha h\nu)^{1/2}$ vs $h\nu$ .....	106
Figure 4.4 Raman Spectra of pure PAM, pure PVA, 70/30, 50/50 and 30/70 blend ratio (a) in the region of 600-1800 $\text{cm}^{-1}$ (b) in the region of 2700-3600 $\text{cm}^{-1}$ .....	109
Figure 4.5 Variation in (a) Max load, Ultimate tensile strength, Young's Modulus, stress at break (b) Elongation at break, Stiffness as a function of PAM/PVA content .....	111
Figure 4.6 (a) TG of pure PAM, pure PVA and blends (b) Dr TG of pure PAM, pure PVA and blends.....	112
Figure 4.7 Scanning Electron Micrograph of (a) Pure PAM (b) Pure PVA .....	114
Figure 4.8 Scanning Electron Micrograph of (a) 70/30 (b) 50/50 (c) 30/70.....	115
Figure 5.1 FTIR Spectra of Pure and blend polymers (a) in the region of 600-3800 $\text{cm}^{-1}$ (b) in the region of 1400-1800 $\text{cm}^{-1}$ .....	123
Figure 5.2 Plot of (a) Absorption coefficient ( $\alpha$ ) vs Wavelength ( $\lambda$ ), (b) Absorption coefficient ( $\alpha$ ) vs Photon Energy ( $h\nu$ ), (c) $(\alpha h\nu)^2$ vs $h\nu$ , (d) $(\alpha h\nu)^{1/2}$ vs $h\nu$ , (e) $\ln \alpha$ vs Photon Energy ( $h\nu$ ).....	128
Figure 5.3 Raman spectra of pure and blend films in the range (a) 600-2000 $\text{cm}^{-1}$ (b) 2700-3500 $\text{cm}^{-1}$ .....	131

Figure 5.4	Variation in Max load, Ultimate tensile strength, Young's Modulus, stress at break, Elongation at break, Stiffness as a function of PAM/PEO content .....	133
Figure 5.5	(a) TG of pure PAM, pure PVA and blends (b) Dr TG of pure PAM, pure PEO and blends .....	135
Figure 6.1	FTIR Spectra of pure PMMA and Their composites (a) in the range 600 – 1800 $\text{cm}^{-1}$ (b) in the range 2800 – 3000 $\text{cm}^{-1}$ .....	153
Figure 6.2	Plot of (a) Absorption coefficient ( $\alpha$ ) vs Wavelength ( $\lambda$ ), (b) Absorption coefficient ( $\alpha$ ) vs Photon Energy ( $h\nu$ ), (c) $(\alpha h\nu)^2$ vs $h\nu$ , (d) $(\alpha h\nu)^{1/2}$ vs $h\nu$ .....	157
Figure 6.3	Variation in Ultimate tensile strength, stress at break, Stiffness, Young's Modulus, Elongation at break as a function of $\text{TiO}_2$ content .....	158
Figure 6.4	DSC curve for PMMA and its composites. ....	159
Figure 6.5	(a) TG of pure PMMA and their composites (b) Derivative TG of pure PMMA and their composites	161
Figure 6.6	Scanning Electron Micrograph of (a) Pure PMMA (b) 0.03% (c) 0.1% (d) 0.5% of $\text{TiO}_2$ .....	162

## List of Tables

Table 1.1	Information obtained by spectroscopy relating to structure and dynamics of polymeric systems.	19
Table 2.1	Physical properties of PVC	33
Table 2.2	Physical properties of PMMA	35
Table 2.3	Physical properties of PAM	37
Table 2.4	Physical properties of PVA	38
Table 2.5	Physical properties of PEO	39
Table 2.6	Physical properties of TiO <sub>2</sub>	40
Table 2.7	Thickness of various polymers and its blends	43
Table 3.1	Assignment of different vibrational modes of PVC, PMMA and various Blends.	82
Table 3.2	Variation of absorption edge and direct/indirect band gap with different blend percentage	85
Table 3.3	TG and DrTG data of Pure PVC, PMMA and their blended samples	92
Table 4.1	Assignments of the FT-IR characterization bands of the pure PAM, pure PVA and pure PAM/PVA blend <sup>38, 39, 40</sup>	105
Table 4.2	Variation of optical (Direct/Indirect) energy gap (E <sub>gopt</sub> ) and absorption edge (ΔE) with different samples	107
Table 4.3	Assignments of the Raman characterization bands of the pure PAM and pure PVA	109
Table 4.4	Assignments of the Raman characterization bands of the PAM/PVA blends	110
Table 4.5	TG and DrTG data of Pure PAM, PVA and their blended samples	113
Table 5.1	Assignments of the FT-IR characterization of bands of the pure PAM, pure PEO and PAM/PEO blend [16, 18, 36-38].	125
Table 5.2	Absorption edge, optical band gap (both direct and indirect) and activation energy values of pure PAM, pure PEO and PAM/PEO polymer blend films.	129
Table 5.3	Assignments of Raman bands of pure PAM, Pure PEO and PAM/PEO blends [37, 41-42].	132
Table 5.4	TG and DrTG data of Pure PAM, PEO and their blended samples	136
Table 5.5	Effect of the Blend Ratio on the Temperatures Corresponding to Different Percentage Weight Losses in PAM/PEO Blends	136
Table 5.6	T <sub>m</sub> (°C), ΔH (J/g), χ <sub>c</sub> (%), of PAM/PEO Blends	138
Table 6.1	Assignment of different vibrational modes of PMMA and its various composites.	152
Table 6.2	Various of absorption edge and direct/indirect band gap with different blend percentage	156
Table 6.3	Glass Transition temperature (T <sub>g</sub> ) °C of different PMMA/ TiO <sub>2</sub> Composites.	159
Table 6.4	TG and DrTG data of Pure PMMA and their composites	162

# Chapter 1

## Introduction

---

### *Abstract*

*This chapter deals with the general introduction and fundamental of polymers, polymer blends and polymer composites. Various applications of polymer blends and composites are also described. The importance of the spectroscopy in the field of polymer science is explained. A detailed literature survey and motivation for selecting this problem is also emphasized at the end of the chapter.*

## 1.1. Introduction to Polymeric age

The earliest known work with polymers was the rubber industry in pre-Columbian Mexico. They combine latex of the rubber tree with the juice of the morning glory plant in different proportions to get rubber with different properties for different products, such as bouncing balls, sandals, and rubber bands. The first modern example of polymer science is the derivatives of the natural polymer cellulose, such as celluloid and cellulose acetate developed by Henri Braconnot, Christian Schönbein and others. But it used as plastic during First World War in 1914.

The first synthetic polymer used on a commercial scale was a phenol-formaldehyde resin known as *Bakelite*, developed in the early 1900s by chemist Leo Baekeland. Hermann Staudinger was the first to propose that polymers consisted of long chains of atoms held together by covalent bonds. The first of what may be called the modern synthetic polymers were developed during the inter-war years. The first commercial manufacture of polystyrene took place in Germany in 1930, poly(methyl methacrylate) in 1936, PVC was used as a plasticized material in 1939 and poly(ethylene terephthalate) in 1943. Polyolefins, polymers derived from olefins, were started to develop around 1950. The first linear thermoplastic polycarbonate was commercially produced in 1960. Polypropylene was manufactured in 1962.

The development and production of a new polymer is an extremely costly process, so the method of reducing these costs is important. For these reasons a great interest was developed during the 1970s and 1980s in the blending of polymers of different types to give either cheaper products or products with properties which were the combination of two or more polymers.

The development of new polymers has not come to an end but polymer chemists continue to develop both new polymers and new polymerization processes for the older polymers. This leads

to the introduction of polymers for special uses. Totally novel types of polymers are also synthesized with a view to investigate whether they might have useful properties.

## 1.2. Introduction of Polymer

The word Polymer is derived from Greek words “poly” means many and “meres” means parts. In simple statement polymer is a long chain molecule which have large number of repeating units which is called monomers. Certain polymers are found in nature like proteins, cellulose, silk etc. while many others like nylon, polystyrene, polyethylene are chemically synthesized.

### 1.2.1. Classification of Polymer

Hundreds of polymers have been synthesized and many more are likely to be produced in future. But fortunately on the basis of their processing characteristic, type of polymerization, on the basis of polymer structure, chemical structures, physical properties, mechanical behavior, thermal characteristics, and stereochemistry, polymers can be classified as follows.

#### **Natural and Synthetic polymer**

Polymers isolated from natural materials are called natural polymers.

Example: cotton, silk, wool etc.

Polymers synthesized from low molecular weight compounds are called synthetic polymers.

Example: Polyethylene, Polyvinyl chloride (PVC), nylon etc.

#### **Based on processing characteristics**

Polymers can also be divided into groups based on their properties. All polymers can be classified in to two major groups based on their thermal processing behavior which is very useful for thermal properties of different polymers.

- **Thermoplastics**

They can be softened in order to process into a desired form when heated are called thermoplastics.

It can be reused and re-fabricated by applying heat and pressure.

Example: Polyvinyl chloride (PVC), Polystyrene (PS), Polypropylene (PP) etc.

- **Thermosets**

Polymers whose individual chains have been chemically linked by covalent bond during their fabrication and once they formed they cannot be thermally processed to re-fabricate are called thermosets.

They resist heat softening, creep and solvent effect. Due to these properties they are useful for composite materials, coatings and adhesive applications.

Examples: Epoxy resins, phenol-formaldehyde resins etc.

- ✚ **Based on polymerization process**

Polymers may also be classified according to their polymerization mechanism as shown below.

- **Addition or Condensation**

Polymer which is polymerized by a sequential addition of monomers is addition polymer.

Example: Polystyrene (PS), Poly Ethylene (PE) etc.

Polymer which is obtained by the random reaction of two molecules is called condensation polymer. As a molecule, a monomer, oligomer or higher molecular weight functional group take part in poly condensation reaction.

Example: Nylon-6, 6, Polycarbonate (PC), etc.

- **Step growth or Chain growth**

Step growth polymerization is a type of polymerization mechanism in which bifunctional or multifunctional monomers react to form a first dimer, then trimer and longer oligomer or eventually long chain polymer. Most condensation polymers are step growth polymer.

Example: Polyester, Polyamide etc.

Chain growth polymerization is technique when unsaturated monomers or molecules add on to the active side on a growing polymer chain, one at a time [1].

And as a molecules radical, anion or cation can take part in polymerization. Most addition polymers are chain growth polymer.

Example: Polystyrene (PS), Polyvinyl chloride (PVC), etc.

- ✚ **Atactic, Isotactic and Syndiotactic Polymers**

On the basis of the configurations, polymers can be classified into three categories viz., atactic, isotactic (cis-arrangement) and syndiotactic (trans-arrangement).

- **Atactic polymer**

Those polymers, in which arrangement of side groups is at random around the main chain, are termed as atactic polymers.

- **Isotactic polymer**

Those polymers in which the arrangement of side groups are all on the same side are known as isotactic polymers.

- **Syndiotactic Polymer**

Whereas, those polymers in which the arrangement of side groups is in alternating fashion is termed as syndiotactic polymers.

### Based on polymer structure

Polymer may also classify based on the chemical structure of their backbone.

- **Homo chain polymer**

Polymers having all carbon atoms along their backbone are called homo chain polymers which are further divided as polyalkylenes, polyalkenylenes and polyalkynylenes depending upon whether there are single, double or triple bonds along their backbone.

Example: Polystyrene (PS), Polyvinyl chloride (PVC), etc.

- **Hetero chain polymer**

Polymers having more than one atom type in their backbone are called hetero chain polymers which are grouped by the types of atoms and chemical groups e.g. carbonyl, amide or ester, etc. located along the backbone.

Example: Polyether, Polycarbonates etc.

Depending on its ultimate form and use, a polymer can also be classified as plastic, elastomers, fibre or liquid resins.

### 1.2.2. Properties

Every polymer has very distinct characteristics but most polymers have the general properties. Polymer properties are broadly divided into several classes. The most basic property of a polymer is the identity of its constituent monomers. The other one is the arrangement of these monomers within the polymer at the scale of a single chain. These basic structural properties play a major role in determining bulk physical properties of the polymer, which describes how the polymer behaves as a continuous macroscopic material. Chemical properties, at the nano-scale, describe how the chains interact through various physical forces. At the macro-scale, they

describe how the bulk polymer interacts with other chemicals and solvents. Some basic properties of polymers are listed below.

- Polymers are very light in weight with great degrees of strength.
- Polymers can be processed in various ways.
- Polymers have many inherent properties that can be further enhanced.
- Polymers can be very resistant to chemicals and also to weather. They only react with particular solvent.
- Polymer can act as both thermally and electrically insulator.
- Polymers have excellent transport properties such as diffusivity.
- Mechanical properties of polymers have made polymer to great interesting materials. Polymers replace many materials with their good physical properties.

### 1.3. Polymer Blends

The polymer industry traces its beginning to the early modification of shellac natural rubber, gutta-percha and cellulose. In 1846, Parkes patented the first polymer blend natural rubber with gutta-percha partially co-dissolved in  $CS_2$ . Blending these two isomers resulted in partially cross linked materials whose rigidity is controlled by composition [2].

#### 1.3.1. What is Polymer Blends?

Blending indicates “an action to combine ingredients into one mass, so that the constituent parts are indistinguishable”. While in plastic processing, it means the physical act of homogenization [3]. Polymer blends are physical mixtures of two or more polymers with/without any chemical bonding between them. The objective of polymer blending is to achieving feasible products with

unique properties and lower cost. Blending technology also provides attractive opportunities for reuse and recycling of polymer wastes.

When two or more polymers are mixed, the phase structure of the resulting material can be either miscible or immiscible. Due to their high molar mass, the entropy of mixing of polymers is relatively low and consequently specific interactions are needed to obtain blends, which are miscible or homogeneous on a molecular scale [4]. Polymer blends exhibit properties that are superior to any one of the component. Miscibility of the constituent polymers decides the structure of the blend which in turn, decides the properties of the blend [5-7]. If there is weak interaction between constituent polymer, miscibility of polymers is weak [8]. Blending offers a unique tool for overcoming the deficiencies of the polymer without much loss in the mechanical properties [9, 10]. Knowledge of the miscibility and phase behavior of polymer blends is essential for controlling the properties of polymer blends.

### 1.3.2. Different kind of Polymer Blends

There are many types of polymer blends, it include from simple binary mixtures of polymer, interpenetrating networks, compatible blends, impact modified polymers, emulsion polymers, engineering polymer blends, thermosets blends, elastomeric blends, liquid crystalline polymer blends, water soluble polymer blends, natural product polymer blends and so on. But polymer blends can be broadly divided in to three categories:

- Immiscible polymer blends

It is also known as heterogeneous polymer blends. If the blend is made of two polymers then the blend structure is not a single phase structure and two glass transition temperatures will be observed.

- Compatible polymer blends

These blends are also immiscible polymer blends but they exhibit macroscopically uniform physical properties, which is caused by strong interaction between the component polymers.

- Miscible polymer blends

They are also known as homogeneous polymer blends. Polymer blends that exhibit a single phase structure. In this case only one glass transition temperature is observed.

### 1.3.3. Properties of Polymer Blends

Polymer blends have been designed, rather than by availability. These polymeric materials must perform under strenuous mechanical, chemical, thermal and electrical conditions imposed by the requirements of a specific application. They are also accepted to stay performed at complex atmospheric conditions. All these factors point toward the need for studies of the properties and performance of polymer blends. For assessing the performance of a polymer blend, mainly study the given properties like mechanical, chemical and solvent effects, thermal, flame retardancy, electrical and optical properties. Polymer blend have very excellent properties like better processing, blow molding, mechanical (creep, impact, stiffness, strength), heat resistance, optical and electrical properties and also have lower cost.

### 1.3.4. Methods for Blending

The properties of a polymer blends are dependent upon the method of preparation. There are a number of methods which have been employed to prepare polymer blends. Some important and most commonly used techniques are as follow.

- **Mechanical-melt mixing**

This is the most important and cheap method to prepare polymer blend in industry. The simplest process for the making of polymer blends from thermoplastic is mixing the polymers in the melt condition in suitable devices like rollers, extruders; kneeling machine etc. under suitable reaction conditions, chemical reaction like chain scissions, cross linking can take place in polymer melt. Grafting reaction can also be achieved by adding suitable monomers to polymer melts in extruders [11].

- **Solution cast techniques**

Solution cast techniques is an important technique utilized to fabricate thin layered films. The solution cast process consists of the solution of the film ingredients in a suitable common solvent which further take place to dry where the solvent is evaporated. When solvent is evaporated, the resultant film is removed from substrate. Advantages of solution casting method as compared to melt process are higher quality with uniform thickness of films, highly pure and clear films with lack of residuals and free from pinholes and it is also possible to produce pattern films.

- **Latex blending**

Latex is a colloidal dispersion of a polymer substance in an aqueous medium. Latex blends are prepared by mixing two polymers where each polymer is present in the form of polymeric microspheres dispersed in a fluid medium [12]. Blends prepared with this method would be expected to have very high interfacial area. The early emulsion polymerization of rubbers and thermoplastic acrylates provided raw ingredients for latex blending. Latex blends were used either directly as paints, adhesive and sealants or they were pelletized or spray dried.

- **Spray or freeze drying**

In spray drying, transformation of fluid of blend materials into a dried particulate form by spraying fluid into a hot drying medium [13]. This is an ideal process, when the end products have precise quality, residual moisture content, bulk density and particle size. On other hand, a technique in which first polymers are heated above glass transition to form good solution then allow polymer solution to freeze certainly lower temperature to achieve solid polymer from solution [14].

- **Fine powder mixing**

In this technique, mixtures of polymer powders have been made to allow for diffusion mixing at higher temperature. Mostly temperatures apply here above glass transition temperature of constituent polymers.

- **In-situ polymerization**

The polymerization of one polymer is conducted in the presence of other polymer. Interpenetrating Polymer Networks are prepared by polymerization of different polymer networks. Polymer electrolytes are prepared by this technique.

### 1.3.5. Application of Polymer Blends

Since industrialization and commercialization, polymer blends tends to direct replacement of the different materials, mostly metal. This is because they can be easily formed in complex shape, corrosion resistant as well as lighter in weight than metals. Blend families tend to be appropriate for certain types of applications which require the special attributes of the major blend component.

Polymer blends are generally used in below mentioned applications: Automotive applications, Electrical and Electronics Applications, Medical Applications, Building and Construction,

Business Machines and Communications, Packaging, Power Tools, different Appliances, Furniture, Recycling materials and so on.

## **1.4. Polymer Composites**

One of the aims of material research is to developed new materials with desirable physical properties for particular application and also to understand the mechanisms which controlling these properties. Polymer composites can be developed by mixing of two or more basic constituents which containing two or more phases. The basic difference between blends and composites is that the two main constituents in the composites remain recognizable while these may not be recognizable in blends [15].

### **1.4.1. What is Polymer Composites?**

Any of the combinations or compositions that comprise two or more materials as separate phases, at least one of which is a polymer, By combining a polymer with another material, such as glass, carbon, or another polymer, it is often possible to obtain unique combinations or levels of properties [16]. The goal of polymer composites is to improve strength, stiffness, or toughness, or dimensional stability by embedding particles or fibers in a polymer matrix or binding phase with low cost.

### **1.4.2. Different kind of Polymer composites**

On the basis of matrix phase, composites can be classified into metal matrix composites (MMCs), ceramic matrix composites (CMCs), and polymer matrix composites (PMCs) [17]. On the basis of the dopant, polymer composites are also further classified. Types of reinforcement are particulate composites (composed of particles), fibrous composites (composed of fibers), and

laminate composites (composed of laminates). Particulate composites are also classified according to the dopant particles like organic or inorganic particle, metal or non metallic particle.

### 1.4.3. Properties of Polymer Composites

Properties of different polymers will determine the application to which it is appropriate. The chief advantages of polymers as matrix are low cost, easy processability, good chemical resistance, and low specific gravity. Different kind of polymers such as thermoplastic polymers, thermosetting polymers, elastomers, and their blends are used for making of polymer composites. Polymer Composites are very popular due to their low cost and simple fabrication methods. It's main advantage of properties are shown below [18]:

- a) High specific strength
- b) High specific stiffness
- c) High fracture resistance
- d) Good abrasion resistance
- e) Good impact resistance
- f) Good corrosion resistance
- g) Good fatigue resistance
- h) Low cost

The main disadvantages of Polymer Composites are:

- a) Low thermal resistance and
- b) High coefficient of thermal expansion.

#### 1.4.4. Methods to make Polymer Composites

The important processing methods of polymer composites are hand lay-up, bag molding process, filament winding, pultrusion, bulk molding, sheet molding, resin transfer molding, injection molding, and so on.

#### 1.4.5. Application of Polymer Composites

Generally plastics, fibers, rubber, adhesives, paints and coatings etc. are based on polymers. One polymer can also be used for more than one application. Polymer composite materials overcome many of the shortcomings of homogeneous materials. They are currently being used in various medical field and many additional applications have been proposed. Polymer composites have also been used as sensor materials for different types of sensing applications [19]. Composites and plastics are used in a wide variety of products from advanced spacecraft to sporting goods [20]. Metal doped polymer provides suitable properties for EMI shielding [21]. In electrical field polymer composites are used in Panels, housing fittings, switchgear, insulators, and connectors. In chemical field they are widely used in Chemical storage tanks, pressure vessels, piping, pump body, valves, etc.

### 1.5. Selection of Polymer blends

In this section we discuss about the selection of polymers and its blends. And literature survey regarding these polymers and its blends are also described.

#### 1.5.1. Polyvinyl chloride (PVC) and Poly methyl methacrylate (PMMA) blend

Poly (vinyl chloride) (PVC) is one of the most important and widely used thermoplastics due to its many important properties like good processability, chemical resistance, low flammability and low cost [22]. Its principal drawback, however, is low thermal stability at processing

temperatures. This deficiency is overcome by adding plasticizers or processing aids in PVC. Especially poly(methyl methacrylate) (PMMA), are used as processing aids for PVC [23]. The aim for modifying PVC by blending is to manufacture new PVC polymers that combine desired physical properties at low cost. Enhancement in ionic conductivity and mechanical strength has been reported in polymer electrolytes by modifying them in the form of blends [24].

First PVC/PMMA blends were studied by Schurer et. al. [25] PVC/ PMMA blends has been studied by different approaches by different workers, it was well described by Chao Zhou et.al. [26] Schurer [27] reported that PVC/ PMMA are miscible only in blends having PVC contents greater than 60%. Rupa Chakrabarti et. al. studied physical and mechanical properties of PVC/PMMA blend and suggested that a substantial increase in toughness accompanied with unusual increase in modulus and ultimate tensile strength occurred after initial stages of PMMA incorporation compared to pure PVC [28]. Wlochowicz and Janicki concluded that PVC / PMMA blends at all compositions are wholly amorphous two-phase system [29]. Varada investigated the miscibility of PVC with PMMA by ultrasonic and refractive index method [30]. They pointed that PVC and PMMA are miscible in all compositions. Shen and Torkelson observed that PVC/ PMMA blends are miscible at all compositions, if they are prepared between  $T_g$  and their lower critical solution temperature [31]. This discrepancy in the miscibility may be due to the different methods used for sample preparation and polymers used are having different molecular weights. S. Ramesh et.al. studied PVC/PMMA blend based polymer electrolytes and reported about interaction of PVC/PMMA blend with lithium triflate salt, ethylene carbonate (EC), dibutyl phthalate (DBP) plasticizers and also with silica [32]. The PVC/PMMA blend is a well-known system in which hydrogen bonds involving the  $\alpha$  hydrogen and the carbonyl group of PMMA are expected. It has been reported' that this type of interaction is competing along with

dipole dipole interactions between the H - C - Cl and C = O groups to ensure miscibility [33]. The present study involves the blending of PVC with amorphous and a rigid polymer, poly (methyl methacrylate) (PMMA) having a very high glass transition temperature ( $T_g$ ). PMMA might be expected to counter balance the fall in mechanical properties of PVC is attributed to the disruption in molecular packing of stiff and rigid chains of PVC [34].

### 1.5.2. Poly acrylamide (PAM) and Poly vinyl alcohol (PVA) blend

PAM is well-known hydrophilic polymer and has been greatly used in the field of agriculture and biomedicine [35, 36]. The electrical and mechanical properties of the ethylene propylene diene monomer (EPDM) and nitrile rubber (NBR) blended with polyacrylamide (PAM) were studied [37]. PAM is a polymer of biomedical and pharmaceutical interest widely studied as hydrogel for blood compatible applications [38]. Polymers of acrylamide are well known for their hydrophilicity and inertness that make them a material of choice in large number of applications in medical and pharmacy [39].

Many researchers have studied the use of PAM hydrogels for controlled release of fertilizers, pesticides or possibly in medicine [40]. Also, it was used for the decontamination of waste water containing radioactivity [41]. Polyacrylamide-based polymers have received a great extent of utility in industry because of their high molecular weight, water soluble property, and ability to receive diverse modification on chemical structure [42, 43]. When PAM dissolved in solvents, the linear structure formed in solution by these macromolecules reduces the drag coefficient, thereby, facilitating the transport of viscous liquids over long distances [44, 45]. When cross-linked, the polymer is insoluble in water and forms a hydrogel system that is capable of absorbing and retaining large quantities of water. The linear form and solubility properties also

offer unique applications such as stabilizing soil matrices, reducing erosion, and improving soil aeration [46, 47].

Poly vinyl alcohol (PVA) films are known to possess high tensile and impact strengths, a high tensile modulus, and excellent resistance to alkali, oil, and solvents [48]. PVA has gained increasing attention in the biomedical field because of its bio inertness [49, 50]. Vargas et al. investigated poly Vinyl Alcohol (PVA) for the phase behavior [51]. Fritz and Breitsmer developed ionically conducting polyelectrolytes based on PVA due to its bio-compatibility and wide spread use in biomedical fields [52]. Because of its superior mechanical properties and better ionic conduction, it has some technological advantages in electrochromic devices and fuel cells, etc [53]. Hydrophilicity of PVA is an advantage for its applications, and also a limiting factor in its characterization because its molecules are prone to aggregate through hydrogen bonding due to its poly hydroxyl groups [54].

Blends of polyvinyl alcohol (PVA) with other polymers have been mechanically characterized by many researchers [55]. PVA and PAM are two well-known polymers and their individual biomedical, mechanical and other properties have been thoroughly investigated [56-58]. PVA is a water soluble, non-toxic, non-immunogenic polymer with a remarkable film forming property [59, 60]. However, its weak mechanical strength restricts its use in those applications where the material has to withstand prolonged stress. Thus, the introduction of other polymeric components into the PVA matrix could improve its mechanical properties [61]. PVA is widely used as a basic material for a variety of biomedical applications [62-64].

The chemical resistance and physical properties of PVA have led to its broad industrial use. Chemically cross linked PVA hydrogels have received increasing attention in biomedical and biochemical applications because of their permeability, biocompatibility and biodegradability

[65-68]. Horia M Nizam El-din et. al. undertaken to investigate the miscibility of PVA with PAM in various proportions [69].

The selection and use of polymers can potentially form hydrogen bonds when two polymers mixed, as well as the study of blends properties, are of importance to find further applications of the resulting blend materials for biomedical and pharmaceutical devices [70].

### **1.5.3. Poly acrylamide (PAM) and Poly ethylene oxide (PEO) blend**

Polyacrylamide (PAM) is highly water-absorbent, forming a soft gel when hydrated. It is used in manufacturing of soft contact lenses, in potable water treatment industry etc [71]. Polyethylene oxide (PEO) is becoming increasingly important in a variety of fields as the most suitable material for optical and electrical applications, because of its advantages such as water solubility, low glass transition temperature, large dipole moment, low cost and easy processability [72, 74]. PAM and PEO may be utilized in many applications established industrially due to their useful physical properties.

### **1.5.4. Poly methyl methacrylate (PMMA) and Titanium Dioxide (TiO<sub>2</sub>)**

In recent years, studies on optical and electrical characteristics of polymers have fascinated much consideration in their application in optical and electronic devices [75, 76]. The optical properties of the polymers can be correctly customized by the addition of dopant depending on their reactivity with host matrix. Optical parameters (e.g. refractive index, optical band gap, etc.) of poly methyl methacrylate (PMMA) depend on its molecular structure and they can be modified. Titanium dioxide or titania (TiO<sub>2</sub>) is a harmless white material widely used in photo electrochemical solar energy conversion and environmental photo catalysis (treatment of polluted water and air) including self cleaning and anti fogging surfaces [77, 78]. It is also commonly used as a high refractive index material in optical filter applications and sensors [79,

80]. Nanostructured TiO<sub>2</sub> is used in solar cell research and displays [81]. TiO<sub>2</sub> thin films are valued for their good durability, high dielectric constant, high refractive index, excellent transparency in the visible range and biocompatibility. In polymer light emitting diode devices, mixing TiO<sub>2</sub> nanoparticles into poly[2-methoxy-5-(20-ethyl-hexyloxy)-para-phenylenevinylene] MEH-PPV results in increased current densities, radiances and power efficiencies [82, 83].

## 1.6. Spectroscopy in Polymer Science

Spectroscopy is defined as science of interaction between electromagnetic radiation and matter. Polymer spectroscopy deals with the application of a wide range of spectroscopic methods to study polymers which have higher molar mass and formed by linking of monomers. The basic information obtained by spectroscopy is always consisting of energy difference, additionally consisting band shapes, intensities and in some cases polarization of signals. Polymer spectroscopy provides two types of information, related to the structure and dynamics of polymers (**Table 1.1**). Information on chemical structure is the main aim of analytical application of polymer spectroscopy as it gives information at molecular level which is very helpful to study other properties of polymers. Polymer spectroscopy and non spectroscopic methods are combining to produce well and pure characterized polymer samples.

**Table 1.1** Information obtained by spectroscopy relating to structure and dynamics of polymeric systems.

<b>Structure</b>	<b>Dynamics</b>
Chemical structure and Tacticity	Movements of polymer chain, segments and side groups
Conformation	Phonons
Crystallinity	Excitons
Electronic Structure	Complex formation and related phenomena

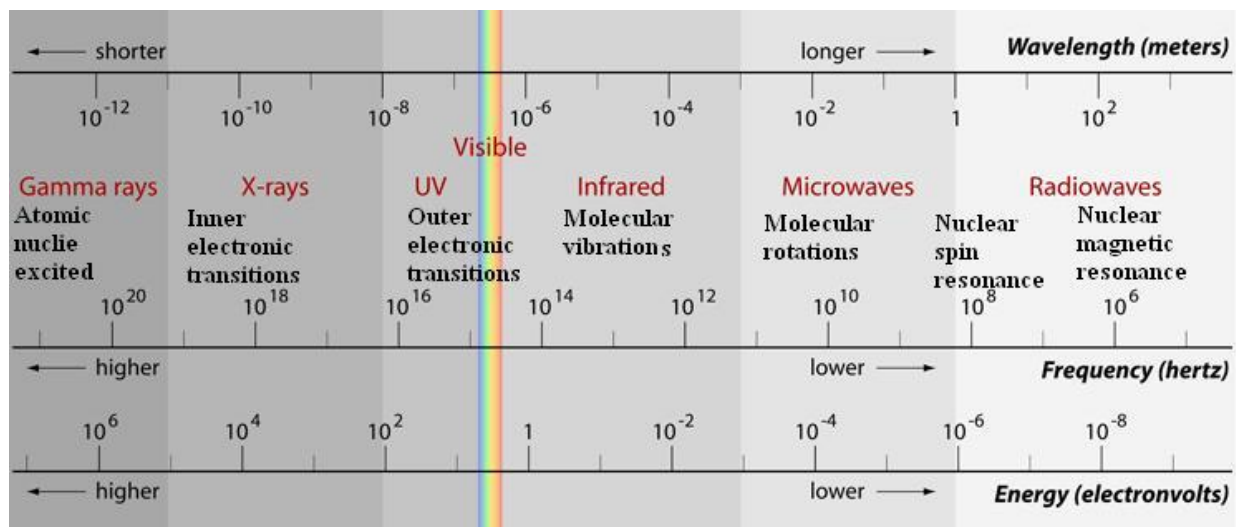


Figure 1.1 Spectral Range of Spectroscopic methods used in spectroscopy.

Information on chemical structure is the main aim of analytical application of polymer spectroscopy. Spectroscopy gives precise information at the molecular level. Polymer spectroscopy involves the investigation of monomers or oligomers and also their interaction with surrounding molecules. In order to get maximum useful information, polymer spectroscopy should be combined with non-spectroscopic methods to study different polymer properties. Spectral range of spectroscopic methods used in polymer spectroscopy is shown in the above

**Figure 1.1.** Whole range can be divided into three parts conveniently [84]:

1. Electronic spectroscopy (ESCA and UV-Vis)
2. Vibrational spectroscopy (IR and Raman)
3. Spin resonance spectroscopy (ESR and NMR)

## 1.7. Objective of the work

To study the mechanical, optical, structural and thermal properties and surface morphology of pure, blends and composites polymer films using spectroscopic techniques. Also to study the

---

effects of different concentrations on the properties of blends and composites polymer films using spectroscopic techniques such as FTIR , Raman, UV- Vis, TGA, and DSC. These studies enable us to understand the issues related to the processing and structure-property relationship for pure polymer and polymer blends/composites.

The motivation for this work is that nobody was tried to correlate mechanical properties, thermal properties and optical properties studied by conventional methods with spectroscopic investigation using FTIR, Raman and UV-Vis spectral studies. But spectroscopic study may be able to provide quick, more reliable and in depth details than the other techniques. Hence decided to study the influence of different concentrations of polymer blend and composite on different properties of pure, blend and composite polymer films with conventional methods and correlate their result with spectroscopic results.

## References

1. Introduction to polymer, R. J. young, Chapman & Hall, ISBN – 0-412-22170-5, 1987.
2. David I. Bower, An Introduction to Polymer Physics, Cambridge University Press, New York, 2002.
3. L. A. Utracki (Edi.), polymer blends hand book, 577-651, Klawer Academic Publishers, 2003.
4. D.J. Walsh, S. Rostami, Adv. Polym. Sci., 70, 119 1985.
5. Olabisi, O.; Robeson, L. M.; Shaw, M. T. Polymer-Polymer Miscibility; Academic Press: New York, 1979.
6. Kwei, T. K.; Wang, T. T. In Polymer Blends; Paul, D. R.; Newman, S., Eds.; Academic Press: New York, 1978.
7. L.A. Utracki, Text Book of Polymer Alloys and Blends (Thermodynamics and Rheology), Hanser, New York 1990.
8. A.V. Rajulu, R.L. Reddy, S.M. Raghavendra, S.A. Ahmed, Eur. Polym. J. 35 (6) 1183, 1999.
9. J.L. Acosta, E. Morales, Solid State Ionics 85, 85 1996.
10. A.M. Rocco, R.P. Pereira, M.I. Felisberti, Polymer 42 5199, 2001.

11. D. Braun, H. Cherdrón, M. Rehahn, H. Ritter, B. Voit, *Polymer synthesis: Theory and Practice*, 4<sup>th</sup> edition, Springer-Verlag Berlin Heidelberg, 2005
12. Jianrong Feng, Mitchell A. Winnik, Richard R. Shivers, Brian Clubb, *Macromolecules*, 28, 7671-7682, 1995.
13. K. Masters, *Spray drying Handbook*, John Wiley & Sons, New York, 4<sup>th</sup> edition 1985.
14. Mar K Alger, *Polymer Science Sictionary*, Chapman & Hall, 1997
15. Josmin P. Jose, Sant Kumar Malhotra, Sabu Thomas, Kuruvilla Joseph, Koichi Goda, and Meyyarappallil Sadasivan Sreekala, *Advances in Polymer Composites: Macro- and Microcomposites – State of the Art, New Challenges, and Opportunities*, Polymer Composites: Volume 1, First Edition, Published by Wiley-VCH Verlag GmbH & Co. KGaA 2012.
16. *McGraw-Hill Encyclopedia of Science and Technology*, 5th edition, published by The McGraw-Hill Companies, Inc.
17. Avila, A.F., Paulo, C.M., Santos, D.B., and Fari, C.A. *Materials Characterization*, 50, 281–291, 2003.
18. *Polymer Composites: Volume 1, First Edition*. Edited by Sabu Thomas, Kuruvilla Joseph, Sant Kumar Malhotra, Koichi Goda, and Meyyarappallil Sadasivan Sreekala, Published by Wiley-VCH Verlag GmbH & Co. KGaA, 2012.
19. J. R. Li, J.R. Xu, M.Q. Zhang, M.Z. Rong. *Carbon* 41 2353-2360, 2003.

20. M. Ueda, I. H. Tan, R. S. Dallaqua, J. O. Rossi, J. J. Barroso, M. H. Tabacniks, Nucl. Instrum. Meth B 206 760, 2003.
21. F. Rodrigues, C. Cohen, C.K. Ober, L.A. Archer, "Principles of Polymer Systems" Eds. D. T. Schanck, D.P. Teston, 2003, Taylor and Francis, New York, London. D. D. L. Chung. Carbon, 1 39 279-285, 2001.
22. Aouachria Kamira and Belhaneche-Bensemera Naima, Polymer Testing., **25** 1101–1108, 2006.
23. Reyne M. Les plastiques modernes: polyme`res, transformations et applications. Paris: Hermes; 1992.
24. Fekete Erika, E. Foldes and B. pukanskszky, Europian Polymer Journal., 41 727-736, 2005.
25. J. W. Schurer, A. de Boer and G. Challa, Polymer.,16 201, 1975.
26. Chao Zhoul et.al, Polymer Bulletin., 58 979–988, 2007.
27. J. W. Schurer, A. de Boer and G. Challa, Polymer.,16 201, 1975.
28. Rupa Chakrabarti, Molay Das and Debabrata Chakraborty, Inc. J Appl Polym Sci., 93 2721-2730, 2004.
29. A. Wlochowicz and J. Janicki, J. App. Poly. Sci., 38 1469, 1989.
30. A. Varada Rajulu, R. Lakshminarayna Reddy and S. M. Raghavendra, Eur.Polym. J., 35 1183, 1999.

31. S. Shen and M. Torkelson, *Macromolecules.*, 25 721, 1992.
32. S. Ramesh, K. H. Leen, K. Kumutha and A. K. Arof, *Spectrochimica Acta., Part A*, 66 1237–1242, 2007.
33. E. Lemieux, R. E. Prud'homme, R. Forte, R. Jbrhme, and P. Teyssib, *Macromolecules*, 21, 2148 1988.
34. Patel G, Sureshkumar MB, Singh NL, Bhattacharya SS, Spectroscopic correlation of mechanical properties of PVC/ PMMA polymer blend. *J Int Acad Phys Sci* 14:91–100, 2010.
35. Lopatin VV, Askadskii AA, Peregudov AS, Vasilev VG Structure and relaxation properties of medical purposed polyacrylamide gels. *J Appl Polym Sci* 96:1043–1058, 2005.
36. Durmaz S, Okay O In homogeneities in poly (acrylamide) gels: position-dependent elastic modulus measurements. *Polym. Bull* 46:409–418, 2001.
37. Salwa El-Sabbagh, Samia M. Mokhtar, Salwa L. Abd-El Messieh, *Journal of Applied Polymer Science*, Vol. 70, 2053–2059, 1998.
38. Peppas, N. A. In *Biomaterials Science*; Ratner, B. Ed.; Academic Press, Inc., New York, p. 63, 1996.
39. A. K. Bajpai and Smitha Bhanu, *J. Mater. Sci. Mater. Med.* 15, 43, 2004.

40. Yousefzadeh P, SohrabpourMand KhadjaviMS, Proceedings of the Research and development of control release formulation of IAEA pesticide Vienna, Austria, 81-89, 1994.
41. Rudenko LI, Sklyar VY, Khan VY, Sklyar VP and Makaro MA, Chernobyl Reports of the All-Union Scientific and Technical Meeting, Ukraine, 10–15, Ministerstvo rossijskoj PO Atomic, Ennergii, Moscow, May 1988.
42. K.E. Lee, B.T. Poh, N. Morad, and T.T. Teng, *Int. J. Polym. Anal. Charact.*, 13, 95, 2008.
43. K.E. Lee, B.T. Poh, N. Morad, and T.T. Teng, *J. Macromol. Sci.*, 46, 240, 2009.
44. Rho T, Park J, Kim C, Yoon H-K, Suh H-K. Degradation of polyacrylamide in dilute solution. *Polym. Degrad. Stab.* 51: 287, 1996.
45. Yang M-H. On the thermal degradation of poly(styrene sulfone)s VIII. Effect of structure on thermal characteristics. *Polym. Degrad. Stab.* 76: 69, 2002.
46. Wallace A, Wallace GA, Abouzam AM. Effect of excess level of a polymer as a soil conditioner on yield and mineral nutrition of plants. *Soil Sci.* 141: 377, 1986.
47. Rosen J, Hellenas KE. Analysis of acrylamide in cooked foods by liquid chromatography tandem mass spectrometry. *Analyst* 127: 880, 2002.
48. F. H. Abd El-Kader, S. A. Gafer, A. F. Basha, S. I. Bannan, M. A. F. Basha, *Journal of Applied Polymer Science*, Vol. 118, 413–420, 2010.
49. Cholakis, C. H.; Zingg, W.; Sefton, M. V. *J Biomed Mater Res.*, 23, 417, 1989.
50. Horiike, S.; Matsuzawa, S. *J Appl Polym Sci* 58, 1335, 1995.

51. Vargas, R. A., Garcia, A., and Vargas, M. A., *Electrochim Acta* 43, 1271, 1998.
52. Fritz, H. P. and Breitsmer, M., *Solid State Ionics* 45, 255, 1991.
53. Rajendran, S. and Mahandran, O., *Ionics* 7, 463, 2001.
54. Coleman, M. M. and Painter, P. C., *Prog. Polym Sci.* 1, 20, 1995.
55. Zhang X, Burgar I, Lourbakos E, Beh H, *Polymer* 45:330S–3312, 2004.
56. Xu N, Zhou D, Li L, He J, Chen W, Wan F, Xue G, *J Appl Polym Sci* 88:79–87, 2003.
57. Barretta P, Bordi F, Rinaldi C, Paradossi G, *J Phys Chem B* 104:11019–11026, 2000.
58. Bajpai AK, Bhanu S In vitro release dynamics of insulin from a loaded hydrophilic polymeric network. *J Mater Sci: Mater Med* 15:43–54, 2004.
59. Chan LW, Hao JS, Heng PWS Evaluation of permeability and mechanical properties of composite polyvinyl alcohol films. *Chem Pharm Bull* 47(10):1412–1416, 1999.
60. Hassan CM, Peppas NA Structure and applications of poly (vinyl alcohol ) hydrogels produced by conventional crosslinking or by freezing/thawing methods. *Adv Polym Sci* 153:37–65, 2000.
61. A. K. Bajpai And Manish Sharma, *Journal of Macromolecular Science, Part A: Pure and Applied Chemistry*, 42:663–682, 2005.
62. Barretta P, Bordi F, Rinaldi C, Paradossi G, *J Phys Chem B* 104:11019–11026, 2000.

63. Russo R, Macinonico M, Petti L, Romano G Physical behaviour of biodegradable alginate-poly(vinyl alcohol) blend films. *J Polym Sci Part B, Polym Phys* 43(10):1205–1213, 2005.
64. Gutzler R, Smulders M, Lange RFM The role of synthetic pharmaceutical polymer excipients in oral dosage forms—poly (ethylene oxide)—graft—poly (vinyl alcohol) copolymers in tablet coatings. *Macromol Symp* 225:81–93, 2005.
65. A. Muhlebach, B. Muller, C. Pharira, M. Hofmann, B. Seiferling And D. J . Guerry, *Polym. Sci. Part A: Polym. Chem.* 35, 3603, 1997.
66. C. K. Yeom and K. H. Lee, *J. Membr. Sci.* 109, 257, 1996.
67. K. J . Kim, S. B. Lee and N. W. Han, *Polym. J.* 25, 129, 1993.
68. H. Matsuyama, M. Teramoto and H. Urano, *J. Membr. Sci.* 126, 151, 1997.
69. Horia M Nizam El-din, Abdel Wahab M El-Naggari and Faten I Ali, *Polym Int* 52:225–234, 2003.
70. Tuncer C, Aykara And Serkan Demirci, *Journal of Macromolecular Science, Part A: Pure and Applied Chemistry*, 43:1113–1121, 2006.
71. A Rawat, H K Mahavar, S Chauhan, A Tanwar, P J Singh, *Indian J Pure & Appl Phys*, VOL 50: 100-104, 2012.
72. Conway B. E., *Electrochemical Supercapacitors: Scientific Fundamental and Technological Applications*, New York: Springer, 1999.

73. Mishra R, Tripathy S P, Sinha D, Dwivedi K K, Ghosh S , Khathing D T, Muller M, Fink D and Chung W H, *Nucl. Instrum. Methods B*, 168 59, 2000.
74. Abdel-Hamid H M, *Solid-State Electron.*, 49 1163, 2005.
75. Acosta JL, Morales E, *Solid State Ion* 85:85, 1996.
76. Kim JY, Kim SH , *Solid State Ion* 124(1–2):91, 1999.
77. C.A. Linkous, *Environ. Sci. Technol.* 34, 44754, 2000.
78. A. Fujishima, T.N. Rao, D.A. Tryk, *J. Photochem. Photobiol. C1* 1, 2000.
79. P. Loebl, M. Huppertz, D. Mergel, *Thin Solid Films* 251 72, 1994.
80. I. Hayakawa, Y. Iwamoto, K. Kikuta, *Sens. Actuators B* 62 55, 2000.
81. A. Hagfeld, B. Didriksson, *Sol. Energy Mater. Sci. Cells* 31 481, 1994.
82. S.A. Carter, J.C. Scott, P.J. Brock, *Appl. Phys. Lett.* 31 1145, 1997.
83. J. Zhang, X. Ju, B. Wang, Q. Li, T. Liu, T. Hu, *Synth. Metals* 118, 181, 2001.
84. Walter Klopffer, *Introduction to Polymer Spectroscopy* by springer-Verlag Berlin Heidelberg 1984.

---

## Chapter 2

# Materials and Experimental Techniques

---

### ***Abstract***

*This chapter deals with the discussion about the structure, properties and utilities of the polymer which were used in the present work. Preparation of films of polymer blends and composites are discussed here. The specification of different characterization techniques, which have been used for the analysis of polymer blends/composites films, are also discussed in this chapter.*

## 2.1. Introduction

This chapter describes a detailed account of the polymeric materials used for the present study, methods to prepare films of polymeric blends/composites and various techniques used for the analysis of polymer blends/composites films. Detailed descriptions of following are considered in this chapter.

- Materials: Properties
- Sample preparation
- Thickness measurement
- Fourier Transform Infra-Red (FTIR) Spectroscopy
- UV-Vis Spectroscopy
- RAMAN Spectroscopy
- Mechanical Properties
- Thermogravimetric Analysis(TGA)
- Scanning Electron Microscopy
- Differential Scanning Calorimeter

## 2.2. Materials

The Materials used in the present study are

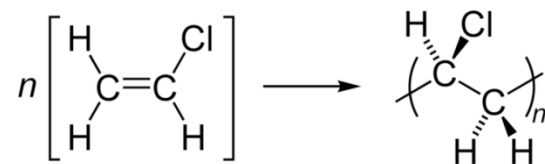
1. Polyvinyl Chloride (PVC)
2. Polymethyl methacrylate (PMMA)
3. Poly Acrylamide (PAM)
4. Polyvinyl Alcohol (PVA)
5. Polyethylene Oxide (PEO)

## 6. Titanium Dioxide (TiO<sub>2</sub>)

### 2.2.1. Polyvinyl Chloride (PVC)

Polyvinyl Chloride (PVC) is the third widely produced plastic [1]. PVC is widely used because it is durable, cheap and easily worked. It has large number of properties, so can be used to make hundreds of products [2]. PVC's are relatively low cost, biological and chemical resistance and workability have resulted in it being used for a wide variety of applications. With the addition of impact modifiers and stabilizers, it has become a popular material for window and door frames. By adding plasticizers, it can become flexible enough to be used in cabling applications as a wire insulator. It has been used in many other applications.

PVC is also widely used vinyl member which is formed by the free radical polymerization of vinyl chloride monomer units as shown below.



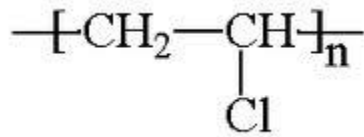
PVC consists of polar molecules which are attracted to each other by electrostatic attraction due to dipole-dipole interaction of a chlorine atom in one atom to a hydrogen atom in another atom. Due to this intermolecular interactions between polymer chain PVC is fairly strong thermoplastic materials.

## PROPERTIES

### ❖ Composition



❖ **Structure of Polyvinyl chloride (PVC)**



❖ **PHYSICAL PROPERTIES OF PVC**

Physical properties of PVC are described below (**Table 2.1**).

**Table 2.1** Physical properties of PVC

Property	PVC
Density [g/cm <sup>3</sup> ]	1.3–1.45
Thermal conductivity [W/(m·K)]	0.14–0.28
Yield strength [MPa]	31–60
Young's modulus [psi]	490,000
Surface resistivity [Ω]	10 <sup>13</sup> –10 <sup>14</sup>
Elongation at break (%)	20–40
Glass temperature (°C)	82 °C
Melting point (°C)	100–260
Specific heat ( <i>c</i> ) (kJ/(kg·K))	0.9

❖ **Other Properties**

- **Weathering stability.** PVC is resistant to aggressive environmental factors, therefore is the material of choice for roofing.
- **Versatility.** PVC can be flexible or rigid.
- **Fire protection.** PVC is a material resistant to ignition due to its chlorine content.
- **Longevity.** PVC products can last up to 100 years and even more.

- **Hygiene.** PVC is the material of choice for medical applications, particularly blood and plasma storage containers.
- **Energy recovery.** PVC has high thermal power; when utilized in incinerators PVC provides power and heat for homes and industries, and all that without any environmental impact
- **Barrier properties.** PVC can be made impervious to liquids, vapors and gases.
- **Eco-efficiency.** Only 43% of PVC's content comes from oil (57% comes from salt); it therefore contributes to the preservation of that highly valuable natural resource.
- **Recyclability.** PVC is very recyclable, more so than many other plastics.
- **Economical efficiency.** PVC is the cheapest of large-tonnage polymers providing many products with the best quality-price ratio.

### 2.2.2. Poly (methyl methacrylate) (PMMA)

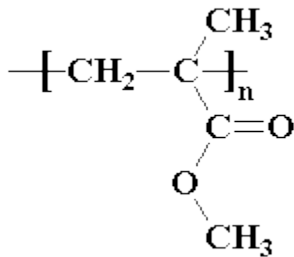
Poly (methyl methacrylate) (PMMA) is a transparent thermoplastic which is the synthetic polymer of methyl methacrylate. PMMA is routinely produced by emulsion polymerization, solution polymerization, and bulk polymerization. It is commercially polymerized by free radical initiators such as peroxides and azo compounds in suspension or for more specialized applications such as for hard contact lenses. PMMA is an amorphous, transparent and colorless thermoplastic which is hard and stiff but brittle. PMMA is a strong and lightweight material. PMMA is often preferred because of its moderate properties, easy handling and processing, and having low cost, but behaves in a brittle manner when loaded. It has good abrasion and UV resistance and excellent optical clarity [3, 4].

## PROPERTIES

### ❖ Composition



### ❖ Structure of Polymethyl methacrylate (PMMA)



### ❖ PHYSICAL PROPERTIES OF PMMA

Physical properties of PMMA are described below (Table 2.2).

**Table 2.2** Physical properties of PMMA

Property	PMMA
Density [g/cm <sup>3</sup> ]	1.18
Thermal conductivity [W/(m·K)]	0.167-0.25
Young's modulus [MPa]	1800-3100
Glass temperature (°C)	85
Melting point (°C)	130–140
Specific heat (c) (kJ/(kg·K))	1.47

### ❖ Application

- Optical instruments:

Production of optical lenses, such as glasses, magnifying glass, various lenses

- Stationery and daily necessities:

Making a variety of drawing tools, teaching model, specimen shield, lamps, all kinds of pens, buttons, hair clips, candy, soap box, household accessories.

- Construction areas:

Indoor and outdoor lighting and non-lighting signal display, ceiling lighting, furniture, partition materials, solar energy collector housings etc.

- Other areas:

Can be used as medical devices, such as additional limbs, dentures, medical optical basic raw material, aero-space equipment, light cover, surface cover plates, car and motorcycle windshields. PMMA finds major applications in automotive industry, as acrylic sheet for bathtubs, sign boards and as composites materials for kitchen sinks, basins and bathroom fixtures.

### 2.2.3. Polyacrylamide (PAM)

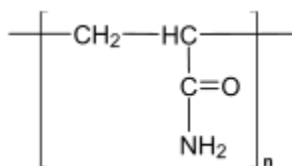
Polyacrylamide (PAM) is a polymer formed from acrylamide subunits. It can be synthesized as a simple linear-chain structure or cross-linked, typically using *N,N'*-methylenebisacrylamide. Polymers of acrylamide are well known for their hydrophilicity and inertness. PAM is well-known hydrophilic polymer and has been greatly used in the field of agriculture and biomedicine [5, 6]. It is water soluble polymer that's why Polyacrylamide-based polymers have received a great extent of utility in industry.

## PROPERTIES

### ❖ Composition



### ❖ Structure of Polyacrylamide (PAM)



## ❖ PHYSICAL PROPERTIES OF PAM

Physical properties of PAM are described below (**Table 2.3**).

**Table 2.3** Physical properties of PAM

Property	PAM
Density [ $\text{g}/\text{cm}^3$ ]	1.5
Thermal conductivity [ $\text{W}/(\text{m}\cdot^\circ\text{C})$ ]	0.56
Glass temperature ( $^\circ\text{C}$ )	160-170
Melting point ( $^\circ\text{C}$ )	230–240

## ❖ Application

Polyacrylamide is not toxic. It is used to coagulate solids in a liquid like in water treatment plant, Enhanced Oil Recovery, used for horticultural and agricultural, to make Gro-Beast toys, which expand when placed in water, can be utilized as an additive in body-powder, used in molecular biology applications as a medium for electrophoresis of proteins and nucleic acids.

### 2.2.4. Polyvinyl Alcohol (PVA)

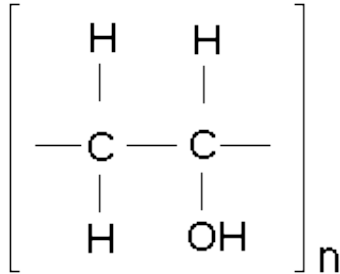
Polyvinyl alcohol is obtained by the direct hydrolysis of poly (vinyl acetate). PVA is a non-toxic, water soluble synthetic polymer that has been commercially produced on a large scale. It has a large number of hydroxyl groups which allows it to react with many types of functional groups. This advantage makes it suitable as biocompatible materials. Polyvinyl alcohol (PVA) has excellent film forming, emulsifying and adhesive properties [7]. It is also resistant to oil, grease and solvents. It is odorless and nontoxic. It has high tensile strength and flexibility, as well as high oxygen and aroma barrier properties. The chemical resistance and physical properties of PVA have led to its broad industrial use. Chemically cross linked PVA have received increasing attention in biomedical and biochemical applications.

## PROPERTIES

### ❖ Composition



### ❖ Structure of Polyvinyl Alcohol (PVA)



### ❖ PHYSICAL PROPERTIES OF PVA

Physical properties of PVA are described below (**Table 2.4**).

**Table 2.4** Physical properties of PVA

Property	PVA
Density [g/cm <sup>3</sup> ]	1.19-1.39
Thermal conductivity [W/(m·K)]	0.2
Refractive Index	1.54
Glass temperature (°C)	75-85
Melting point (°C)	180-190
Specific heat ( <i>c</i> ) (kJ/(kg·K))	1.67

### ❖ Application

PVA has been widely utilized in diverse fields, ranging from thickening agent to controlled release systems [8]. It has been widely used as a basic material for a variety of biomedical applications [9]. PVA is useful as thickener and modifier, useful in water transfer printing process, as hard contact lens solution as a lubricant, used in the

formation of polymer encapsulated nano beads, to making protective chemical-resistant gloves, for packaging purpose, as an additive for strength to concrete and cements.

### 2.2.5. Polyethylene Oxide (PEO)

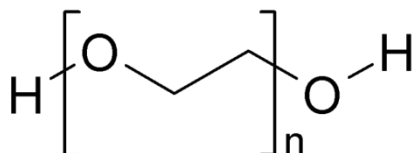
Polyethylene Oxide is a polyether compound with many applications from industrial manufacturing to medicine. PEO is synthetic polymer of ethylene oxide monomer. Polyethylene oxide is non-toxic, odorless, neutral, lubricating, nonvolatile and nonirritating and is used in a variety of pharmaceuticals and in medications as a solvent, dispensing agent, ointment and suppository bases [10].

#### PROPERTIES

##### ❖ Composition



##### ❖ Structure of Polyethylene Oxide (PEO)



##### ❖ PHYSICAL PROPERTIES OF PEO

Physical properties of PEO are described below (**Table 2.5**).

**Table 2.5** Physical properties of PEO

Property	PEO
Density [g/cm <sup>3</sup> ]	1.15-1.26
Thermal conductivity [W/(m·K)]	0.17
Refractive Index	1.45
Glass temperature (°C)	-67
Melting point (°C)	65-75

### ❖ Application

PEO has good chemical stability, both acid and alkali - resistant, corrosion-resistant. It is useful to enhance water dispersibility and water-based coatings, Anti dusting agent in agricultural formulations, Coupling agent, humectants, solvent and lubricant in cosmetics and personal care bases, Dye carrier in paints and inks, Low volatile, water soluble, and noncorrosive lubricant without staining residue in food and package process, Plasticizer to increase lubricity, Softener and antistatic agent for textiles.

#### 2.2.6. Titanium Dioxide (TiO<sub>2</sub>)

Titanium dioxide, also known as titanium (IV) oxide or Titania, is the naturally occurring oxide of titanium, chemical formula TiO<sub>2</sub>. Generally it comes in two different forms, rutile and anatase.

## PROPERTIES

### ❖ Composition



### ❖ PHYSICAL PROPERTIES OF TiO<sub>2</sub>

Physical properties of TiO<sub>2</sub> are described below (**Table 2.6**).

**Table 2.6** Physical properties of TiO<sub>2</sub>

Property	TiO <sub>2</sub>
Molar Mass [g/mol]	79.866
Density [g/cm <sup>3</sup> ]	4.23
Refractive Index	2.488
Melting point (°C)	1843

## ❖ Application

TiO<sub>2</sub> has a wide range of applications, from paint to sunscreen to food coloring. Titanium dioxide is the most widely used white pigment because of its brightness and very high refractive index. TiO<sub>2</sub> is useful in cosmetic and skin care products, as a UV absorber, as a photo catalyst.

## 2.3. Methods

### 2.3.1. Blend preparation

All the polymeric blends, studied here, are prepared by solution cast technique. All the polymer, dopant and solvent are purchased from local chemical supplier. Methods of preparation of all blends are described below.

#### i. Preparation of PVC and PMMA blends

The polymeric blends of PVC and PMMA were prepared in different weight proportion by solution cast technique. The weighed fractions of PVC and PMMA were dissolve in acetone plus toluene solution in 1:3 fraction at room temperature and stirred for approximately 24 hrs at different proportions starting from 90/10, 80/20, 70/30, 60/40, 50/50, 30/70. And the solution was cast on a clean and flat petty dish. Then petty dish is kept open at room temperature to evaporate the solvent. Then the films were lifted from the petty dish and used for further analysis and characterization.

#### ii. Preparation of PAM and PVA blends

The blend films were prepared by the solution casting method in three different weight percentages 30:70, 50:50 and 70:30 of PAM and PVA using distilled water as solvent at room temperature. The gel like solution was cast on a clean and flat Teflon dish. Then the

dish is kept in bulb oven to evaporate the solvent. After drying the films, it's used for further analysis and characterization.

### iii. Preparation of PAM and PEO blends

The blend films of PAM/PEO in three different weight proportions (30:70, 50:50 and 70:30) were prepared by the solution casting method using distilled water as solvent. After stirring for 12 hours at room temperature, we get homogenous gel like solution. Then solution was cast on a clean and flat Teflon dish to evaporate solution. After getting dry, the films are used for further analysis and characterization.

### 2.3.2. Composites Preparation

We have studied PMMA and  $\text{TiO}_2$  composites here. These composites are also made by solution cast techniques in different weight proportion.

#### i. Preparation of PMMA and $\text{TiO}_2$ composites

The weighed fractions of PMMA and  $\text{TiO}_2$  were dissolve in Tetra hydrofuran (THF) solution at room temperature and stirred for approximately 12 hrs for homogeneous solution at different weight percentage of  $\text{TiO}_2$  starting from 0.01%, 0.03%, 0.05%, etc. The solution was cast on a flat petty dish which is cleaned with acetone. The solution was allowed to spread uniformly in all direction in the petty dish. Then petty dish is kept open at room temperature to evaporate the solvent. Then the films were lifted from the petty dish for the experimental analysis.

### 2.3.3. Thickness Measurement

The thickness of the synthesized blends and composites are measured by a sensitive digital vernier caliper. Least count of the instrument is 0.001 mm. The thickness of all blends and

composites films are measured at 5 different places, choose randomly, and then average of it is taken in the count. The obtained thickness is given in **Table 2.7**.

**Table 2.7** Thickness of various polymers and its blends

Sr. No.	Polymer film	Thickness(mm)
1.	Pure PVC	0.23
	PVC+PMMA (90:10)	0.19
	PVC+PMMA (80:20)	0.18
	PVC+PMMA (70:30)	0.11
	PVC+PMMA (60:40)	0.26
	PVC+PMMA (50:50)	0.28
	PVC+PMMA (30:70)	0.27
	Pure PMMA	0.30
2.	Pure PAM	0.06
	PAM+PVA (70:30)	0.07
	PAM+PVA (50:50)	0.06
	PAM+PVA (30:70)	0.05
	Pure PVA	0.07
3.	Pure PAM	0.06
	PAM+PEO (70:30)	0.12
	PAM+PEO (50:50)	0.14
	PAM+PEO (30:70)	0.06
	Pure PEO	0.06
4.	Pure PMMA	0.31
	PMMA+ TiO <sub>2</sub> (0.03%)	0.25
	PMMA+ TiO <sub>2</sub> (0.1%)	0.15
	PMMA+ TiO <sub>2</sub> (0.3%)	0.17
	PMMA+ TiO <sub>2</sub> (0.5%)	0.42

## 2.4. Experimental Techniques and Instruments

The Pure and Blend samples were characterized with different characterization techniques to study the structural, physical, chemical, optical, thermal properties and surface morphology. Different characterization techniques with their working principle have been discussed as below.

### 2.4.1. Fourier Transform Infrared (FTIR) Spectroscopy

Infrared spectroscopy has been a useful technique for materials analysis for over several years. An infrared spectrum represents a fingerprint of a sample with absorption peaks which correspond to the frequencies of vibrations between the bonds of the atoms [11, 12].

The molecules are excited to a higher energy state when they absorb infrared radiation [13-15]. The absorption of infrared radiation is a quantized process. Only selected frequencies (energies) of infrared radiation will be absorbed by a molecule. In the absorption process, those frequencies of infrared radiation, which match the natural vibrational frequencies of the molecule, will be absorbed, and the energy absorbed will serve to increase the amplitude of the vibrational motions of the bonds in the molecule [16]. All bonds in a molecule are not capable of absorbing infrared radiation, even if the frequency of the radiation exactly matches that of the bond motion. Only those bonds which have a permanent dipole moment are capable of absorbing infrared radiation. The changing electrical dipole of the bond can then couple with the electromagnetic field of the incoming radiation. Every different type of bond has a different natural frequency of vibration. Since the same type of bond in two different compounds is in a slightly different environment, because each different compound is a unique combination of atoms, no two compounds produce the exact same infrared spectrum. Therefore, infrared spectroscopy can result in a positive identification of every different kind of materials. In addition, the size of the peaks in the spectrum is a direct indication of the amount of material present. (Nicolet Corporation) [17].

Fourier transform infrared spectroscopy is preferred methods of infrared spectral analysis for several reasons:

- It is a non-destructive technique
- It provides a precise measurement method which requires no external calibration
- It can increase speed, collecting a scan every second
- It can increase sensitivity
- It has greater optical throughput
- It is mechanically simple with only one moving part

Fourier Transform Infrared (FT-IR) spectrometry was developed in order to overcome the limitations encountered with dispersive instruments, such as slow scanning process and measuring all of the infrared frequencies simultaneously, Which were overcome by developing optical device called an interferometer. The interferometer produces a signal which has all of the infrared frequencies “encoded” into it. The signal can be measured very quickly.

Interferometers produces interfering signal which is the combination of two beam signal which is called interferogram. But an analyst requires a frequency spectrum to make identification. Interferogram signal cannot be interpreted directly so decoding of the individual frequencies is required. This can be done by a technique called the Fourier transformation. This transformation is performed by the computer which then presents the user with the desired spectral information for analysis [17].

FTIR spectroscopy has been classified into two major areas: non-reflection techniques and reflection techniques. Attenuated Total Reflectance (ATR) spectroscopy is an internal reflection technique used in combination with FTIR. ATR spectroscopy is often considered as a technique to study the surface of different materials, such as thin films or opaque solids. The ATR technique requires an internal reflection element (IRE), such as the ATR crystal. The sample,

which has lower refractive index, is in contact with the crystal. Thus an absorbing medium is in contact with a reflecting one. An incident beam enters the ATR crystal from one of the side faces and is totally reflected at the interface with the sample. The sample is able to absorb light in accordance with its spectrum through the penetration of an evanescent wave up to few microns and reflected back into the crystal. Some energy is removed from the reflected beam; it's called Attenuated Total Reflectance (ATR). The decrease in the reflected beam intensity results in an absorption spectrum. This spectrum can then be interpreted in terms of the physical and chemical structure and properties of the materials.

The normal instrumental process is as follows:

1. **The Source:** Infrared energy is emitted from a glowing black-body source. This beam passes through an aperture which controls the amount of energy presented to the sample.
2. **The Interferometer:** The beam enters the interferometer where the “spectral encoding” takes place. The resulting interferogram signal then exits the interferometer.
3. **The Sample:** The beam enters the sample compartment where it is transmitted through or reflected off of the surface of the sample, depending on the type of analysis being accomplished. This is where specific frequencies of energy are absorbed.
4. **The Detector:** The beam finally passes to the detector for final measurement. The detectors are designed to measure the special interferogram signal.
5. **The Computer:** The measured signal is digitized and sent to the computer where the Fourier transformation takes place. The final infrared spectrum is then presented to the user for interpretation and any further manipulation.

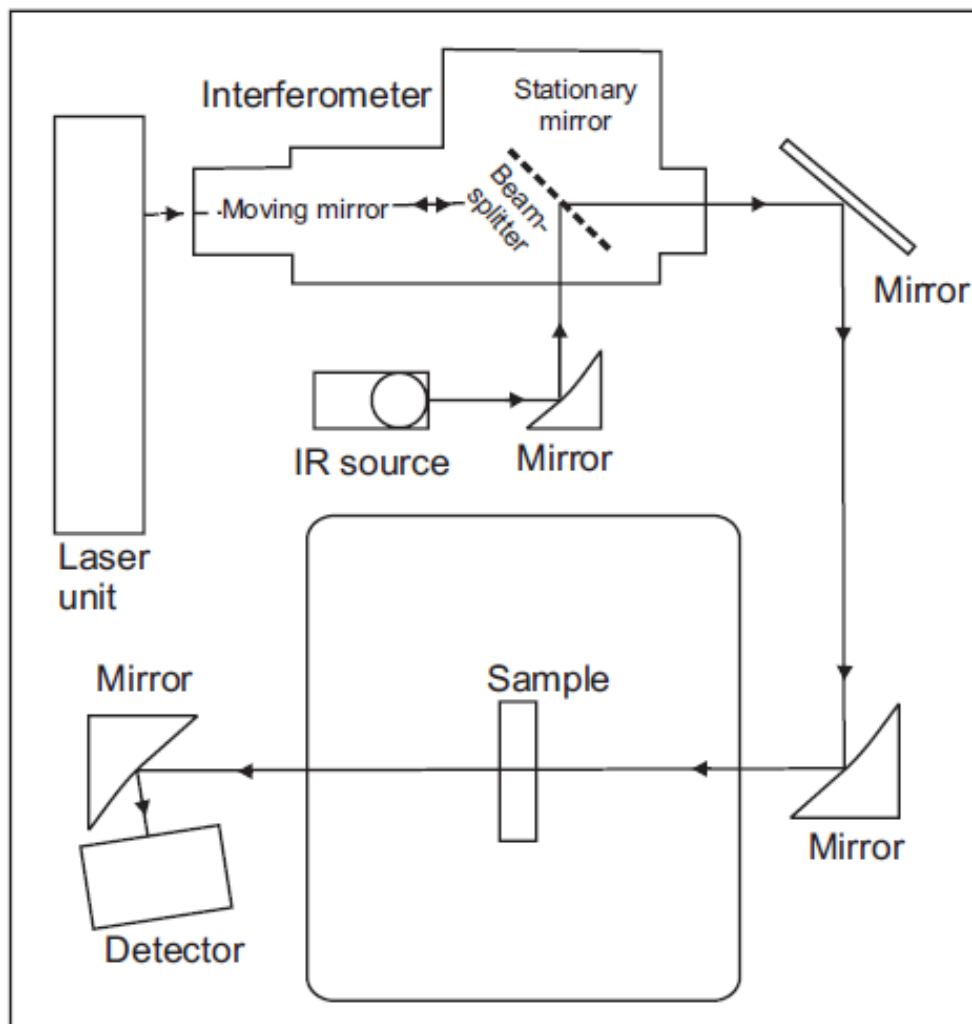


Figure 2.1 Schematic Diagram of an Infrared Spectrophotometer

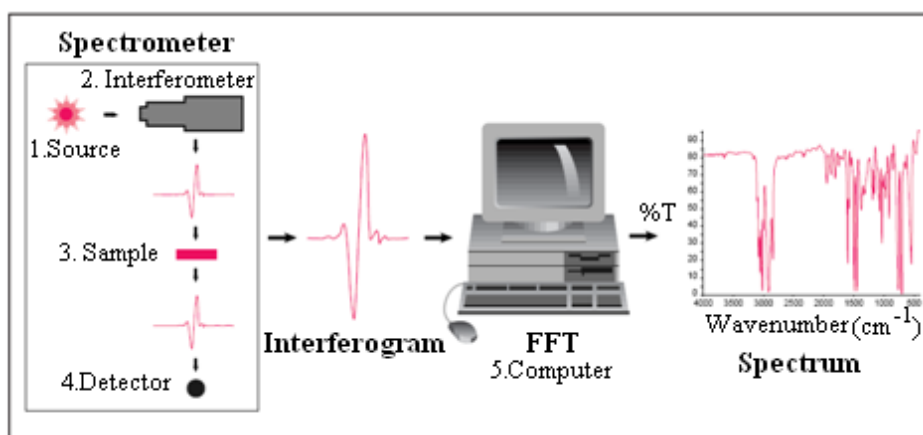


Figure 2.2 Analysis of IR spectroscopy data

Because there needs to be a relative scale for the absorption intensity, a background spectrum must also be measured. This is normally a measurement with no sample in the beam. This can be compared to the measurement with the sample in the beam to determine the “percent transmittance.” This technique results in a spectrum which has all of the instrumental characteristics removed and all spectral features which are present are strictly due to the sample.

The detectors employed are much more sensitive and the optical throughput is much higher. The sensitivity benefits enable identification of even the smallest of contaminants. These advantages, along with several others, make measurements made by FTIR extremely accurate and reproducible. Thus, it is a very reliable technique for positive identification of any sample. Thus, the Fourier Transform Infrared (FT-IR) technique has brought significant practical advantages to infrared spectroscopy.

#### 2.4.2. UV-Vis Spectroscopy

**Ultraviolet–visible spectroscopy** or **ultraviolet-visible spectrophotometry** (**UV-Vis** or **UV/Vis**) refers to absorption spectroscopy or reflectance spectroscopy in the ultraviolet-visible spectral region. Ultraviolet and visible spectrophotometry is the most preferable in laboratories. It concerned with the identification and measurement of organic and inorganic compounds. UV-Visible spectrometry used for its simplicity, versatility, speed, accuracy and cost-effectiveness.

#### **The Origin of the Absorption**

Valence electrons can generally be found in one of three types of electron orbital:

1. Single bond ( $\sigma$  bonding orbitals)
2. Double or triple bonds ( $\pi$  bonding orbitals)

### 3. Non-bonding orbitals (lone pair electrons)

Sigma bonding orbital tend to be lower in energy than  $\pi$  bonding orbital, which in turn are lower in energy than non-bonding orbital. When electromagnetic radiation of the correct frequency is absorbed, a transition occurs from one of these orbitals to an empty orbital, usually an anti-bonding orbital like  $\sigma^*$  or  $\pi^*$  (**Figure 2.3**).

1. The exact energy differences between the orbital depend on the atoms present and the nature of the bonding system. Most of the transitions from bonding orbital involve only  $\pi \rightarrow \pi^*$ ,  $n \rightarrow \sigma^*$  and  $n \rightarrow \pi^*$  transitions [18].

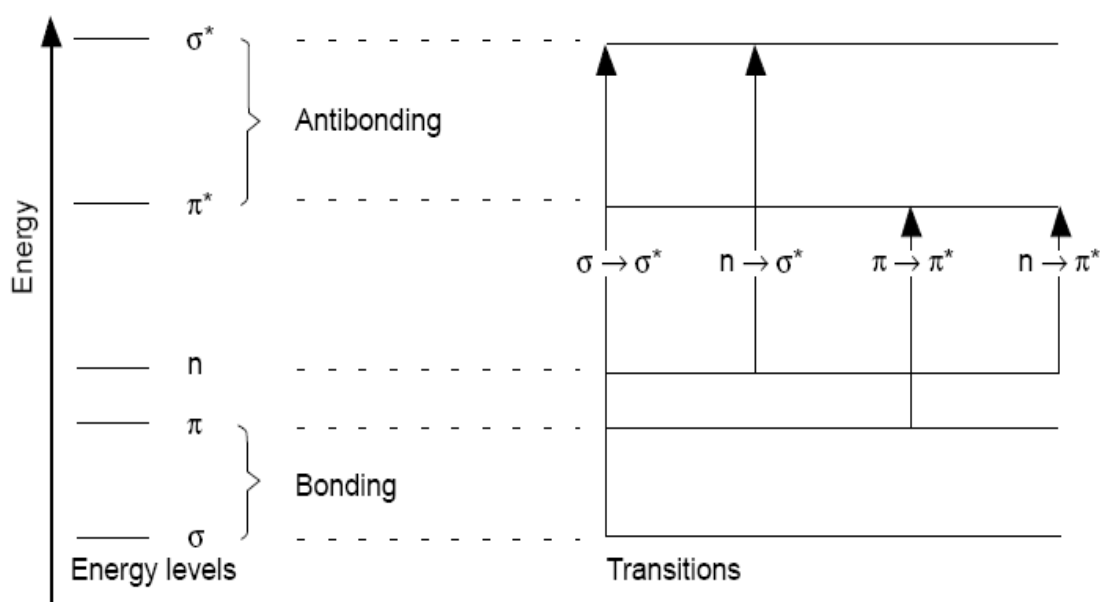


**Figure 2.3** Different molecular orbital transitions

### Instrumentation

The minimum requirements of an instrument to study absorption spectra (spectrophotometer) are shown in **Figure 2.4**.

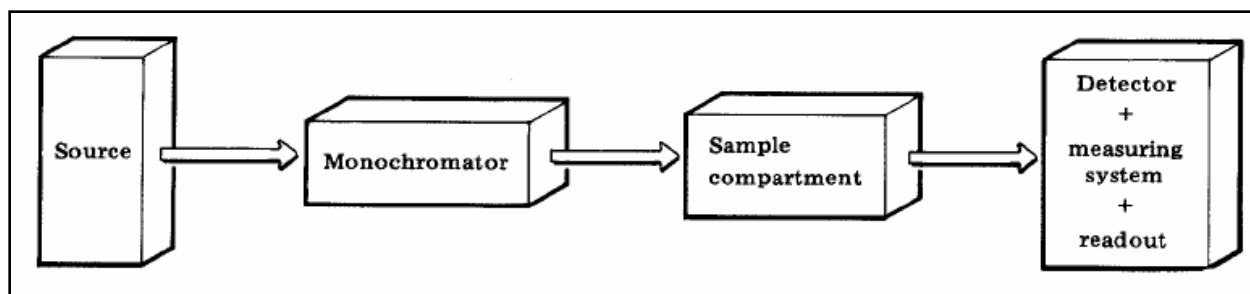


**Figure 2.4** Essential elements of UV-Vis Spectrophotometer

1. A source of radiation of appropriate wavelengths.
2. A means of isolating light of a single wavelength and getting it to the sample compartment - monochromator and optical geometry.
3. A means of introducing the test sample into the light beam - sample handling.
4. A means of detecting and measuring the light intensity.

### **Source**

Source should be stable during the measurement period, i.e. that the intensity of emitted radiation should not fluctuate, and that there should be enough intensity over large wavelength region. No single lamp provides radiation across the whole of the range required, so two are used. Ultraviolet light is generally derived from a deuterium arc that provides emission of high intensity and visible light is normally supplied by a tungsten lamp or tungsten-halogen lamp. Recently, xenon lamp sources have been introduced, and these cover the UV and visible range.

### **Monochromator**

The function of a monochromator is to produce a beam of monochromatic (single wavelength) radiation that can be selected from a wide range of wavelengths. The radiation is separated according to its frequency/wavelength by a monochromator followed by a narrow slit. The slit

ensures that the radiation is of a very narrow waveband i.e. it is monochromatic. Two basic methods of wavelength selection may be noted, filters and a dispersing system (e.g. a prism or diffraction grating).

### **Detectors**

Detection of the radiation passing through the sample or reference cell can be achieved by detectors. The four principal types of detectors found in spectrophotometers are the photoconductive cell, the photomultiplier, the silicon diode and the diode array. A photomultiplier or a photodiode converts photons of radiation into tiny electrical currents and a semiconducting cell emits electrons when radiation is incident on it.

### **Measuring Systems**

A spectrophotometer ends with the provision of a signal (normally an electrical voltage) that is proportional to the absorption by a sample at a given wavelength. The signal handling and measuring systems can be as simple as an amplifier and a meter or as elaborate as a personal computer and printer, depending on the application.

Traditionally, the preferred technique was double-beam geometry in the sample handling area (**Figure 2.5**). Double-beam operation is achieved by a time-sharing system in which the light path is directed (by rotating sectional mirror or similar device) alternately through the sample and the reference cell. Modern instruments are self-calibrating, though the accuracy of the calibration can be checked if necessary. Wavelength checks are made by passing the sample beam through glass samples (containing holmium oxide) that have precise absorption peaks, and the absorption is calibrated by passing the sample beam through either a series of filters, each with a specific and known absorption, or a series of standard solutions.

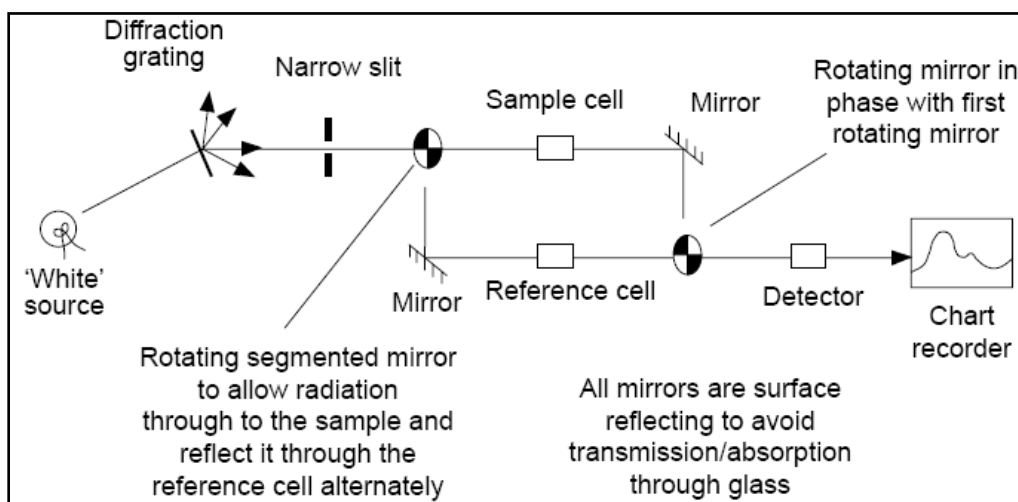


**Figure 2.5 Schematic Diagram of UV-Vis Spectrophotometer**

### Beer-Lambert law

The method is most often used in a quantitative way to determine concentrations of an absorbing species, using the Beer-Lambert law [19]:

$$A = \log_{10}(I_0/I) = \epsilon \cdot c \cdot L$$

where  $A$  is the measured absorbance,  $I_0$  is the intensity of the incident light at a given wavelength,  $I$  is the transmitted intensity,  $L$  the path length through the sample, and  $c$  the concentration of the absorbing species. For each species and wavelength,  $\epsilon$  is a constant known as the molar absorptivity or extinction coefficient. In the range of wavelengths where a sharp increase of absorption appears in the substance, the Tauc relation for dependence of absorbance on wavelength or light photon energy applies [20].

The absorption ( $A$ ) and transmission ( $T$ ) of samples were carried out by UV-Vis spectrometer.

The absorption coefficient was determined from the UV-Vis spectra using the formula:

$$\alpha = A/d \quad \dots (2)$$

Where  $A$  is the absorbance and  $d$  is the thickness of the film. When a band gap exists, the absorption coefficient has the following dependence on the energy of the incident photon [21, 22].

$$\alpha h\nu = B(h\nu - E_g)^x \quad \dots (3)$$

Where  $\alpha$  is the absorption coefficient of the substance,  $E_g$  is the substance optical gap,  $h$  is plank's constant,  $\nu$  is a corresponding frequency  $x$  is the parameter that gives the type of electron transition and factor  $B$  depends on the transition probability and can be assumed to be constant within the optical frequency range [23]. The band gap ( $E_g$ ) depends on many parameters, e.g. on crystalline materials, on their anisotropy, temperature, pressure, on effect of external electric and magnetic forces [24]. As explained Tauc [25], approximate absorption edges and optical activation energies can be calculated from the absorption spectra using equation (3).

The study of optical absorption gives information about the band structure of solids. Insulators/semiconductors are generally classified into two types: (1) direct band gap and (2) indirect band gap. In direct band gap semiconductors, the top of the valence band and the bottom of the conduction band both lie at the same position, zero crystal momentum (wave vector). If the bottom of the conduction band does not correspond to zero crystal momentum, then it is called an indirect band gap semiconductor. In indirect band gap materials, transition from valence to conduction band should always be associated with absorption of a phonon of the right magnitude of crystal momentum [26].

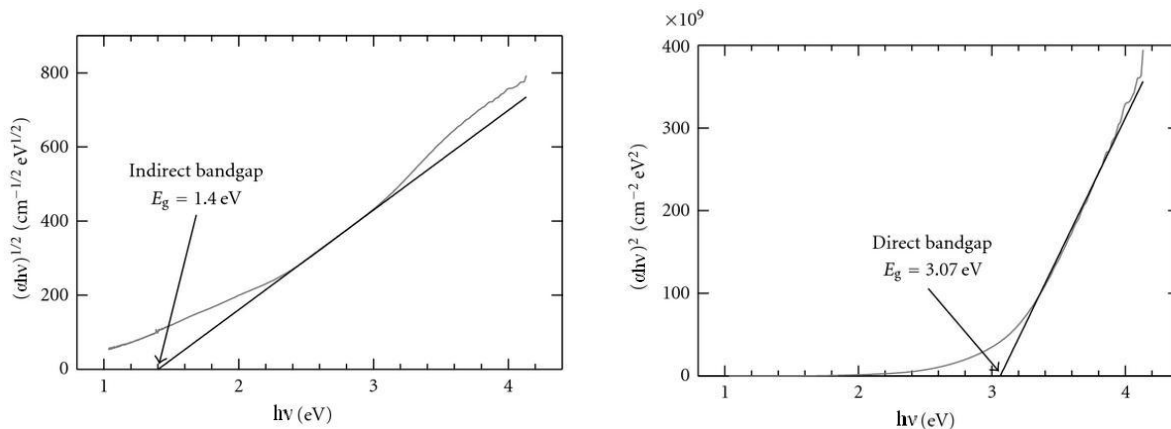


**Figure 2.6** Tauc's plot of Indirect and Direct energy band gap

Optical absorption studies on pure and doped films were carried out to determine the optical constants such as optical band gap ( $E_g$ ) and the position of the fundamental band edge. According to Shahada *et al* [27], it was observed that two distinct linear relations were found, corresponding to different inter band absorption processes. The lower energy range of  $x = 2$  is typical of an indirect allowed transition. The indirect optical energy gap can be obtained from the plot of  $(\alpha h\nu)^{1/2}$  versus  $h\nu$ , while the direct energy gap,  $x = 1/2$ , can be obtained from the plot of  $(\alpha h\nu)^2$  versus  $h\nu$ , is believed to be appropriate for the higher energy absorption (use equation 3). The intercept on the energy axis on extrapolating the linear portion of the curves to zero absorption value may be interpreted as the value of the band gap as shown in **Figure 2.6**.

### 2.4.3. RAMAN Spectroscopy

#### Introduction

Raman spectroscopy is a spectroscopic technique based on inelastic scattering of monochromatic light. Raman spectroscopy [28-33] provides the ability to study the interactions of the vibrational and rotational energies of atoms or groups of atoms within molecules. The excitation energy causes a change in the induced dipole moment, or polarisability, of the molecule. Laser sources and the excitation wavelengths for Raman spectroscopy may range from the ultraviolet (UV) to

the near infrared (NIR) and the resultant spectral pattern is interpreted similarly to the infrared spectrum of the molecule. Inelastic scattering means that the frequency of photons in monochromatic light changes upon interaction with a sample. Photons of the laser light are absorbed by the sample and then reemitted. Frequency of the reemitted photons is shifted up or down in comparison with original monochromatic frequency, which is called the Raman effect. This shift provides information about vibrational, rotational and other low frequency transitions in molecules. Raman spectra result from vibrational motions that cause a change in a source-induced molecular dipole moment. Raman spectroscopy can be used to study solid, liquid and gaseous samples.

The Raman effect is based on molecular deformations in electric field  $E$  determined by molecular polarizability,  $\alpha$ . The laser beam can be considered as an oscillating electromagnetic wave with electrical vector  $E$ . Upon interaction with the sample it induces electric dipole moment  $P = \alpha E$  which deforms molecules. Because of periodical deformation, molecules start vibrating with characteristic frequency  $\nu_m$ . When the polarization in the molecules couples to a vibrational state that is higher in energy than the state they started in, then the original photon and the scattered photon differ in energy by the amount required to vibrationally excite the molecule. The Raman effect corresponds to the absorption and subsequent emission of a photon via an intermediate quantum state of a material.

Amplitude of vibration is called a nuclear displacement. In other words, monochromatic laser light with frequency  $\nu_0$  excites molecules and transforms them into oscillating dipoles. Such oscillating dipoles emit light of three different frequencies (**Figure 2.7**):

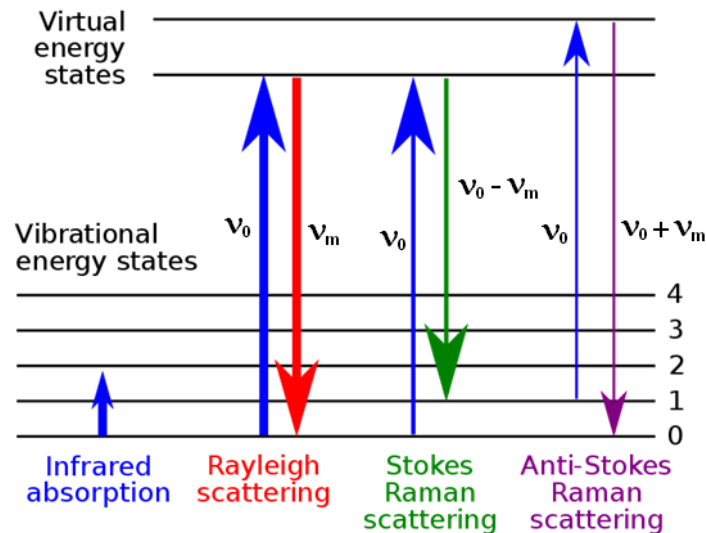


**Figure 2.7** Energy level diagram of the states involved in Raman signal.

1. A molecule with no Raman-active modes absorbs a photon with the frequency  $\nu_0$ . The excited molecule returns back to the same basic vibrational state and emits light with the same frequency  $\nu_0$  as an excitation source. This type of interaction is called an elastic **Rayleigh scattering**.
2. A photon with frequency  $\nu_0$  is absorbed by a Raman-active molecule which at the time of interaction is in the basic vibrational state. Part of the photon's energy is transferred to the Raman-active mode with frequency  $\nu_m$  and the resulting frequency of scattered light is reduced to  $\nu_0 - \nu_m$ . This Raman frequency is called Stokes frequency, or just "**Stokes**".
3. A photon with frequency  $\nu_0$  is absorbed by a Raman-active molecule, which, at the time of interaction, is already in the excited vibrational state. Excessive energy of excited Raman active mode is released, molecule returns to the basic vibrational state and the resulting frequency of scattered light goes up to  $\nu_0 + \nu_m$ . This Raman frequency is called Anti- Stokes frequency, or just "**Anti-Stokes**".

About 99.999% of all incident photons in spontaneous Raman undergo elastic Rayleigh scattering. This type of signal is useless for practical purposes of molecular characterization. Only about 0.001% of the incident light produces inelastic Raman signal with frequencies  $\nu_0 \pm \nu_m$ . Spontaneous Raman scattering is very weak and special measures should be taken to distinguish it from the predominant Rayleigh scattering. Instruments such as notch filters, tunable filters, laser stop apertures, double and triple spectrometric systems are used to reduce Rayleigh scattering and obtain high-quality Raman spectra.

### **Instrumentation**

A Raman system typically consists of four major components (**Figure 2.8**):

1. Excitation source (Laser).
2. Sample illumination system and light collection optics.
3. Wavelength selector (Filter or Spectrophotometer).
4. Detector (Photodiode array or CCD).

A sample is normally illuminated with a laser beam in the ultraviolet (UV), visible (Vis) or near infrared (NIR) range. Scattered light is collected with a lens and is sent through interference filter or spectrophotometer to obtain Raman spectrum of a sample. Since spontaneous Raman scattering is very weak the main difficulty of Raman spectroscopy is separating it from the intense Rayleigh scattering. In many cases the problem is resolved by simply cutting off the spectral range close to the laser line. People use commercially available interference (notch) filters which cut-off spectral range of the laser line. This method is efficient in stray light elimination but it does not allow detection of low-frequency Raman modes in the range below  $100 \text{ cm}^{-1}$ .

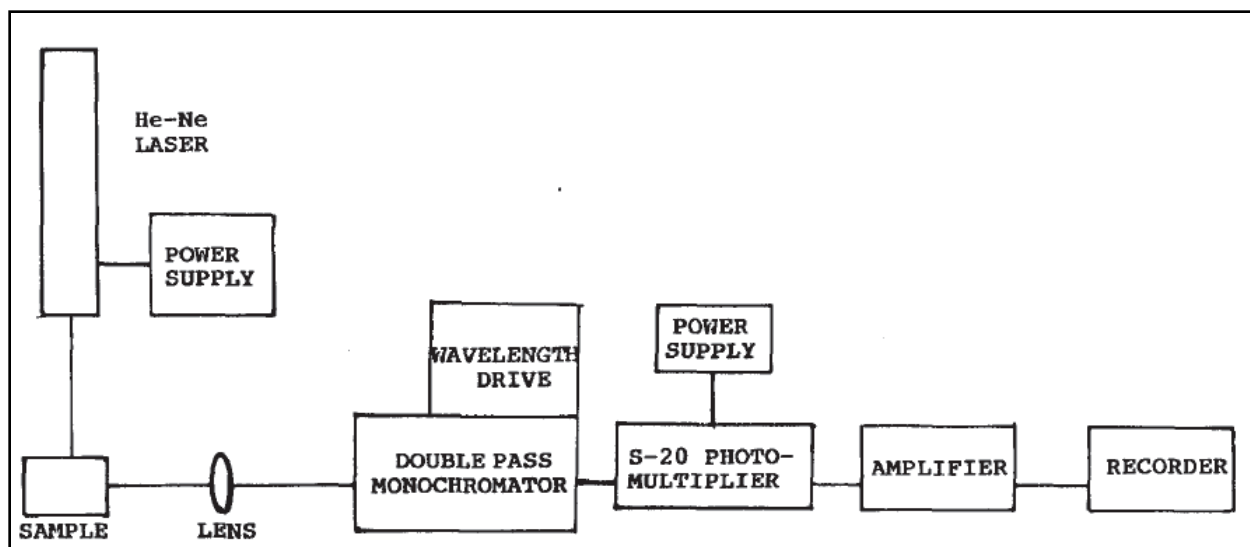


**Figure 2.8** Scheme of Raman Spectrometer

Stray light is generated in the spectrometer mainly upon light dispersion on gratings and strongly depends on grating quality. Raman spectrometers typically use holographic gratings which normally have much less manufacturing defects in their structure than the ruled one. In such systems Raman-active modes with frequencies as low as  $3\text{-}5\text{ cm}^{-1}$  can be efficiently detected. Nowadays, more and more often researchers use multi-channel detectors like Photodiode Arrays (PDA) or a Charge-Coupled Devices (CCD) to detect the Raman scattered light. In many cases CCD is becoming the detector of choice for Raman spectroscopy.

### Ways to improve Raman signal intensity

Raman signal is normally quite weak and people are constantly improving Raman spectroscopy techniques. Many different ways of sample preparation, sample illumination or scattered light detection were invented to enhance intensity of Raman signal. Some of techniques are shown below.

Stimulated Raman (SR)

Coherent Anti-Stokes Raman (CARS)

Resonance Raman (RR)

Surface-Enhanced Raman Spectroscopy (SERS)

Surface-Enhanced Resonance Raman Spectroscopy (SERRS)

#### 2.4.4. Mechanical Testing Facility

The LR30K advanced materials testing machine incorporates an extensive range of features making it ideal for performing complex as well as routine testing applications up to 30 kN.

Lloyd LR30K is a versatile instrument can be used for many types of tests. Possible tests are given below:

1. Load-elongation from zero loads to breaking load
2. Percentage elongation above and below the yield point.
3. Tearing test
4. Compression test
5. Adhesion test etc.

Lloyd Testing machine has the following basic components

- Load frame – It is usually consisting of two strong supports for the machine.
- Load cell - A force transducer or other means of measuring the load is required.
- Cross head - A movable cross head is controlled to move up or down. Usually this is a constant rate of extension. Machines can program the crosshead speed.
- Means of measuring extension or deformation- It is a measure of the response of the test specimen to the movement of the cross head.

- Output device - A means of providing the test result is needed. Machine has a computer interface for analysis and printing.

The specimen is placed in the machine between the grips. It can automatically record the change in gauge length during the test. Tensile properties indicate how the material will react to forces being applied in tension. A tensile test is a fundamental mechanical test where a carefully prepared specimen is loaded in a very controlled manner while measuring the applied load and the elongation of the specimen over some distance. Tensile tests are used to determine the modulus of elasticity, elastic limit, elongation, proportional limit, and reduction in area, tensile strength, yield point, yield strength and other tensile properties. The main product of a tensile test is a load versus elongation curve which is then converted into a stress versus strain curve. A typical engineering stress-strain curve is shown below **Figure 2.9**[34].

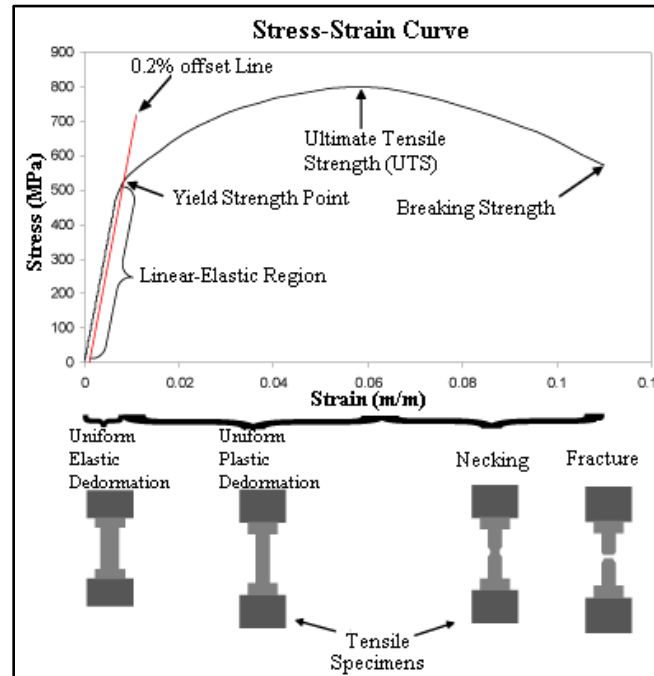


**Figure 2.9** A typical stress versus strain curve

The machine itself can record the displacement between its cross heads on which the specimen is held and it gives stress versus strain curve (**Figure 2.9**). And software automatically derived different mechanical properties from that data.

### **Linear-Elastic Region**

As shown in the curve, the stress and strain initially increase with a linear relationship. This is the linear-elastic portion of the curve and it indicates that no plastic deformation has occurred. In this region of the curve, when the stress is reduced, the material will return to its original shape. In this linear region, the line obeys the relationship defined as *Hooke's Law* where the ratio of stress to strain is a constant. The slope of the line in this region where stress is proportional to strain is constant and is called the *Young's modulus*. *Elastic limit* is the greatest stress, the material can withstand without any measurable permanent strain remaining on the complete release of load.

### **Yield Point**

At some point, the stress-strain curve deviates from the straight-line relationship. From this point on in the tensile test, some permanent deformation occurs in the specimen and the material is said to react plastically to any further increase in load or stress. The material will not return to its original condition when the load is removed. To determine the yield strength using this offset, the point is found on the strain axis (x-axis) of 0.002, and then a line parallel to the stress-strain line is drawn. This line will intersect the stress-strain line slightly after it begins to curve, and that intersection is defined as the yield strength with a 0.2% offset. Knowledge of the yield point is very crucial when designing a material as it generally represents an upper limit of the load that can be applied to material.

## Ultimate Tensile Strength

The ultimate tensile strength (UTS) is the maximum engineering stress level reached in a tension test. The strength of a material is its ability to withstand external forces without breaking.

## Breaking load

Load at which specimen breaks is called breaking load. It is expressed in grams weight.

### 2.4.5. Differential Scanning Calorimeter (DSC)

Differential Scanning Calorimetry (DSC) is a technique in which the heat flow rate difference into a substance and a reference is measured as a function of temperature while the substance and reference are subjected to a controlled temperature program. DSC uses the temperature difference developed between the sample, and a reference for calculation of the heat flow. An exotherm indicates heat flowing out of the sample, while an endotherm indicates heat flowing in.

Two types of DSC systems are commonly in use:

#### Power-compensation DSC:

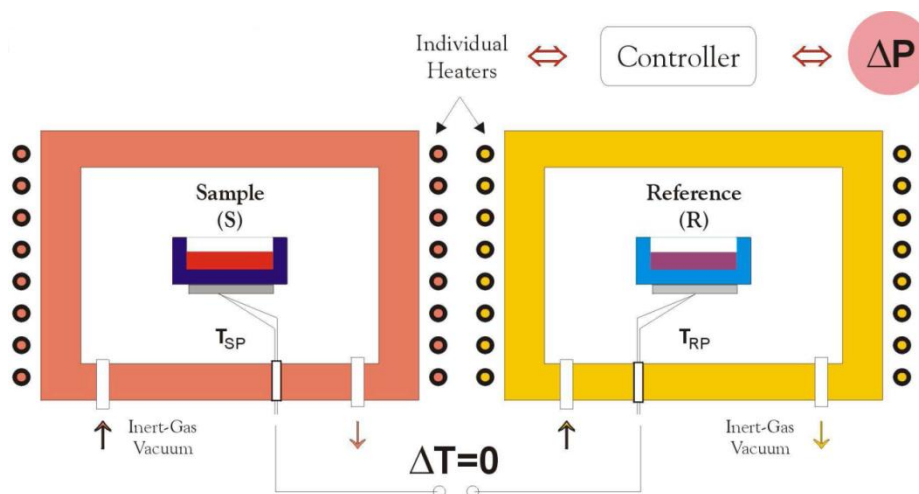
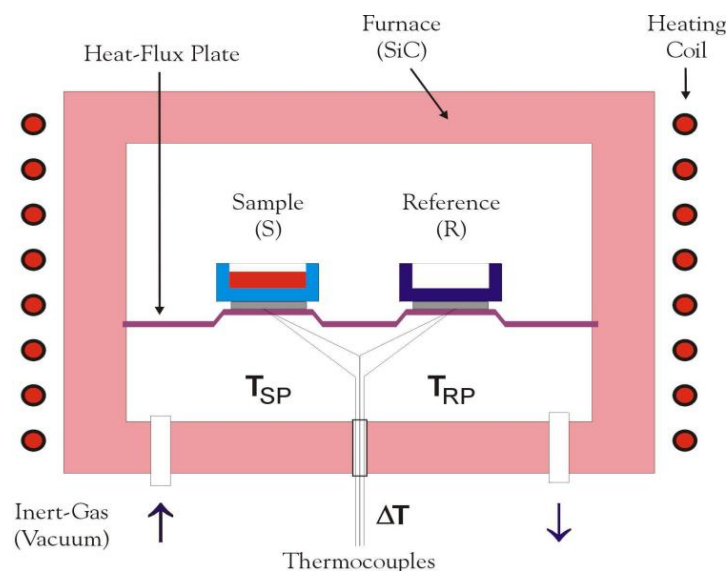


Figure 2.10 Cross section of Power-compensation DSC

In power compensation DSC (**Figure 2.10**), the specimen and reference temperatures are controlled independently using separate furnaces. The temperature difference between the sample and reference is maintained to zero by varying the power input to the two furnaces. This energy is then a measure of the enthalpy or heat capacity changes in the test specimen S relative to the reference R.

### Heat-flux DSC:

In Heat flux DSC (**Figure 2.11**), the test specimen S and reference material R (usually an empty sample pan + lid) are enclosed in the same furnace together with a metallic block with high thermal conductivity that ensures a good heat-flow path between S and R. The enthalpy or heat capacity changes in the specimen S lead to temperature differences relative to R. This results in a certain heat-flow between S and R. The temperature difference  $\Delta T$  between S and R is recorded and further related to the enthalpy change in the specimen using calibration experiments.



**Figure 2.11** Cross section of main components of a typical heat-flux DSC cell.

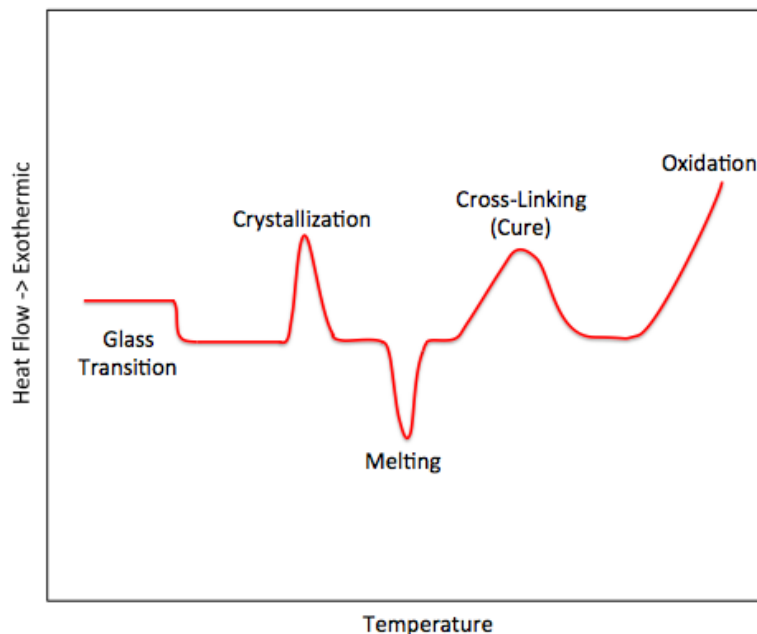


**Figure 2.12** A typical DSC curve for polymer

Measuring principle of DSC is to compare the rate of heat flow to the sample and to reference which are heated or cooled at the same rate. Changes in the sample that is associated with absorption or evolution of heat cause a change in the differential heat flow which is then recorded as a peak. The area under the peak is directly proportional to the enthalpic change and its direction indicates whether the thermal event is endothermic or exothermic. The plot heat flow versus temperature (**Figure 2.12**) gives information about glass transition temperature, crystallization, melting temperature, cross-linking and oxidation process of the materials. Glass transition temperature, crystallization and melting temperature are described as below.

### **Glass Transition Temperature:**

When we heat the polymer, after certain temperature, behavior of the graph changed suddenly pointing downward, which indicates endothermic reaction taken place. The glass transition ( $T_g$ ) is the temperature assigned to a region above which materials are fluid or rubbery and below which they are immobile and rigid [35].

**Crystallization Temperature:**

When we heated above  $T_g$ , at a particular temperature Polymer will have gained enough energy to move into order arrangement called crystalline state. When polymers fall into this state they gives of energy, so we get a peak in DSC heat flow versus temperature plot. *Crystallization* is a process in which polymer from the amorphous state is transformed into the crystalline state from either solution or the melt and at which temperature crystallization occurs is called polymer crystallization temperature  $T_c$  [36].

**Melting Temperature:**

If polymer further heated after  $T_c$ , It will reach another thermal transition, called melting. It is the transition from the crystalline state to the melt. Melting is a transition with an increase of disorder of the system. When polymer reached melting temperature  $T_m$ , polymer chains come out of their order arrangement and become free to move around [37].

**2.4.6. Thermal Gravimetric Analysis (TGA)**

Thermo-gravimetric analysis (TGA) or thermo-gravimetry (TG) is a technique where the mass of a polymer is measured as a function of temperature or time while the sample is subjected to a controlled temperature program in a controlled atmosphere [38]. TGA gives weight loss curve with respect to different temperature.

The basic instrumental requirements for TGA are a precision balance with a pan loaded with the sample, and a programmable furnace. The furnace can be programmed either for a constant heating rate, or for heating to acquire a constant mass loss with time. Sample is heated under the different gas environment. Basically nitrogen gas is used in TGA.

## TGA Instrumentation

The essential components of the TGA instrument, are an analytical microbalance, furnace, temperature programmer, sample holder, an enclosure for establishing the required atmosphere, and a means of recording and displaying the data. Typical arrangements of the components for TGA are shown in the **Figure 2.13**.

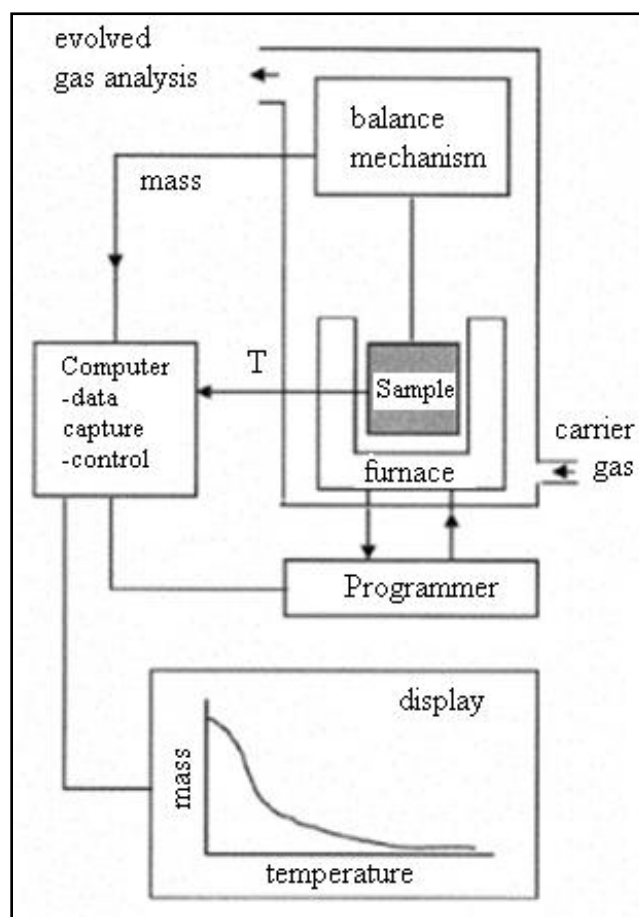


**Figure 2.13** Scheme of Thermal gravimetric analysis

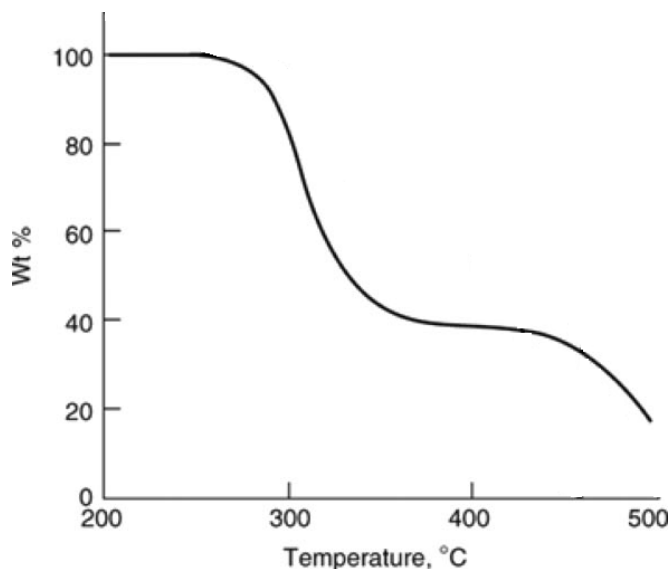


**Figure 2.14** A typical thermal degradation TGA curve

There are three ways in which a polymer degrades: random scission, systematic chain scission or the combination of two. Random scission along the chain produces radicals or other reactive species. These reactive species continue to break down into progressively smaller species, which become volatile and are lost or they may attack other polymer chains leading to cross-linked polymers, which are less prone to degradation and ultimately lead to high temperature residue referred to as a char [39]. A generalized degradation plot of polymer is shown in the **Figure 2.14**.

TGA measurements record only the loss of volatile fragments of polymers, caused by decomposition. TGA cannot detect any chemical changes or degradation of properties caused by cross-linking. In TGA measurement one should take care of materials, sample weight and heating rate.

TGA is commonly used to determine characteristics of materials that exhibit either mass loss or gain due to decomposition, oxidation, or loss of volatiles (such as moisture). Common applications of TGA are (1) materials characterization through analysis of characteristic decomposition patterns, (2) studies of degradation mechanisms and reaction kinetics, (3)

determination of organic content in a sample, and (4) determination of inorganic (e.g. ash) content in a sample, which may be useful for corroborating predicted material structures or simply used as a chemical analysis.[Wikipedia]

#### 2.4.7. Scanning Electron Microscopy (SEM)

Microscopy is the study of the fine structure and morphology of objects with the use of microscope [40, 41]. Microscopes range from optical microscopes to transmission electron microscopes, which resolve details on micrometer level to nanometer level. In microscopy resolution and contrast are key parameter.

The scanning electron microscope (SEM) is capable of producing high resolution image of sample surface. SEM images have a three dimensional appearance and are useful for judging the surface structure of sample. SEM forms an image by scanning a probe, a focused electron beam, across the specimen [42].

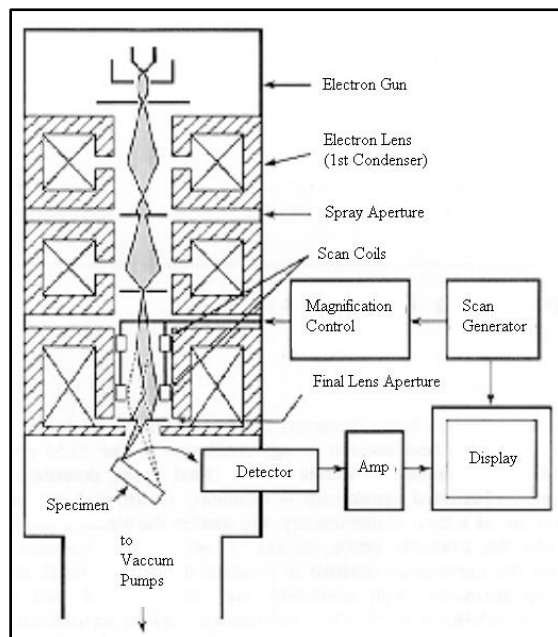


Figure 2.15 Cross section and lab image of Scanning electron microscope

The SEM consists of electron column which containing the lens system, a specimen chamber, detectors as well as imaging and recording units as shown in **Figure 2.15**. Different parts of SEM are described below:

**Electron gun:** located at the top of the column where free electrons are generated by emission from a tungsten filament.

**Condenser lenses:** after electron beam passes the anode two condenser lenses converges the beam and make pass through a focal point.

**Apertures:** the function of apertures is to reduce and exclude extra electrons in the lenses and also to determine the spot size of beam at specimen which is very important to determine resolution and depth of field [43, 44].

**Scanning system:** images are formed by scanning the electron beam across the specimen using deflection coils inside the objective lens [44].

**Specimen chamber:** at the end, the specimen stage and controls are located. The secondary electrons from the specimen are attracted to detectors by positive charge.

Modern SEM mostly uses a PC to control the electron beam, to select the signals and to record and store the digital images [45]. Microscope column and the specimen chamber are evacuated using high vacuum pumps at a pressure of at least  $5 \times 10^{-5}$  Torr, which is necessary to allowing the beam electrons to travel from the cathode to the specimen with little interaction with the residual gas molecules.

**Sample Preparation:** As SEM utilizes vacuum conditions, special preparation must be done to the sample. All metal are conductive and require no preparation before being used. While non-metal

samples are non conductive so they needs to be made conductive by covering the samples with a thin layer of conductive material. This is done by a using a device called “sputter coater”.

Now when electrons are coming from source, they can be controlled by field emission. The probe size is reduced by demagnification of the filament image using two electromagnetic lenses and then focusing onto the specimen surface by using an objective lens. The probe is scanned on the specimen surface by two set of scanning coils, controlled by the same scan generator used to observe the image. The signal is detected by a low noise scintillation-photomultiplier-amplifier system and modulates the display signal. Once the probe is focused and corrected for astigmatism, the magnification can be changed by changing the size of the scanned area without refocusing [46].

## **2.5. Experiment specification detail**

### **2.5.1. Fourier Transform Infrared Spectroscopy**

The FTIR spectra of all polymer blend samples have been recorded on a JASCO- FTIR-4100 Spectrometer, between  $4000\text{ cm}^{-1}$  and  $600\text{ cm}^{-1}$  in the ATR mode.

### **2.5.2. UV-Vis Spectroscopy**

The absorption spectra and transmission spectra of samples were taken in the range of 200-800 nm using Perkin-Elmer Lambda 25 UV-VIS spectrophotometer.

### **2.5.3. FT-RAMAN Spectroscopy**

Fourier Transform Raman spectra of pure and blend polymers were obtained with a Bruker RAM II Vertex-70 FTIR spectrometer equipped with FRA106 Raman module. Spectral resolution was  $4\text{ cm}^{-1}$ . The samples were excited with  $\lambda = 1064\text{ nm}$  by diode laser pumped Nd:YAG solid state laser with maximum output power 150 mW.

#### 2.5.4. Mechanical Analysis

Mechanical properties of all polymer blend samples of PVC/PMMA have been reported in this study. These measurements were made on Lloyds LR30 K instrument with a crosshead speed of 10 mm/min and a gauge length of 10 mm. The measurements were repeated for five times and their mean value is reported here. All testing were carried out at room temperature. Pores or nicks free samples were used for measurements. Access to this instrument was available at Textile Engineering Department, Faculty of Technology and Engineering, The M. S. University of Baroda, Vadodara, for this work.

#### 2.5.5. Differential Scanning Calorimeter

For the DSC measurements SII Exstar-6000, operating in dynamic mode (heating rate=10 °C/min) in N<sub>2</sub> gas environment, was employed. Samples in appropriate amount were placed in sealed aluminum pans. Prior to use the calorimeter was calibrated with metal standards; an empty aluminum pan being used as a reference.

#### 2.5.6. Thermal Gravimetric Analysis

Thermo-gravimetric (TG) and DTG measurements were made on EX STAR TGA instrument with heating rate 10°C/min under nitrogen atmosphere. The samples were taken 5–10 mg in an aluminum pan.

#### 2.5.7. Scanning Electron Microscopy

For present work, Scanning Electron Microscopy Model: JEOL make Scanning Electron Microscope, model number JSM 6380LV at ERDA, Vadodara have been used. The working distance (WD, sample distance from objective lens) is varied from 15 mm to 20 mm as per resolution of the images. The spot size is also varied from 30 to 60 nm. The

accelerating voltage is fixed at 20 kV and filament current is kept nearly 85  $\mu\text{A}$  to 100  $\mu\text{A}$  to conduct morphological analysis. Inside the SEM chamber, the vacuum is created less than  $10^{-7}$  torrs (within 5 minutes) for minimizing impurities and viewing the sharp surfaces of the sample. The magnifications of the images are varied as per the image clarity.

## 2.6. References

1. W. V. Titow. PVC technology. Springer. pp. 6–. ISBN 978-0-85334-249-6, 31<sup>st</sup> December 1984.
2. Chanda, Manas; Roy, Salil K. Plastics technology handbook. CRC Press. pp. 1–6. ISBN 978-0-8493-7039-7, 2006.
3. Joel R. Fried, Polymer Science and Technology, Prentice hall of India Private Limited, New Delhi, 2000.
4. V. R. Govariker, N. V. Viswanathan and Jaydev Sreedher, Polymer Science, New age International (P) Ltd., Publishers Edition 1, 1996.
5. Lopatin VV, Askadskii AA, Peregudov AS, Vasilev VG, J Appl Polym Sci 96:1043–1058, 2005.
6. Durmaz S, Okay O, Polym Bull 46:409–418, 2001.
7. Chan LW, Hao JS, Heng PWS, Chem Pharm Bull 47(10):1412–1416, 1999.
8. Morita, R., R. Honda and Y. Takahashi, Journal of Controlled Release, 90(1): 109-117, 2000.
9. Gutzler R, Smulders M, Lange RFM, Macromol Symp 225:81–93, 2005.
10. Smolinske, Susan C. Handbook of Food, Drug, and Cosmetic Excipients. Boca Raton: CRC Press. p. 287. ISBN 0-8493-3585-X, 1992.
11. B. P. Straughan and S. Walker, editors, Spectroscopy, volume 2, John Wiley and Sons, 1976.
12. A. H. Fawcett, editor, Polymer spectroscopy, John Wiley and Sons, 1996.
13. D. L. Pavia, G. M. Lampman and J. George S. Kriz, "Introduction to Spectroscopy", W.B Saunders Company, p.13, 1979.

14. C. D. Craver and J. Chares E Carraher, "Applied Polymer Science 21st Century", Elsevier, p.709, 2000.
15. P. C. Painter and M. M. Coleman, "Fundamentals of polymer science", Technomic Publishing Company, Inc., p.145, 1997.
16. B. P. Straughan and S. Walker, editors, Spectroscopy, volume 2, John Wiley and Sons, 1976.
17. Nicolet Corporation, Introduction to Fourier Transform Infrared Spectroscopy
18. Fundamentals of Analytical Chemistry 8th Ed., by Douglas A. Skoog, Donald M. West, F. James Holler, Stanley R. Crouch. 2003.
19. [http://en.wikipedia.org/wiki/Ultraviolet%E2%80%93visible\\_spectroscopy](http://en.wikipedia.org/wiki/Ultraviolet%E2%80%93visible_spectroscopy)
20. J. Tauc, R. Grigorovici, A. Vanku, Phys. Stat. Sol. 15, 627, 1966.
21. Davis DS, Shalliday JS, Phys Rev 118:1020, 1960.
22. Thutupalli GM, Tomlin SG, J Phys D Appl Phys 9:1639, 1976.
23. J. Tauc, in Amorphous and Liquid Semiconductors, Springer, Heidelberg, 1974.
24. J.M. Ziman, in Principles of the Theory of Solids, Cambridge University Press, Cambridge, 1979.
25. J. Tauc, R. Grigorovici, A. Vanku, Phys. Stat. Sol. 15, 627, 1966.
26. V. B. Achari, T. J. R. Reddy, A. K. Sharma, V. V. R. N. Rao, Ionics, 13:349–354, 2007.
27. L. Shahada, M. E. Kassem, H. I. Abdelkader, and H. M. Hassan, J. Appl. Polym. Sci. 65, 1653, 1997.
28. J. R. Ferraro and K. Nakamoto, "Introductory Raman Spectroscopy", Academic Press, p.3, 1994.

29. J. G. Grasselli, M. K. Snavely and B. J. Bulkin, "Chemical applications of Raman spectroscopy", Wiley, p.3, 1981.
30. P. Hendra, C. Jones and G. Warnes, "Fourier transform Raman spectroscopy", Ellis Horwood Limited, p.3, 1991.
31. G. Grasselli and B. J. Bulkin, "Analytical Raman spectroscopy", John Wiley & Sons, Inc., p.3, 1991.
32. G. Socrates, "Infrared and Raman characteristic group frequencies : tables and charts", John Wiley & Sons, Inc., p.3, 2001.
33. I. R. Lewis and H. G. M. Edwards, "Handbook of Raman spectroscopy", Marcel Dekker, p.3, 2001.
34. <http://www.ndt-ed.org/EducationResources/CommunityCollege/Materials/Mechanical/Tensile.htm>
35. Paul Gabbott, Principles and Applications of Thermal Analysis, Blackwell Publishing Ltd, 2008
36. Joseph D. Menczel, R. Bruce Prime, Thermal Analysis Of Polymers- Fundamentals and Applications, John Wiley & Sons, 2009
37. Joseph D. Menczel, R. Bruce Prime, Thermal Analysis of Polymers- Fundamentals and Applications, John Wiley & Sons, 2009
38. Earnest, C. M., Compositional Analysis by Thermogravimetry, ASTM STP 997. ASTM International, Philadelphia, 1988.
39. PST 522E – Manual and Program of Synthesis and Characterization of Macromolecules Lecture, Chapter 12, polymer science and technology, Istanbul technical University
40. L. C. Sawyer and D. T. Grubb, Polymer Microscopy, Chapman and Hall, P.16, 1987.

41. M. J. Folkes and P. S. Hope, Polymer blends and alloys, Chapman and Hall, p. 109, 1993.
42. J. Goldstein, D. E. Newbyry, D. C. Joy, C. E. Lyman, P. Echlin, E. Lifshin, L. C. Sawyer and J. R. Michael, Scanning Electron Microscopy and X-ray Microanalysis, 3<sup>rd</sup> ed., Plenum, New York, 2003.
43. M.T. Postek, K. S. Howard, A. H. Johnson and K. L. McMichael, Scanning Electron Microscopy: A student handbook, Ladd Research Ind. Inc. Williston, VT, 1980.
44. I. M. Watt, The principles and Practice of Electron Microscopy, Cambridge Univ. Press., Cambridge, England, 1985.
45. Rudolf Reichelt, science of Microscopy, Vol. I, Eds. P. W. Hawkers, John C. H. spence, Springer Science and Business Media, New York, 2007.
46. L. C. Sawyer, D. T. Grubb and Gregory F. Meyers Polymer Microscopy, 3<sup>rd</sup> ed., Chapman and Hall, 1987.

## Chapter 3

# Characterization of PVC/PMMA Blends

---

### *Abstract*

*This chapter gives an account of the characteristics of PVC/PMMA blend in different weight proportion (70/30, 50/50 and 30/70) which is prepared by solution cast technique. These blends are investigated by spectroscopic techniques like FTIR, UV-Vis and RAMAN. Mechanical, Thermal and Morphological properties are investigated. The results obtained from different characterization techniques show the blending effect of different properties. These properties of PVC/PMMA blends are correlated with spectroscopic investigation.*

### 3.1. Introduction

PVC is one of the most important and widely used thermoplastic polymers because of its well-known performance and properties like low cost, good processability, chemical resistance and low flammability. The modification of polyvinyl chloride (PVC) to obtain different PVC copolymers and blends is of great significance to the plastics industry. The aim for modifying PVC by blending is to manufacture new PVC polymers that combine desired physical properties at low cost. Blending technique has gained a lot of commercial as well as academic importance. In addition to blending, we can also improve stiffness by adding inorganic dopant materials whereas using rubbery phase improves toughness of the polymers.

Polymers and their blends are often processed in the melt, which makes them thermally stable. Several studies show that blending can alter the decomposition of individual polymers [1-4]. PVC has low thermal stability which is its major drawbacks. Several polymers are mixed with PVC as plasticizers or processing aids. PMMA is used as processing aids for PVC [5]. I. C. Mc Neil et. al. [6] studied PVC/PMMA mixtures and showed that methacrylate (MMA) monomer formed at a much lower temperature than that of PMMA depolymerization when heated alone. D. Braun et al [7, 8] studied the thermal degradation of PVC with PMMA have shown that at higher concentrations of PMMA exhibit some stabilization of PVC, while lower concentrations leads to destabilization. Naima Belhaeche- Bensemra et. al. [9] showed that PMMA exerted a stabilizing effect on the thermal degradation of PVC by reducing de-hydro chlorination.

Miscibility and phase behavior of polymer blends is essential for controlling the properties of polymer blends. PVC/ PMMA blends has been studied by different approaches by different workers, it was well described by Chao Zhou et.al.[10], Schurer [11] reported that PVC/ PMMA are miscible only in blends having PVC contents greater than 60%. Rupa Chakrabarti et. al. [12]

studied physical and mechanical properties of PVC/PMMA blend and suggested that a substantial increase in toughness accompanied with unusual increase in modulus and ultimate tensile strength occurred after initial stages of PMMA incorporation compared to pure PVC. Wlochowicz and Janicki [13] concluded that PVC / PMMA blends at all compositions are wholly amorphous two-phase system. Varada [14] investigated the miscibility of PVC with PMMA by ultrasonic and refractive index method. They pointed out that PVC and PMMA are miscible in all compositions. Kamira Aouachria and Naima Belhaneche-Bensemra [15] studied about miscibility of PVC/PMMA blend. Shen and Torkelson [16] observed that PVC/ PMMA blends are miscible at all compositions, if they are prepared between  $T_g$  and their lower critical solution temperature. This discrepancy in the miscibility may be due to the different methods used for sample preparation and polymers used are having different molecular weights.

In the past recent years, the importance of using PVC/PMMA blend polymer electrolytes was used by many researchers. S. Ramesh et.al. [17] studied PVC/PMMA blend based polymer electrolytes and reported about interaction of PVC/PMMA blend with lithium triflate salt, ethylene carbonate (EC), dibutyl phthalate (DBP) plasticizers and also with silica. Vijay V. Soman and Deepali S. Kelkar [18] have suggested about the interaction among Camphor Sulphonic Acid (CSA), PVC, PMMA and PVC/PMMA blend in different weight percentage. PMMA might be expected to counter balance the fall in mechanical properties of PVC is attributed to the disruption in molecular packing of stiff and rigid chains of PVC[18].

The PVC and PMMA blend is a well known system in which hydrogen bonding type of specific interaction involving  $\alpha$ -hydrogen of PVC and the carbonyl group of PMMA is expected [19].

The matrix structure of the blend is different than pure polymers which in turn affects the physical properties of the blend including the mechanical properties. Infrared spectroscopy is a tool to find out the possible interaction between the polymer matrixes. Several researchers have used this technique to study such interactions between polymers [20, 21].

Several research groups have reported the interaction by the study of shift of the peaks, developments of new peaks, changes in shapes like changes in peak intensity, development of shoulders in the existing peaks in the FTIR spectrum [22, 23]. In recent years, studies on optical and electrical characteristics of polymers have fascinated much consideration in their application in optical and electronic devices [24, 25]. Electrical and optical properties of polyvinyl alcohol thin films doped with metal salts have been investigated by Abd et al. [26]. Refractive index is an important optical parameter for the design of prisms, windows and optical fiber [27]. The absorbance process plays an important role in the optical properties of polymers. From the absorption spectra, it is possible to understand variation of molecular formation of polymer structures.

In the present chapter we studied different properties of PVC/PMMA blends in different weight percentage by different characterization techniques. We report evidence from Fourier Transform Infrared (FTIR) Spectroscopy for hydrogen bonding type interaction between  $\alpha$ -hydrogen of PVC and carbonyl group of PMMA which supports earlier studies done by several researchers. We have also studied some optical properties such as absorption coefficient, optical (direct/indirect) energy band gap, Refractive Index, optical dielectric constant and constant B. In addition, Mechanical Properties of Blends, Thermal Characteristics by Thermal Gravimetric Analysis (TGA), and surface morphology by Scanning Electron Microscopy (SEM) are reported.

The effects of different blending weight percentage on these properties have been discussed and behaviors of all properties are investigated.

## 3.2. Results and Discussion

### 3.2.1. FTIR Analysis

Infrared spectroscopy is a tool to find out the possible interaction between the two polymer matrixes. The interaction can be studied by shift of the peaks, developments of new peaks, changes in shapes like changes in peak intensity, development of shoulders in the existing peaks in the FTIR spectrum. Complexation may shift the polymer peak frequencies. FTIR would be sensitive both in situations where complexation has occurred in crystalline or amorphous phase [28]. **Figure 3.1 (a, b)** shows the FTIR spectrum of Pure PVC, Pure PMMA and other polymer Blends. FTIR-ATR spectrum reveals molecular interactions between PVC and PMMA. Different Vibrational modes of Pure PVC, Pure PMMA and their Blends are described in **Table 3.1**. The following characteristic frequencies, C-Cl stretching ( $834\text{ cm}^{-1}$ ), Trans C-H wagging ( $957\text{ cm}^{-1}$ ), C-O stretching ( $1141\text{ cm}^{-1}$ ), C-O-C stretching ( $1190\text{ cm}^{-1}$ ), C-H anti symmetric stretching ( $1481\text{ cm}^{-1}$ ), C=O stretching ( $1723\text{ cm}^{-1}$ ) and -CH stretching ( $2911\text{ cm}^{-1}$ ) shows a shift in the frequency towards the higher frequency side. While the following characteristic frequencies, -CH<sub>2</sub> deformation ( $1331\text{ cm}^{-1}$ ), C-H rocking ( $1236\text{ cm}^{-1}$ ) remains unchanged and the cis C-H wagging ( $613\text{ cm}^{-1}$ ), C-H symmetric stretching ( $1385\text{ cm}^{-1}$ ) and -CH<sub>3</sub> stretching + -CH<sub>2</sub> Symmetric Stretching ( $2951\text{ cm}^{-1}$ ) shows a decrease in trend.

Rupa Chakrabarti et. al. [12] studied physical and mechanical properties of PVC/PMMA blend and suggested, hydrogen bond interaction between C-Cl group of PVC and C=O group of PMMA. So here also peak shifting are observed for C-Cl stretching group ( $834\text{ cm}^{-1}$  to  $844\text{ cm}^{-1}$ ) towards higher wave number side and for C=O stretching group ( $1723\text{ cm}^{-1}$  to  $1732\text{ cm}^{-1}$ )

**Table 3.1** Assignment of different vibrational modes of PVC, PMMA and various Blends.

Vibrational Modes ↓	Peak No.	Pure Sample	Wave number (cm <sup>-1</sup> )				
			90/10	80/20	60/40	40/60	
-CH stretching	1	PVC	2911	2915	2920	2915	2911
-CH <sub>2</sub> deformation	2		1331	1328	1331	1332	1332
C-H rocking	3		1236	1233	1236	1236	1237
Trans C-H wagging	4		957	957	960	962	964
C-Cl stretching	5		834	832	844	841	841
cis C-H wagging	6		613	605	608	616	618
-CH <sub>3</sub> stretching	7	PMMA	2996	3004	2993	2992	2994
-CH <sub>3</sub> stretching + -CH <sub>2</sub> Symmetric Stretching	8		2951	2961	2946	2950	2950
-CH <sub>2</sub> Anti Symmetric Stretching	9		2851	2852	2852	2842	2841
C=O stretching	10		1723	1737	1732	1727	1726
C-H anti symmetric stretching	11		1481	1495	1495	1483	1483
C-H deformation	12		1434	1426	1434	1434	1434
C-H symmetric stretching	13		1385	1371	1371	1384	1385
-CH <sub>2</sub> twist	14		1238	1233	1236	1237	1237
C-O-C stretching	15		1190	1195	1194	1191	1191
C-O stretching	16		1141	1150	1149	1146	1145
C-C stretching	17	985	985	960	986	986	

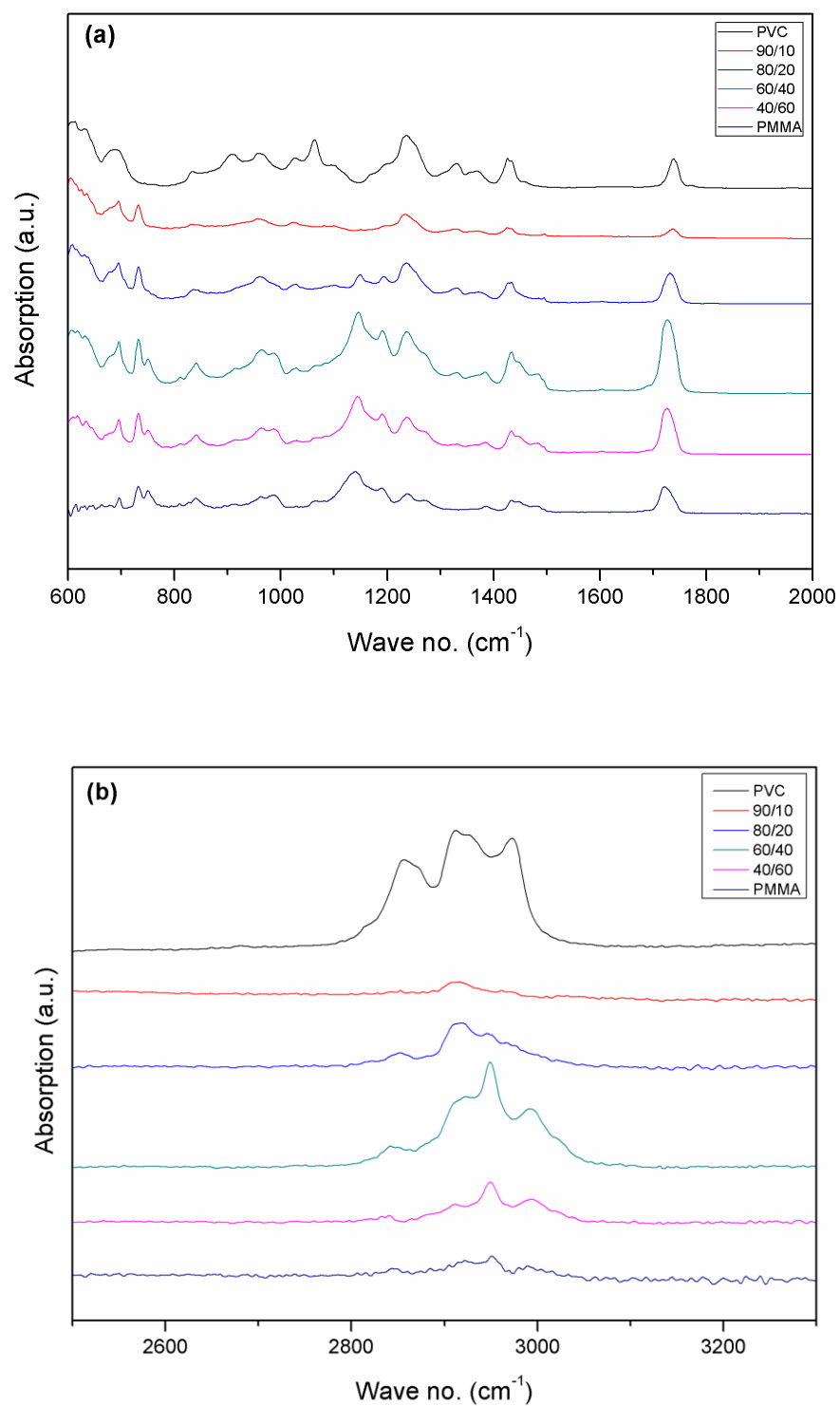


**Figure 3.1** FTIR Spectra of pure PVC, pure PMMA and Their blends (a) in the range 600 – 2000  $\text{cm}^{-1}$  (b) in the range 2500 – 3300  $\text{cm}^{-1}$

towards higher wave number side, which clearly indicate the hydrogen bonding intermolecular interaction between PVC and PMMA polymer chains. These peaks are shifted towards higher wave number side which reveals increase in the strength of the bonds. S. Ramesh [17] has reported the shift in the carbonyl absorption peak to higher wave number side from  $1721\text{ cm}^{-1}$  to  $1732\text{ cm}^{-1}$ . Our results also verify these results.

### 3.2.2. UV-Vis Analysis

The absorbance process plays an important role in the optical properties of polymers. From the absorption spectra, it is possible to understand variation of molecular formation of polymer structures. From the absorption spectra, **(Figure 3.2 (a))**, a sharp increase in absorption below 220 nm, which corresponds to  $\pi\rightarrow\pi^*$  transitions of carbonyl groups in macromolecules is observed [29]. The absorption edges were observed around 250 to 300 nm **(Figure 3.2 (b))**. A shift in band edges toward the higher wavelengths with different absorption intensity for PVC doped PMMA was observed. These shifts indicate the formation of inter/ intra bond between PVC and PMMA. The direct optical energy gap, can be obtained from the plot of  $(\alpha h\nu)^2$  versus  $h\nu$  (photon energy) **(Figure 3.2(c))**, while indirect energy gap obtained from the plot of  $(\alpha h\nu)^{1/2}$  versus  $h\nu$  **(Figure 3.2(d))**, is believed to be appropriate for the higher energy absorption **(Eq. 2)**. The intercept on the energy axis on extrapolating the linear portion of the curves to zero absorption value may be interpreted as the value of the band gap. The various optical properties obtained for different samples are listed in **Table 3.2**. These results are in consistence with FTIR results. Also, the shift in absorption edge reflects the variation in the optical energy band gap. Absorption edge shifted towards higher wavelength side as the PMMA content in PVC increases. It is clear that the indirect optical energy band gap increases with increasing PMMA content. The existence and

variation of optical energy gap may be explained by invoking the occurrence of local cross linking within the amorphous phase of PMMA and PVC.

**Table 3.2** Variation of absorption edge and direct/indirect band gap with different blend percentage

PVC/PMMA blend percentage	Absorption edge ( $\Delta E$ ) (eV)	Direct band gap ( $E_{g(\text{Dir})}$ )	Indirect band gap ( $E_{g(\text{Indir})}$ )
Pure PVC	3.91	4.09	3.65
80/20	4.05	4.21	3.92
60/40	4.11	4.24	4.05
40/60	4.19	4.30	4.15
Pure PMMA	4.42	4.46	4.31

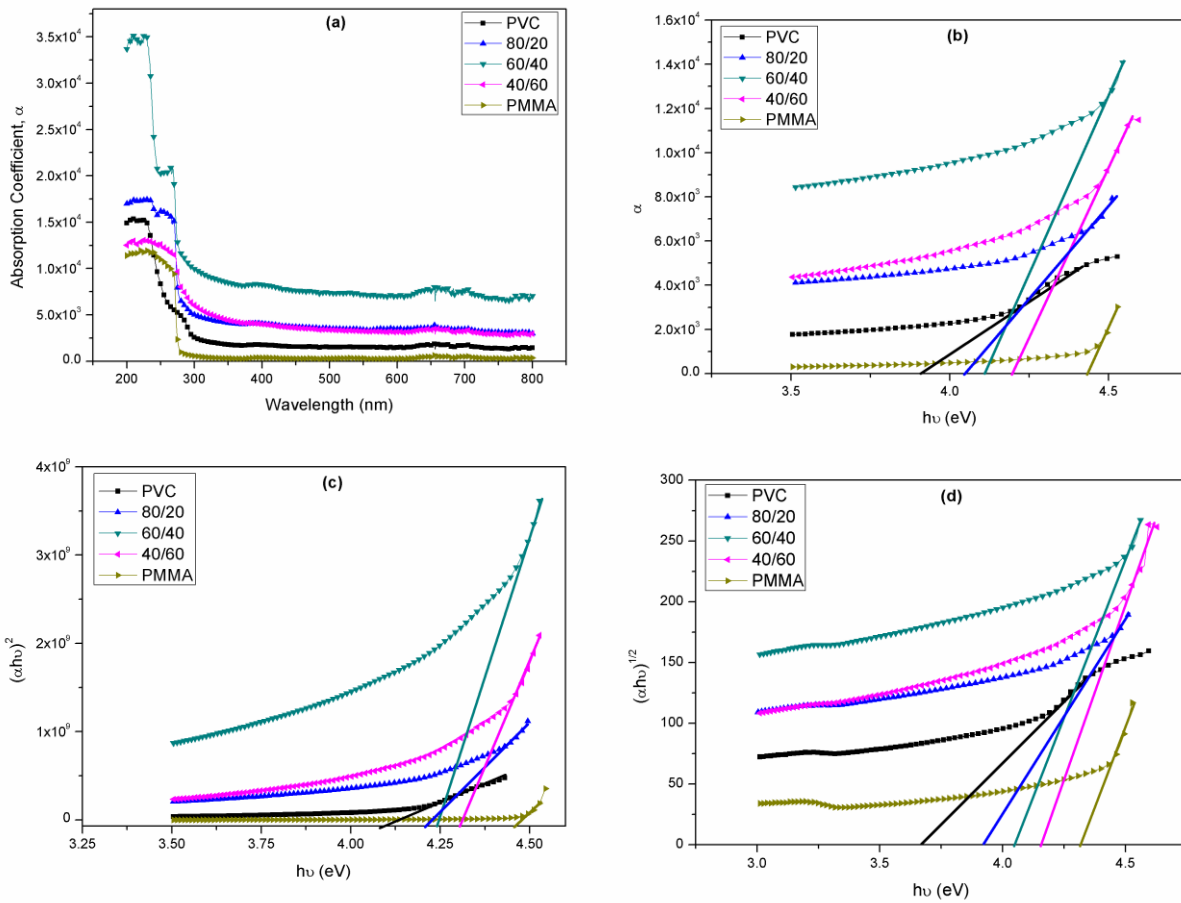


**Figure 3.2** Plot of (a) Absorption coefficient ( $\alpha$ ) vs Wavelength ( $\lambda$ ), (b) Absorption coefficient ( $\alpha$ ) vs Photon Energy ( $h\nu$ ), (c)  $(\alpha h\nu)^2$  vs  $h\nu$ , (d)  $(\alpha h\nu)^{1/2}$  vs  $h\nu$

### 3.2.3. RAMAN Analysis

The Raman spectra of the blends of PVC and PMMA are shown in **Figure 3.3**. Spectral shifts have been observed in the blends of PVC/PMMA polymers. The same trend can be found from both IR and Raman data, i.e. a shift in the C-Cl stretching region of PVC and a clear shift of the carbonyl stretching (C=O) of the PMMA component.

The C-Cl stretching peak shows the shift towards higher wave number. i.e. blue shift for the blends spectra ( $828\text{ cm}^{-1}$  to  $867\text{ cm}^{-1}$ ). The magnitude of the blue shift of the C=O stretching mode of PMMA ( $1917\text{ cm}^{-1}$  to  $1935\text{ cm}^{-1}$ ) is shown in **Figure 3.3(a, b)**. Both peaks shows maximum peak shift for 80/20 wt % content, which is indicating strong hydrogen bonding between two polymers.

The hydrogen bonding which occurs between C-Cl group in PVC and C=O group in PMMA is significant. Spectral changes in the C-Cl stretching region and C=O stretching region of the blends are a mixed contribution from both the C-Cl...O=C interaction and the local conformational structures of pure polymers, PVC and PMMA.

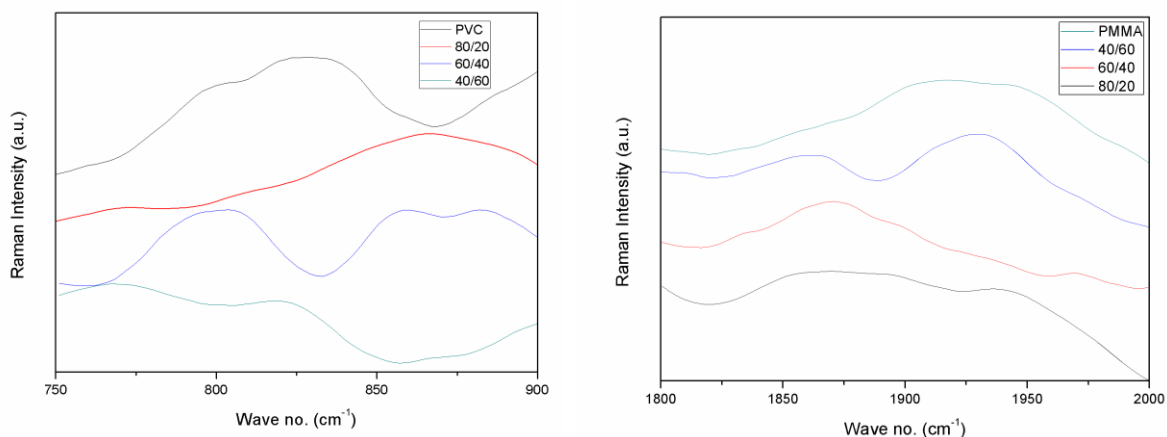


**Figure 3.3** Raman Spectra of Pure PVC, Pure PMMA and their blends (a) in the C-Cl stretching region of PVC (b) in the C=O stretching region of PMMA

### 3.2.4. Mechanical Analysis

Mechanical properties of PVC-PMMA polymer blend were carried out to study the Young's modulus (YM), Ultimate Tensile Strength (UTS), Stress at Peak load and Elongation at Break (EB). The values of all mechanical parameters obtained for PVC/PMMA blends are higher than the values of the Pure PVC except the blend of 10% of PMMA.

Young's Modulus (YM) values corresponding to PMMA % is shown in **Figure 3.4**. The **Figure 3.4** shows that PVC/PMMA blends exhibit lower YM to the extent of 10% of PMMA, beyond which there is sudden increase in YM and it reaches maximum value for 20% of PMMA and after that it again exhibits a decreasing trend. The values of Ultimate Tensile Strength (UTS) and Stress at Peak load for PVC/PMMA blends are shown in **Figure 3.4** corresponding to PMMA %. All these values also exhibit minimum value at 10% of PMMA and then give maximum value at 20% of PMMA. After 20% of PMMA, blend exhibit decreasing trend but their corresponding values of such properties for different blends are quite high in comparison to pure PVC.

The breaking elongation of various blends of PVC/PMMA is shown in **Figure 3.4**, confirmed our expectation. In this case there is a sudden jump in its values initially up to a level of 10% PMMA. Beyond which there is a steady decrease in its values which also confirmed by a decrease in Young's Modulus (YM), Ultimate tensile strength (UTS) etc. The introduction of PMMA into PVC increases the Mechanical properties such as Young's Modulus (YM), Ultimate Tensile Strength (UTS) and Stress at Peak load. The different Young's Modulus (YM) values in PVC blends are due to the difference in cross linking density provided by PMMA with different weight fraction values.

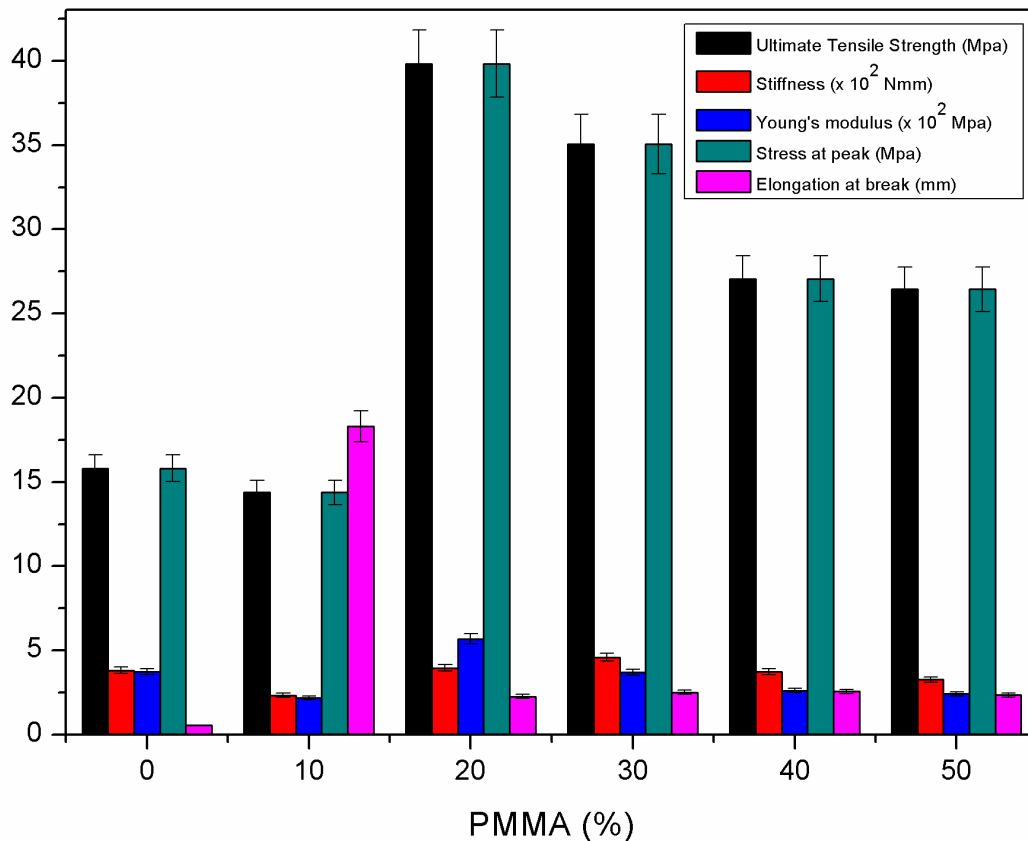


**Figure 3.4** Variation in Ultimate tensile strength, Stiffness, Young's Modulus, stress at peak, Elongation at break, as a function of PMMA content

In general polymers having either a high degree of crystallinity, cross linking or rigid chain exhibit a high strength and low extendibility, thereby giving a high Young's Modulus (YM) values, high stress at peak value and low elongation value [30]. PVC is a hard and strong materials and it shows the dipole-dipole type attraction as a result of electrostatic interaction between the chlorine atom of one chain and hydrogen atom of another. When PMMA is blended with PVC these interaction are weakened by the presence of PMMA up to 10% of PVC. Beyond 10% of PMMA, we observed reversal behavior of PMMA affecting on PVC. So the mechanical properties increase beyond 10% of PMMA and exhibit higher values at 20% of PMMA. Because

at 20% of PMMA, the interaction between PVC and PMMA molecules is higher and the dipole-dipole attraction is also reaches at maximum value.

### 3.2.5. Thermal gravimetric Analysis

The thermo grams, **Figure 3.5 (a)** of PVC, PMMA, and its various blends with PMMA clearly point out general increase in thermal stability of the blends. The increase in the onset temperature of degradation for the blends in both the stages of degradations is a leading feature of the thermal characteristics of such blends, which further increase with increasing proportion of PMMA. The initial weight loss was observed for all samples due to moisture evaporation. The major weight losses occurred in the range of 240 – 360 °C for all the blend samples. The difference in the thermal decomposition was observed clearly from derivative TG (DrTG) curve as shown in **Figure 3.5 (b)**.

The thermo gravimetric data for pure PVC, pure PMMA and their blend films are given in **Table 3.3**. From thermographs, initial weight loss occurs, which is attributed due to the presence of moisture and impurities at the time of loading the samples [31]. After complete dehydration, above 100 °C, no further weight loss is observed for PVC, until irreversible decomposition commenced at approximately around 253 °C. and it shows a weight loss of 59.95%. The loss may be due to the decomposition of PVC occurred [32]. When the temperature rose to 383°C, the samples exhibit a gradual weight loss of about 78.14%. This shows that the occurrence of another irreversible decomposition. For PMMA, single decomposition peak around 378 °C is observed which start at 325 °C and end at 426 °C with almost weight loss 99.37%. PMMA showed one main decomposition weight loss in this region.

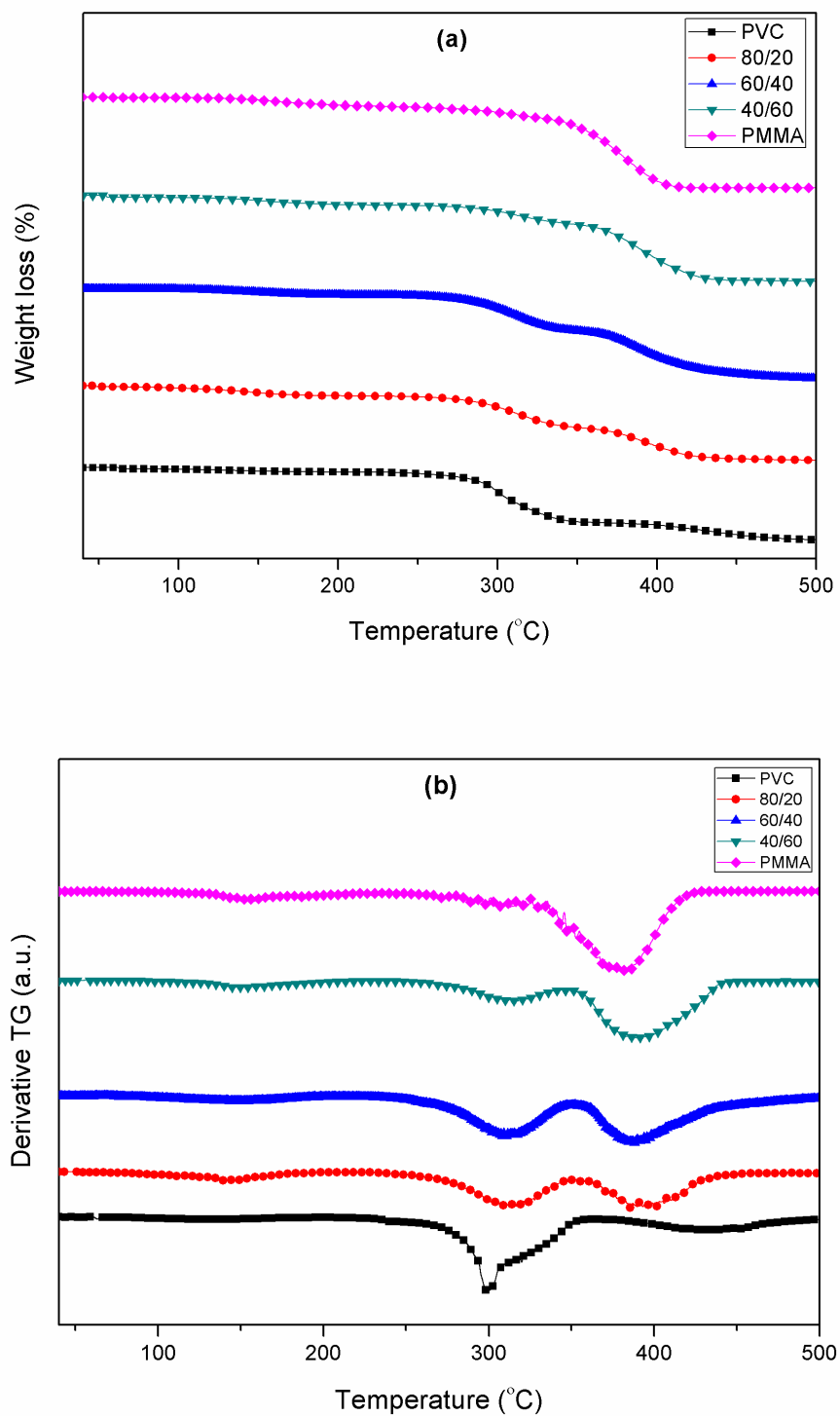


Figure 3.5 (a) TG of pure PVC, pure PMMA and their blends (b) Derivative TG of pure PVC, pure PMMA and their blends

For the 80/20 wt % PVC/PMMA blend film, the first decomposition took place at 266 °C which induced 46.66% weight loss and second decomposition occurred at 357 °C which showed weight loss of 78.35 %. This indicates that the film is stable up to 266 °C. Since the first decomposition of 80/20 wt % blend film occurred at higher temperature and bore a lower weight loss, this proves that the thermal stability increased with addition of PMMA. Polymers of higher PVC content and lower PMMA amount are proven to have a relatively good stability as they have the first decomposition at higher temperature bearing a lower weight loss. From the table we conclude that 80/20 wt % have maximum thermal stability. For 60/40 wt % and 40/60 wt %, the first decomposition occurred at 248 °C and 265 °C with 47.83 % and 31.12 % weight loss respectively and second decomposition took place at 356 °C and 353 °C with 95.13 % and 93.58 % weight loss.

$T_p$  (peak temperature) of DrTG was a function of blend weight percentage.  $T_p$  was used as a measure of thermal stability. The shift in  $T_p$  toward higher temperature showed thermal stability of the blend was higher than the pure PVC.  $T_p$  was maximum for 80/20 wt%, so this blend was more stable. This higher thermal stability was observed for 80/20 blend sample by TGA and DrTG which was due to the intermolecular cross-linking reaction giving highly compatible impact blend system [33]. TGA curves indicated the possibility of a strong hydrogen bond intermolecular interaction between PVC and PMMA due to  $-CHCl$  groups of PVC and  $C=O$  group of PMMA [34].

**Table 3.3 TG and DrTG data of Pure PVC, PMMA and their blended samples**

PVC/PMMA	Temperature(°C)			Weight loss (%)
	Starting	Ending	T <sub>p</sub>	
100/0	253	352	300	59.95
	383	479	432	78.14
80/20	266	353	316	46.66
	357	446	397	78.35
60/40	248	349	312	47.83
	356	462	388	95.13
40/60	265	343	313	31.12
	353	451	388	93.58
0/100	325	426	378	99.37

### 3.2.6. Scanning Electron Microscopy

SEM micrographs of pure PVC and Pure PMMA are shown in **Figure 3.6 (a, b)**. The SEM micrographs of brittle fractured surface of blends with various amount of PVC in PMMA are shown in **Figure 3.6 (c – d)**. These micrographs show almost discrete phases and clearly indicate changed surface morphologies of the various blends compared to that of pure PVC. As the amount of PMMA increases, the morphology of blends shows a uniform dispersion of PVC particles in the blends. But for other than 80/20 wt% SEM micrograph shows agglomeration in blend system, while 80/20 wt% have good homogeneity (**Figure 3.6(c)**). From this image one can show, the blend exhibit uniform morphological feature without any phase separation. In phase mixing homogeneity occurs at the lower level of PMMA (for 20% of PMMA), however, it is absent in higher concentration of PMMA in PVC polymer matrix. This may probably be

recognized to the increase in mechanical and thermal properties as it shows the regularity in stiff chain structure of PVC.

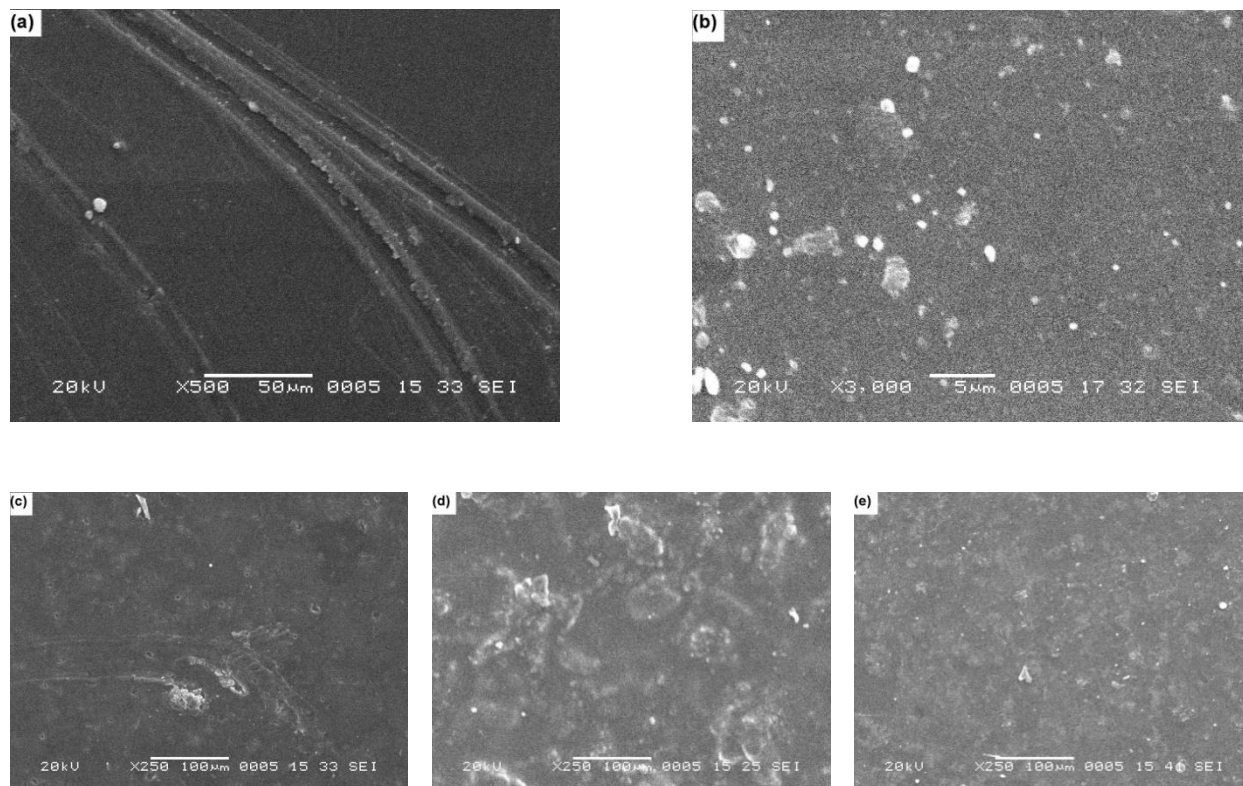


**Figure 3.6** Scanning Electron Micrograph of (a) Pure PVC (b) Pure PMMA (c) 80/20 (d) 60/40 (e) 40/60

### 3.3. Conclusions

From the FTIR and Raman spectra, it is observed that strong hydrogen bond interaction between C-Cl group of PVC and C=O group of PMMA occurs. For 80/20 wt% has maximum peak shifting on higher wave number side is observed. Mechanical properties, mainly ultimate tensile strength and young's modulus, increase beyond 10% of PMMA and exhibit maximum value for 80/20 wt% of PVC/PMMA blend. From TGA, we observed that 80/20 wt% have maximum thermal stability than pure polymers. SEM analysis showed that other than 80/20 wt%, all others

---

have agglomeration in blends system, while 80/20 wt% has good homogeneity. So from above conclusion, In 80/20 wt% of PVC/PMMA exhibit good and enhanced properties than pure constituents.

### 3.4. References

1. A. Kaminska, H. Kaczmarek, J. Thermal Anal., 29, 1017, 1984.
2. L. Goulet, R. E. Prud'homme, Eur. Polym. J., 22, 529, 1986.
3. E. J. Moskala, D. W. Lee, polym. Degr. Stab., 25, 11, 1984.
4. K. Kuzelova, Z. Vymazal, Eur. Polym. J., 35, 361, 1999.
5. M. Reyne, " Les plastiques: Polymeres, transformations et applications", Edition HERMES, Paris, P.96, 1992.
6. I. C. McNeil, D. Neil, Eur. Polym. J., 1970, 6, 143. [] I. C. McNeil, D. Neil, Eur. Polym. J., 6, 569, 1970.
7. D. Braun, B. Böhringer, W. Knoll, N. Fisher, S. Kömmerling, Die Angew, Makromol. Chem., 181, 23, 1990.
8. D. Braun, B. Böhringer, N. Eidam, N. Fisher, S. Kömmerling, Die Angew, Makromol. Chem., 216, 1, 1994.
9. Naima Belhaeche- Bensemra, Belkacem Belabed, Abdelmalik Bedda, Macromol. Symp., 180, 203-215, 2002.
10. Chao Zhou et.al, Polymer Bulletin., 58, 979–988, 2007.
11. J. W. Schurer, A. de Boer and G. Challa, Polymer.,16 201, 1975.
12. Rupa Chakrabarti, Molay Das and Debabrata Chakraborty, Inc. J Appl Polym Sci., 93, 2721-2730, 2004.
13. A. Wlochowicz and J. Janicki, J. App. Poly. Sci., 38, 1469, 1989.
14. A. Varada Rajulu, R. Lakshminarayna Reddy and S. M. Raghavendra, Eur. Polym. J., 35, 1183, 1999.

15. Aouachria Kamira and Belhaneche-Bensemra Naima, *Polymer Testing.*, 25, 1101–1108, 2006.
16. S. Shen and M. Torkelson, *Macromolecules.*, 25, 721, 1992.
17. S. Ramesh, K. H. Leen, K. Kumutha and A. K. Arof, *Spectrochimica Acta., Part A*, 66 1237–1242, 2007.
18. Vijay V. Soman and Deeplai S. Kelkar, *Macromol. Symp.*, 277 152-161, 2009.
19. H. Jager, E. J. Vorenkamp, G. Challa, *Polymer commun.*, 24, 290, 1983.
20. Naima Belhaeche- Bensemra, Belkacem Belabed, Abdelmalik Bedda, *Macromol. Symp.*, 180, 203-215, 2002.
21. Kamira Aouachriaa, Naima Belhaneche-Bensemra, *Polymer Testing*, 25, 1101-1108, 2006.
22. A. P. Rhode, R. Frech, *Solid State Ionics*, 121, 91, 1999.
23. S. York, R. Frech, A. Snow, D. Glatzhofer, *Electrochim Acta*, 46, 1533, 2001.
24. Acosta JL, Morales E, *Solid State Ion* 85:85, 1996.
25. Kim JY, Kim SH, *Solid State Ion* 124(1–2):91, 1999.
26. Abd E I, Kader F H, Osman W H, Ragab H S, Sheap A M, Rizk M S & Basha M A F, *J polym Matter*, 21, 49, 2004.
27. Ma H L, Zhang X H & Lucas J, *J Non-cryst solids*, 101, 128, 1993.
28. S. Rajendran, T. Uma, *Mater. Lett.* 44, 208, 2000.
29. M. Hammama, M.K. El-Mansy, S.M. El-Bashirb M.G. El-Shaarawy, *Desalination*, 209, 244-250, 2007.
30. S. Kim Chi and M. Oh Seung, *Electrochim Acta.*, 46, 1323-31, 2001.

31. T. Shodai, B.B. Owens, H. Ohtsuka and J. Yamaki, *J. Electrochem. Soc.* 141, 2978-2981, 1994.
32. Stephan A M, Saito Y, Muniyandi N, Renganathan N G, Kalyanasundaram S, Elizabeth R N *Solid State Ionics* 148: 467–473, 2002.
33. El-Kader FH, Gafer SA, Basha AF, Bannan SI, Basha MAF , Thermal and optical properties of gelatin/poly(vinyl alcohol) blends. *J Appl Polym Sci* 118:413–420, 2010.
34. Vijay V. Soman, Deepali S. Kelkar, FTIR Studies of Doped PMMA - PVC Blend System, *Macromol. Symp.*, 277, 152–161. DOI: 10.1002/masy.200950319, 2009.

## Chapter 4

# Characterization of PAM/PVA Blends

---

### *Abstract*

*This chapter gives an account of the characteristics of Poly acrylamide(PAM) and Poly vinyl alcohol (PVA) blend in different weight proportion (70/30, 50/50 and 30/70 wt %) which is prepared by solution cast technique. These blends are investigated by spectroscopic techniques like FTIR, UV-Vis and RAMAN. Mechanical, Thermal and Morphological properties are also investigated. The results obtained from different characterization techniques show the effect of blending on different properties. These properties of PAM/PVA blends are correlated with spectroscopic investigation.*

## 4.1. Introduction

In the recent trends, polymer blends cover many different product areas. Their applications in different fields increase drastically. The polymer blends are widely used in biomedical field. The accomplishment of polymer as bio materials depends on their mechanical and thermal properties which allow different shapes with low production cost. Biological polymers have poor mechanical properties. So considering these factors, we prepared polymer blends which have good mechanical, thermal and optical properties with good compatibility.

The selection and use of polymers can potentially form hydrogen bonds when two polymers are mixed, as well as the study of the properties of the blends are of importance to find further applications of the resulting blend materials for biomedical and pharmaceutical devices [1]. PAM is well-known hydrophilic polymer and has been greatly used in the field of agriculture and biomedicine [2, 3]. The electrical and mechanical properties of the ethylene propylene diene monomer (EPDM) and nitrile rubber (NBR) blended with polyacrylamide (PAM) were studied [4]. PAM is a polymer of biomedical and pharmaceutical interest widely studied as hydrogel for blood compatible applications [5]. Polymers of acrylamide are well known for their hydrophilicity and inertness that make them a material of choice in large number of applications in medical and pharmacy [6]. Many researchers have studied the use of PAM hydrogels for controlled release of fertilizers, pesticides or possibly in medicine and also as electrolyte solution [6-8]. Also, it was used for water retention in arid soils [9]. Polyacrylamide-based polymers have received a great extent of utility in industry because of their high molecular weight, water soluble property, and ability to receive diverse modification on chemical structure [10, 11]. When PAM is dissolved in solvents, the linear structure formed in solution. Which reduces the drag coefficient and thereby, facilitating the transportation of these viscous liquids over long distances

[12, 13]. When cross-linked, the polymer is insoluble in water and forms a hydrogel system that is capable of absorbing and retaining large quantities of water. The linear form and solubility properties are also offer unique applications such as stabilizing soil matrices, reducing erosion, and improving soil aeration [9, 14-15].

Poly vinyl alcohol (PVA) films are known to have high tensile and impact strengths, a high tensile modulus, and excellent resistance to alkali, oil, and solvents [16]. PVA has gained increasing attention in the biomedical field because of its bio inertness [17, 18]. Vargas et al. [19] investigated poly Vinyl Alcohol (PVA) for the phase behavior. Fritz and Breitsmer developed ionically conducting polyelectrolytes based on PVA, because of its bio-compatibility and wide use in biomedical fields [20, 21]. Because of its superior mechanical properties and better ionic conduction, it has some technological advantages in electro chromic devices and fuel cells, etc. [22] Hydrophilic nature of PVA is beneficial for its applications, and also a limiting factor in its characterization because its molecules combine through hydrogen bonding due to its poly hydroxyl groups [23]. The chemical resistance and physical properties of PVA have led to its broad industrial use. Due to its oleophobic nature, PVA is useful as membrane for water waste treatment as well as filtration membrane [24, 25]. Chemically cross linked PVA hydrogels have received increasing attention in biomedical and biochemical applications because of their permeability, biocompatibility and biodegradability [26-28]. Hydrogel blend of Polyacrylamide and Poly Vinyl Alcohol can be used as proton exchange membrane [29]. Blends of polyvinyl alcohol (PVA) with other polymers have been mechanically characterized by many researchers [30-32]. Horia M Nizam El-din et. al. undertaken to investigate the miscibility of PVA with PAM in various proportions [31]. PVA and PAM are two well-known polymers and their individual biomedical, mechanical and other properties have been thoroughly investigated [6, 32-

33]. PVA is a water soluble, non-toxic, non-immunogenic polymer with a remarkable film forming property [34, 35]. However, its weak mechanical strength restricts its use in those applications where the material has to withstand stretched stress. The introduction of other polymeric components into the PVA matrix could improve its mechanical properties [36].

## 4.2. Results and Discussion

### 4.2.1. FTIR Analysis

FTIR is very important technique for the study of the molecular interactions. The width and intensity of spectral bands, as well as the position of peaks are all sensitive to environmental changes and to conformations of the macromolecule at molecular level. These differences would be derived from chemical interactions resulting in the band shifts and broadening. If the polymers are compatible, there should be considerable differences between the infrared spectra of the blend and the pure components [37]. So we can study the compatibility as well as intermolecular interactions between two polymers.

**Figure 4.1 (a, b)** shows FTIR absorption spectra of pure PAM, pure PVA and PAM/PVA blend with different concentrations recorded at room temperature in the region  $400 - 4000 \text{ cm}^{-1}$ . FTIR absorption bands, positions and its assignments of all prepared composite films are listed in **Table 4.1** [38-40]. De-convolution was made for two spectral regions  $1500 - 1800 \text{ cm}^{-1}$  and  $2600 - 3700 \text{ cm}^{-1}$  as shown in **Figure 4.2 (a, b)**. From the deconvolution, the spectral peaks are well separated which are listed in **Table 4.1**.

The IR spectrum of PAM exhibiting bands at  $3105 \text{ cm}^{-1}$  and  $3302 \text{ cm}^{-1}$  which were assigned to a symmetric and asymmetric stretching vibration of N-H, bands at  $2763 \text{ cm}^{-1}$  and  $2926 \text{ cm}^{-1}$  assigned to -CH symmetric and asymmetric stretching respectively, bands at  $1728 \text{ cm}^{-1}$  (C=O

stretching) and  $1600\text{ cm}^{-1}$  assigned to (N–H bending) [41, 42]. The band at  $1652\text{ cm}^{-1}$  corresponds to the asymmetric stretching vibration of  $-\text{COO}^-$  groups while bands at  $1434\text{ cm}^{-1}$  (C–N stretching),  $1375\text{ cm}^{-1}$  ( $-\text{CH}_2$  wagging),  $1359\text{ cm}^{-1}$  (C–H bending),  $1254\text{ cm}^{-1}$  ( $-\text{NH}_2$  wagging),  $1097\text{ cm}^{-1}$  (C–C stretching) were also detected [38].

For pure PVA, the bands at  $3000\text{ cm}^{-1}$  to  $3600\text{ cm}^{-1}$  assigned to  $-\text{OH}$  stretching region and  $1565\text{ cm}^{-1}$  assigned to bending vibration of hydroxyl group [42]. The band corresponding to methylene group ( $-\text{CH}_2$ ), asymmetric and symmetric stretching vibrations occurs at about  $2925\text{ cm}^{-1}$  and  $2759\text{ cm}^{-1}$ . The band at about  $936\text{ cm}^{-1}$  corresponds to C–O stretching of acetyl groups, present on the PVA backbone [43, 44]. PVA spectrum also exhibited peaks at  $1433\text{ cm}^{-1}$ ,  $1360\text{ cm}^{-1}$ ,  $1254\text{ cm}^{-1}$ ,  $1119\text{ cm}^{-1}$  and  $1042\text{ cm}^{-1}$  which assigned as O–H & C–H bending,  $-\text{CH}_2$  out of plane bending,  $-\text{CH}_2$  bending, C–O–C asymmetric and symmetric Stretching respectively. A band at  $1727\text{ cm}^{-1}$  is corresponding to the C=O group present in PVA [45]. The spectra of the blend films are characterized by the presence of the absorption bands typical of the pure polymer. The peaks appeared in the range  $3,000\text{ cm}^{-1}$ – $2,800\text{ cm}^{-1}$  indicates the presence of  $-\text{CH}_2$  groups in all the spectra. Bands of PAM at  $3302\text{ cm}^{-1}$  and  $3105\text{ cm}^{-1}$  which are stretching vibration of  $-\text{NH}_2$  group involved in both inter and intra molecular interaction of hydrogen bond coupled with  $-\text{OH}$  group of PVA at  $3145\text{ cm}^{-1}$  and  $3305\text{ cm}^{-1}$  when PVA added into PAM polymer matrix. Spectra of blends clearly indicate the increase in the intensity of bands in the region of  $3000\text{ cm}^{-1}$  to  $3600\text{ cm}^{-1}$ . But intensity of this broad band is maximum for 50/50 blend ratio than the others and peak shifting (at  $3149\text{ cm}^{-1}$  and  $3342\text{ cm}^{-1}$ ) in this region is towards higher wave number side, which indicates the strong hydrogen bonding between PAM and PVA due to  $-\text{CONH}_2$  groups in PAM and  $-\text{OH}$  group in PVA, hence this blue shift of IR band indicating enhancement of bond strength [46-48].

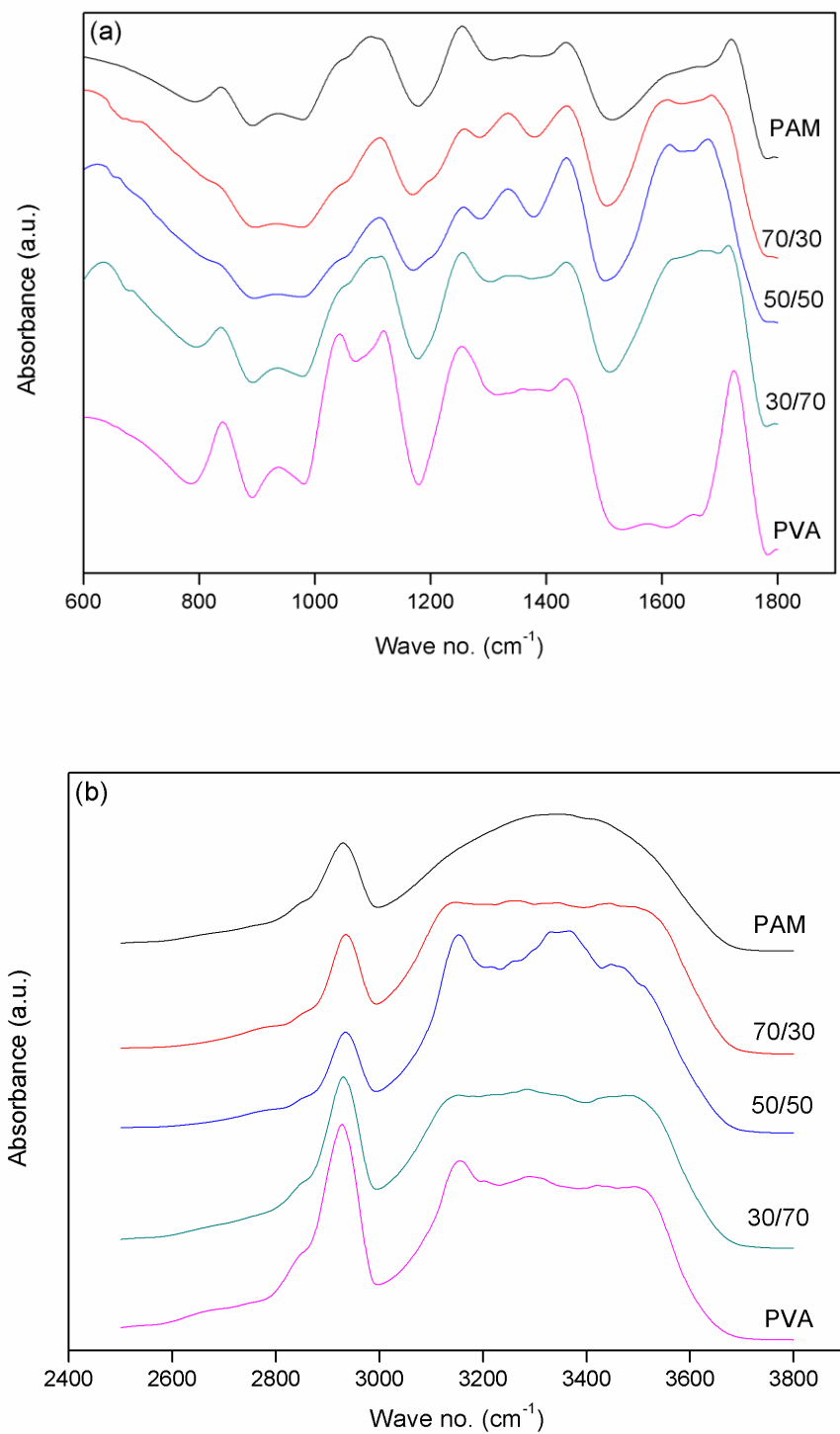


**Figure 4.1** FTIR Spectra of pure PAM, pure PVA, 70/30, 50/50 and 30/70 blend ratio (a) in the region of 600-1800  $\text{cm}^{-1}$  (b) in the region of 2500-3800  $\text{cm}^{-1}$

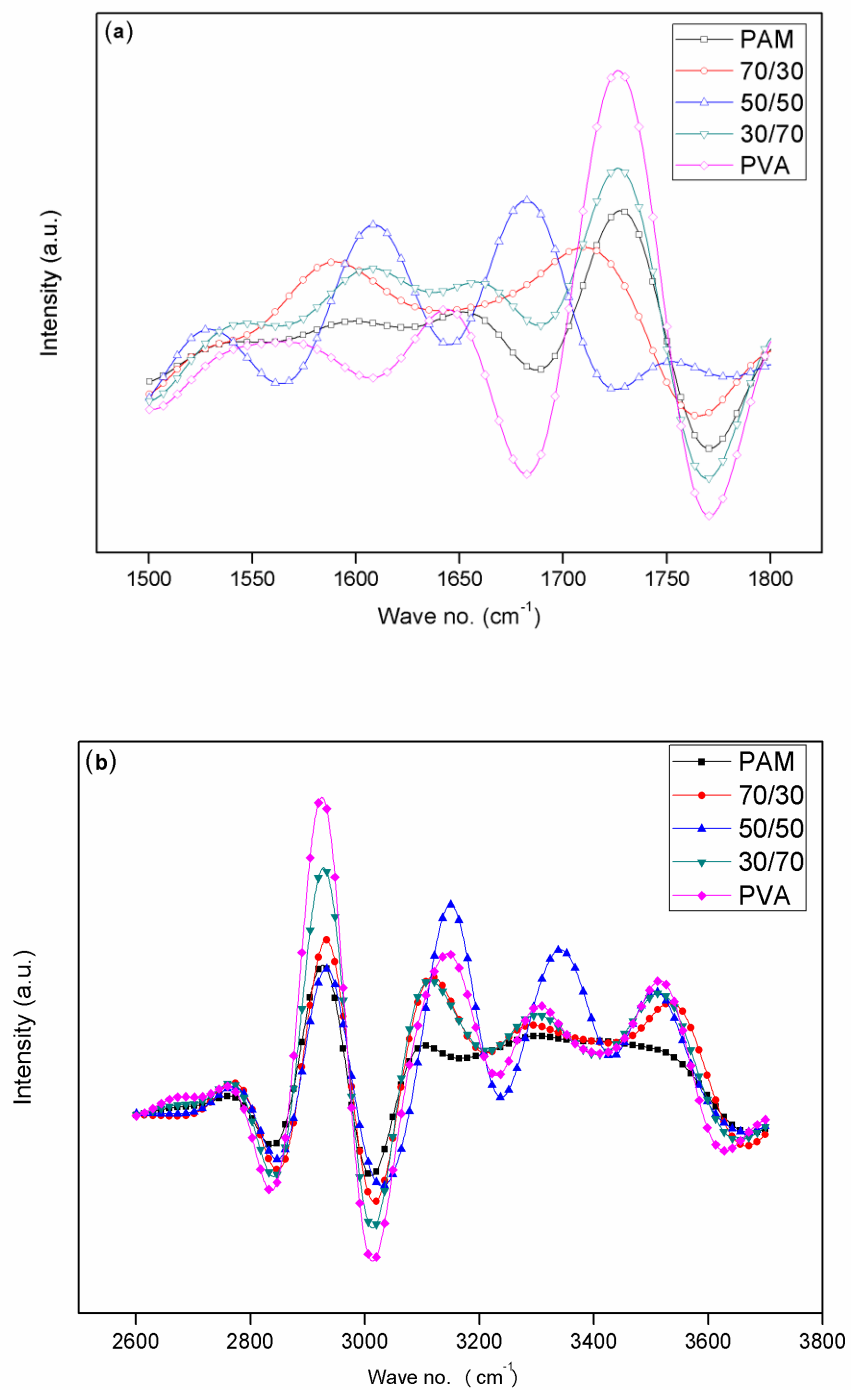


**Figure 4.2** Deconvolution spectra of pure PAM, pure PVA, 70/30, 50/50 and 30/70 blend ratio (a) band in the region of 1500-1800 cm<sup>-1</sup> (b) band in the region of 2600-3700 cm<sup>-1</sup>

**Table 4.1** Assignments of the FT-IR characterization bands of the pure PAM, pure PVA and pure PAM/PVA blend<sup>38, 39, 40</sup>

Wave no. (cm <sup>-1</sup> )	Assignment (PAM)	Wave no. (cm <sup>-1</sup> )	Assignment (PVA)	70/30	50/50	30/70
936	C–O symmetric Stretching	936	C–O symmetric Stretching	933	934	934
1097	C–C asymmetric Stretching	1042	C–O–C symmetric Stretching	1112	1112	1115
1254	–NH <sub>2</sub> wagging	1119	C–O–C asymmetric Stretching	1258	1256	1254
1328	C–H bending	1254	–CH <sub>2</sub> bending	1334	1334	1333
1359	–CH <sub>2</sub> wagging	1360	–CH <sub>2</sub> out of plane bending	1435	1435	1435
1434	C–N stretching	1433	O–H & C–H bending	1529	1529	1547
1600	N–H bending	1565	O–H & C–H bending	1590	1608	1607
1652	Asymmetric stretching of –COO <sup>-</sup>	1644	C=C stretching		1683	1658
1728	C=O stretching	1727	C=O symmetric stretching	1711	1752	1727
2763	C–H symmetric stretching	2759	–CH <sub>2</sub> symmetric stretching	2770	2770	2764
2926	C–H asymmetric stretching	2925	–CH <sub>2</sub> asymmetric stretching	2932	2933	2927
3105	N–H symmetric stretching	3145	O–H stretching	3118	3149	3114
3302	N–H asymmetric stretching	3301	O–H stretching	3291	3342	3301
		3516	O–H stretching	3534	3507	3515

Other IR bands of PAM had distinct shift as shown in the **Table 4.1**. For 50/50 there is maximum shift for different IR peaks. For 50/50, bending vibration of N-H (1600 cm<sup>-1</sup>) blue shifted by 8 cm<sup>-1</sup> to 1608 cm<sup>-1</sup>, asymmetric stretching of –COO<sup>-</sup> (1652 cm<sup>-1</sup>) blue shifted by 31 cm<sup>-1</sup> to 1683 cm<sup>-1</sup>, the C=O stretching vibration also blue shifted by 24 cm<sup>-1</sup> from 1728 cm<sup>-1</sup> to 1752 cm<sup>-1</sup>. Other vibrational peaks are also blue shifted as shown in the **Table 4.1**. No shift is observed for C-N stretching vibration. Peak at 936 cm<sup>-1</sup> due to CO symmetric stretching of PVA and PAM is not shifted but intensity of this peak is increased for 30/70 blend ratio while for 50/50 and 70/30 blend ratio its intensity is very negligible.

#### 4.2.2. UV-Vis Analysis

The optical absorption (UV-Vis) spectra of pure PAM/PVA and their blends in the wavelength range 200-800 nm are shown in **Figure 4.3(a)**. From the figure pure PVA has a small weak absorption band at 272 nm. This band attributed to the  $\pi \rightarrow \pi^*$  transition of C–O group of PVA [49]. Intensity of this absorption peak is slightly increased for 30/70 wt % and then almost

disappears for other blends ratio. This may be due to the increase of number of C–O group of the PVA which is also confirmed by IR spectrum that C–O stretching group intensity is maximum for 30/70 wt% while in others it almost disappears. In all the spectra we can see a sharp increase of light absorption below 220 nm which corresponds to  $n \rightarrow \pi^*$  transition of amine carbonyl groups in PAM macromolecules [49]. Absorption of 50/50 wt% is maximum from all the pure and blends polymer systems in visible region. From the absorption spectra one can show that absorption edges are slightly shifted toward higher wavelength with the increase of PVA content.

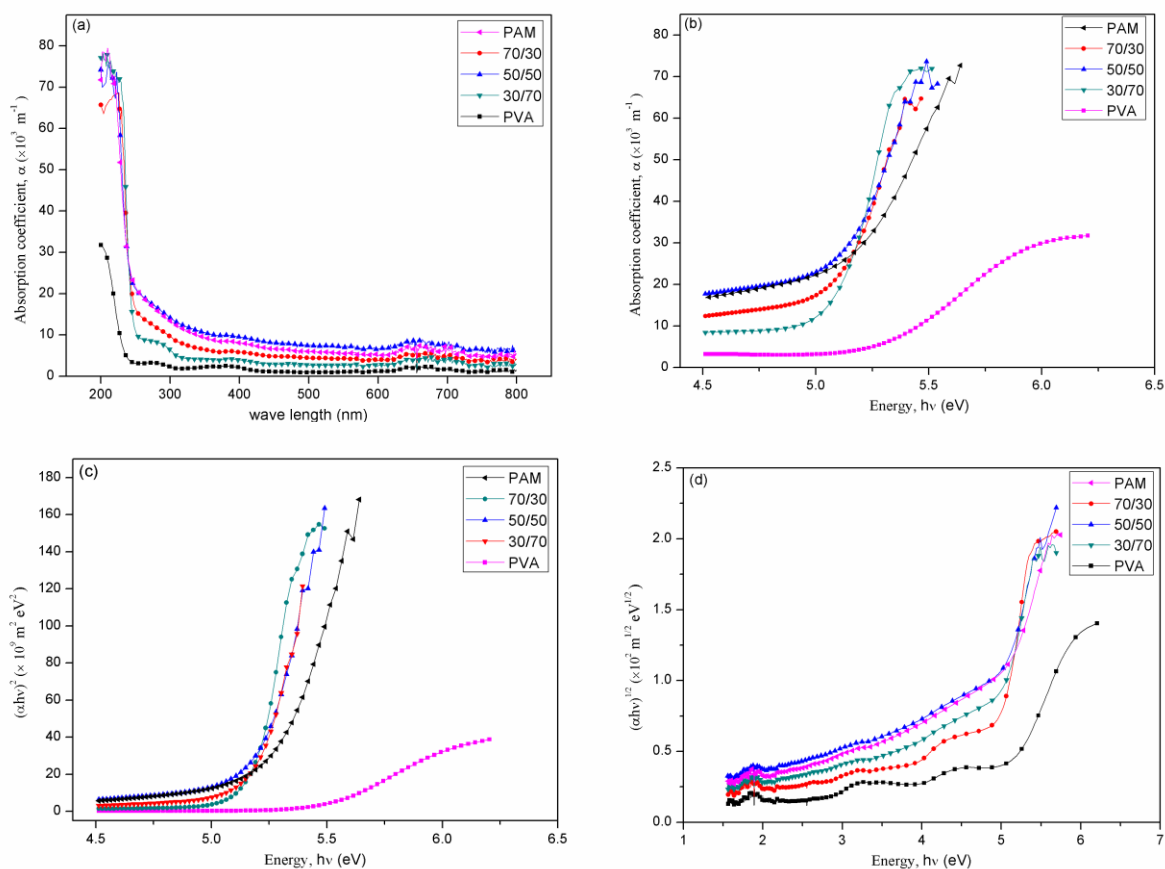


**Figure 4.3** Plot of (a) Absorption coefficient ( $\alpha$ ) vs Wavelength ( $\lambda$ ), (b) Absorption coefficient ( $\alpha$ ) vs Photon Energy ( $h\nu$ ), (c)  $(\alpha h\nu)^2$  vs  $h\nu$ , (d)  $(\alpha h\nu)^{1/2}$  vs  $h\nu$

**Table 4.2** Variation of optical (Direct/Indirect) energy gap ( $E_g^{opt}$ ) and absorption edge ( $\Delta E$ ) with different samples

PAM/PVA	Optical energy gap ( $E^{opt}$ )		Absorption edge (eV)
	Direct (eV)	Indirect (eV)	
Pure PAM	5.35	4.57	4.97
70/30	5.18	4.84	5.10
50/50	5.14	4.75	4.99
30/70	5.15	4.82	5.07
Pure PVA	5.47	4.87	5.24

The absorbance process plays an important role in the optical properties of polymers. The absorption coefficient was determined from the UV-VIS spectra using the formula:

$$\alpha = A/d \quad (1)$$

Where A is the absorbance and d is the thickness of the film. The Tauc relation for dependence of absorbance on photon energy is [50].

$$\alpha(\nu) = B(h\nu - E_g)^x/h\nu \quad (2)$$

Where  $\alpha(\nu)$  is the absorption coefficient,  $E_g$  is the optical gap of the substance, h is plank's constant,  $\nu$  is the corresponding frequency, x is the parameter that gives the type of electron transition. It was observed that two distinct linear relations were found for  $x = 1/2$  (Direct transition) and  $x = 2$  (Indirect transition), corresponding to different inter band absorption processes [51] and factor B depends on the transition probability and can be assumed to be constant within the optical frequency range [51, 52].  $E_g$  is the optical energy gap. On the basis of equation 2, direct and indirect band gap and absorption edge were determined. The position of the absorption edge, the direct band gap and indirect band gap were obtained from the plot of  $\alpha$  vs  $h\nu$ ,  $(\alpha h\nu)^2$  vs  $h\nu$  and  $(\alpha h\nu)^{1/2}$  vs  $h\nu$  shown respectively in **Figure 4.3 (b)**, **Figure 4.3 (c)** and **Figure 4.3 (d)**. The values of the absorption edge and the direct/indirect band gap were

determined by extrapolation of the linear portions of these curves to zero absorption. The values of various optical parameters are shown in the **Table 4.2**.

Absorption edge, direct and indirect band gap were decreased as we increase PVA contents in PAM polymer matrix and they become minimum at 50/50 wt%. This may show that as a result of blending, there is the change in the number of final states in the band gap [51, 53]. And also increase in the number of defects which leads to increase in the density of localized states in the band structure which led to a decrease in the optical band gap [16].

### 4.2.3. RAMAN Analysis

Raman spectroscopy used for the qualitative analysis of the interaction of PVA with PAM. **Figure 4.4 (a, b)** shows FT-Raman Spectra of pure PAM, pure PVA and their blends. **Table 4.3** lists the assignments for the bands of pure polymers.

For PAM, the bands near  $854\text{ cm}^{-1}$  corresponding to C-C stretching region of PAM. The band at  $1107\text{ cm}^{-1}$  attributed to the C-O-C stretching modes of PAM. The band near  $1400\text{ cm}^{-1}$  assigned mainly to the C-N stretching vibration. A band near  $1711\text{ cm}^{-1}$  attributed to C=O stretching mode of the PAM polymer chain. In the range of the stretching vibrations of the  $-\text{CH}_2$  groups, a band at  $2914\text{ cm}^{-1}$  indicates the  $-\text{CH}_2$  stretching. Two overlapped bands, around  $3124\text{ cm}^{-1}$  and  $3248\text{ cm}^{-1}$ , are due to  $-\text{NH}_2$  symmetric and asymmetric stretching respectively.

For PVA, broad peak near  $786\text{ cm}^{-1}$  and  $988\text{ cm}^{-1}$  are from C-C stretching vibration and C-O-C stretching of PVA respectively. Two overlapped peak of  $-\text{CH}_2$  wagging and  $-\text{CH}_2$  twisting are appeared at  $1333\text{ cm}^{-1}$  and  $1398\text{ cm}^{-1}$  with the hump at  $1577\text{ cm}^{-1}$  which attribute to the  $-\text{CH}_2$  deformation vibration. Band appear at  $2875\text{ cm}^{-1}$  is due to  $-\text{CH}_2$  stretching while  $3100\text{ cm}^{-1}$  and  $3350\text{ cm}^{-1}$  are mainly due to  $-\text{OH}$  stretching of PVA. For the blends of PAM/PEO Raman band values are shown in **Table 4.4**. From the table we can see the peak shifting towards higher wave

number side. Peak shift observed for all blends, which indicates the intermolecular interaction between PAM and PVA. Maximum peak shift is observed for 50/50 wt% of PAM/PVA blend due to maximum intermolecular interaction.

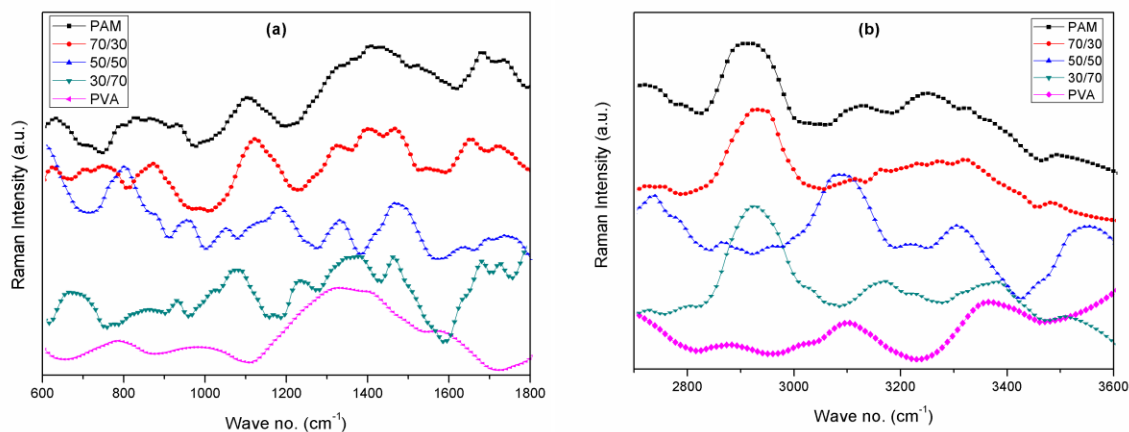


**Figure 4.4** Raman Spectra of pure PAM, pure PVA, 70/30, 50/50 and 30/70 blend ratio (a) in the region of 600-1800  $\text{cm}^{-1}$  (b) in the region of 2700-3600  $\text{cm}^{-1}$

**Table 4.3** Assignments of the Raman characterization bands of the pure PAM and pure PVA

Wave no. ( $\text{cm}^{-1}$ )	Assignment (PAM)	Wave no. ( $\text{cm}^{-1}$ )	Assignment (PVA)
854	C-C stretching	786	C-C Stretching
1107	C-O-C stretching	988	C-O-C Stretching
1400	C-N stretching	1333	-CH <sub>2</sub> wagging
1711	C=O Stretching	1577	O-H & C-H bending
2914	-CH <sub>2</sub> stretching	2875	-CH <sub>2</sub> Stretching
3124	-NH <sub>2</sub> symmetric stretching	3145	O-H stretching
3248	-NH <sub>2</sub> asymmetric stretching	3301	O-H stretching

**Table 4.4** Assignments of the Raman characterization bands of the PAM/PVA blends

Assignment	70/30	50/50	30/70
C–C Stretching	749	800	weak
C-C stretching	875	957	934
C-O-C stretching	1117	1186	1078
–CH <sub>2</sub> wagging	1321	1330	1355
C-N stretching	1466	1475	1464
O–H & C–H bending, C=O Stretching	1659	1740	1680
–CH <sub>2</sub> stretching	2933	3085	2923
O–H stretching, –NH <sub>2</sub> symmetric stretching	Over Lapped	3222	3171
–NH <sub>2</sub> stretching	3271	3305	3388
O–H stretching	weak	3546	3501

For 50/50 there is maximum shift for different Raman peaks. For 50/50, Mainly stretching vibration of C-N ( $1400\text{ cm}^{-1}$ ) blue shifted by  $75\text{ cm}^{-1}$  to  $1475\text{ cm}^{-1}$ , the C=O stretching vibration also blue shifted by  $29\text{ cm}^{-1}$  from  $1711\text{ cm}^{-1}$  to  $1740\text{ cm}^{-1}$ . Other vibrational peaks are also blue shifted as shown in the **Table 4.4**.

Addition of PVA into PAM polymer matrix, bands of PAM at  $3124\text{ cm}^{-1}$  and  $3248\text{ cm}^{-1}$  which are symmetric and asymmetric stretching vibration of –NH<sub>2</sub> group involved in inter molecular interaction of hydrogen bond coupled with –OH group of PVA at  $3145\text{ cm}^{-1}$  and  $3301\text{ cm}^{-1}$ . Spectra of blends clearly indicate the increase in the intensity with well separated bands in the region of  $3000\text{ cm}^{-1}$  to  $3600\text{ cm}^{-1}$ . But intensity of this broad band is maximum for 50/50 blend ratio than the others and peak shifting (at  $3149\text{ cm}^{-1}$  and  $3171\text{ cm}^{-1}$ ) in this region is toward higher wave number side, which indicates the strong hydrogen bonding between PAM and PVA due to –CONH<sub>2</sub> groups in PAM and –OH group in PVA.

#### 4.2.4. Mechanical Analysis

Mechanical properties of PAM/PVA were carried out to study the young's modulus (Y.M.), Ultimate tensile strength (UTS), stiffness, elongation at break, stress at break, Max load taken by films as shown in **Figure 4.5(a, b)**. Mechanical properties of blends were greatly influenced by

the introduction of PVA into PAM polymer matrix, which reveals the enhanced mechanical properties such as YM, UTS, stress at break and max load. The different mechanical properties values in blends are due to the different cross linking density provided by PVA with different weight percentage of PVA [55]. Polymers have either higher crystallinity, cross linking or rigid chain exhibit a higher strength and lower extensibility that is why young's modulus and ultimate tensile strength values are higher and will give lower elongation value [55, 56].

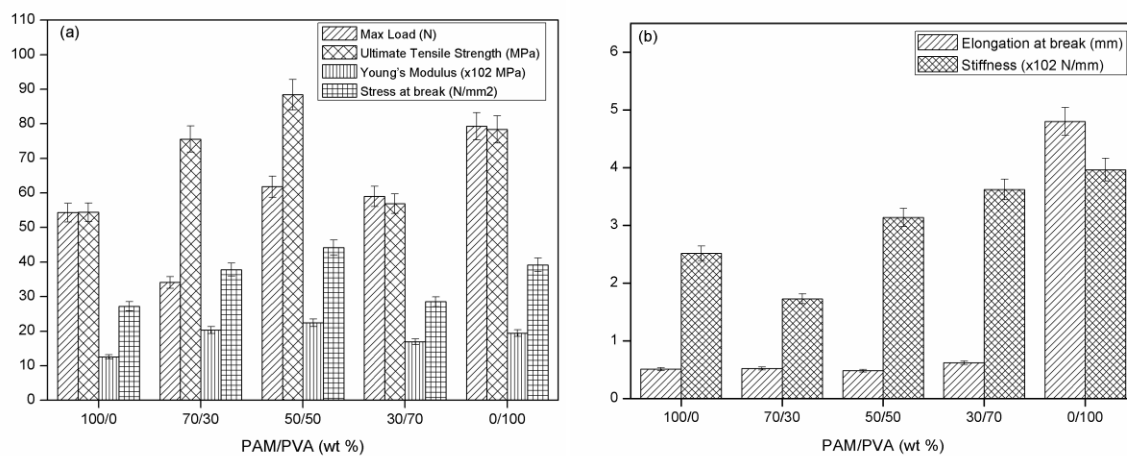


**Figure 4.5** Variation in (a) Max load, Ultimate tensile strength, Young's Modulus, stress at break (b) Elongation at break, Stiffness as a function of PAM/PVA content

From the graph our results also agrees with the above conclusion. For 50/50 blend ratio the YM and UTS values are higher but elongations have lower value. Blend of PVA with PAM effectively improve the mechanical properties. When PVA is blend with PAM, interaction at molecular level occurs, which reveals the enhancement of mechanical properties. Enhancement in mechanical properties is due to the possibility of a strong hydrogen bonding between  $-\text{CONH}_2$  groups in PAM and  $-\text{OH}$  group in PVA. This interaction becomes maximum for 50/50 wt% therefore we obtain maximum value of mechanical properties. This can also be correlated with IR analysis.

#### 4.2.5. Thermal gravimetric Analysis

The thermal degradation behavior of both pure polymer PAM and PVA and their blend samples were examined by TGA as shown in **Figure 4.6 (a)**. The initial weight loss for all samples observed due to moisture evaporation. Next decomposition was major weight loss. This may correspond to structural decomposition of polymer blends and higher weight loss in this region indicates the existence of chemical degradation. The major weight losses occur in the range of 180-390 °C for all the samples. The difference in the thermal decomposition is observed clearly from derivative TG (DrTG) curve as shown in **Figure 4.6 (b)**. Other than PVA, three thermal decomposition peaks ( $T_p$ ) were observed. Relevant data is shown in **Table 4.5**.

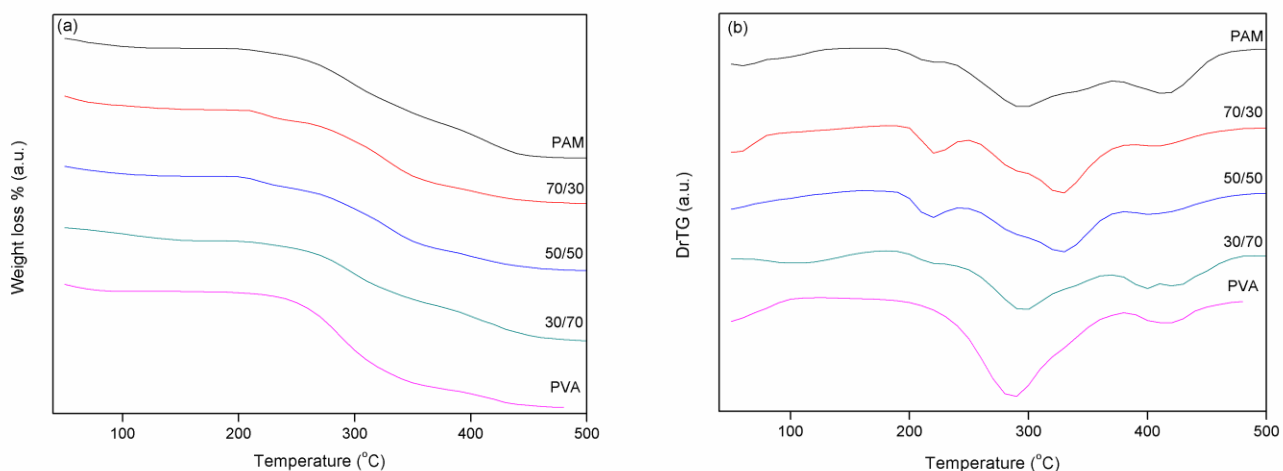


**Figure 4.6** (a) TG of pure PAM, pure PVA and blends (b) Dr TG of pure PAM, pure PVA and blends

**Table 4.5 TG and DrTG data of Pure PAM, PVA and their blended samples**

PAM/PVA	Temperature(°C)			Weight loss (%)
	Starting	Endin g	T <sub>p</sub>	
100/0	184	220	203	8.4
	230	369	294	31.7
	377	489	415	78.1
70/30	188	246	219	13.7
	248	382	325	50.2
	391	484	407	72.9
50/50	188	241	220	12.8
	250	380	330	47.9
	382	488	405	69.2
30/70	185	221	209	10.9
	228	368	295	32.2
	375	484	400	67
0/100	175	380	290	40.2
	382	475	416	86.2

T<sub>p</sub> (Peak Temperature) of DrTG is a function of blend weight percentage. T<sub>p</sub> was used as a measure of thermal stability. Thermal stability of blend is higher than the pure PAM, as indicated by the shift in T<sub>p</sub> towards higher temperature. T<sub>p</sub> was maximum for 50/50 wt %, so this blend is more stable. This higher thermal stability was observed for 50/50 blend sample by TGA and DrTG were due to the intermolecular crosslinking reaction which gave highly compatible impact blend system [16, 54]. From the data obtained by TGA indicates the possibility of a strong hydrogen bonding between PAM and PVA due to –CONH<sub>2</sub> groups in PAM and –OH group in PVA, which is also confirmed by our FTIR study.

From TGA, we conclude that the thermal stability regions of the blend samples were higher than the PAM and stability enhanced by increasing PVA content in PAM polymer matrix and it become more stable for 50/50 wt%.

#### 4.2.6. Scanning Electron Microscopy

From SEM image for PAM and PVA (**Figure 4.7(a), (b)**), smooth and homogeneous surface with some straps obtained. Formation of homogeneous blends was mostly caused by the interaction of hydrogen bonds between functional groups of blend components [57].

As shown **Figure 4.8 (a), (b)** and **(c)**, blends surfaces have heterogeneous mesh type morphology. This is possibly due to PVA, linear polymer, cross linked with PAM may form clusters/domains of chains bonding via hydrogen bond between  $-\text{CONH}_2$  groups in PAM and  $-\text{OH}$  group in PVA. At low content of PVA, crosslinking density is low. So the network chains have good movement and arrange themselves to make mess type of domain network. As PVA content increase, mesh/domain size goes on shrinking. A change in morphology toward smaller domains of a dispersed PVA is expected to give rise to an improvement in the mechanical properties. From SEM micrograph, interaction between PAM and PVA is much greater than others and surface of 50/50 blend ratio is rougher than the other blends. SEM analysis also indicates enhancement in thermal and mechanical properties.

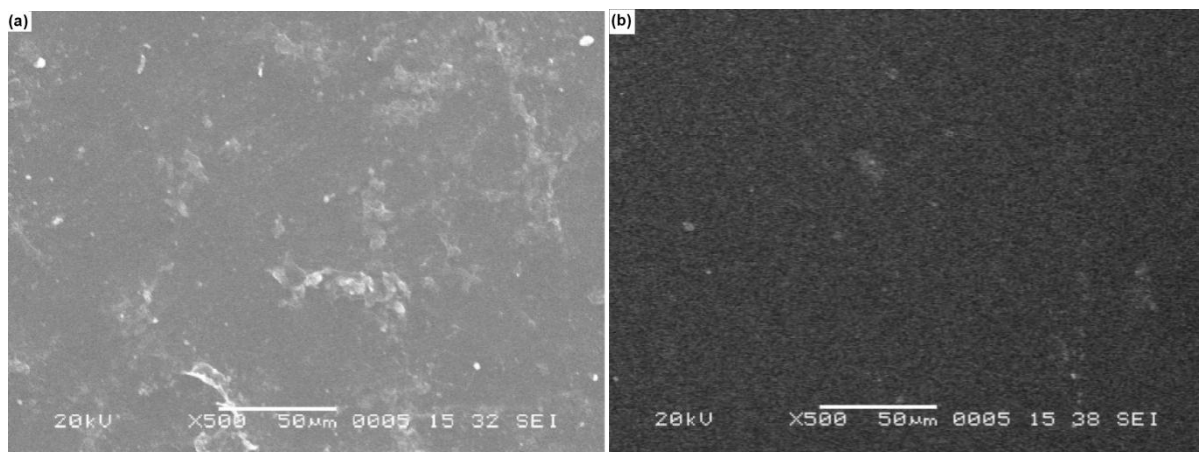


**Figure 4.7** Scanning Electron Micrograph of (a) Pure PAM (b) Pure PVA

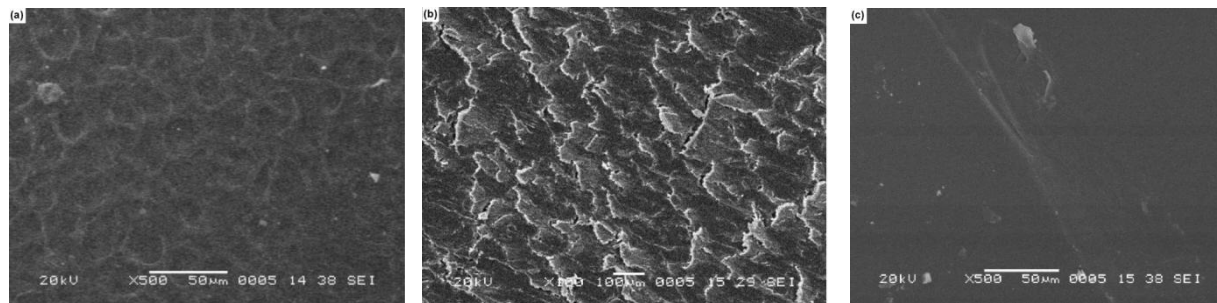


**Figure 4.8** Scanning Electron Micrograph of (a) 70/30 (b) 50/50 (c) 30/70

### 4.3. Conclusions

FTIR and Raman analysis confirmed the conclusion about the specific hydrogen bonding interaction between  $-\text{CONH}_2$  groups in PAM and  $-\text{OH}$  group in PVA. The maximum blue shift of IR peaks of 50/50 wt% implies that bond strength is increased. And that's why; thermal stability and mechanical properties are increased maximum for 50/50 wt%. So we directly correlate enhancement of thermal stability and mechanical properties by noticing the blue shift of IR peak which are contributed to intermolecular interaction between polymers. From UV-Vis studies, noticeable changes in absorption spectra were observed and change in various optical parameters also confirmed that intermolecular interaction occur between PAM and PVA. The position of absorption edge was slightly shifted towards higher wavelength side. Morphological changes in the blend samples were also explained and result was also correlated with the other studies. So from this study we concluded that blend of PAM/PVA with 50/50 wt% is most suitable and compatible with most enhancing properties.

#### 4.4. References

1. Tuncer CA, Serkan D. *Journal of Macromolecular Science, Part A: Pure and Applied Chemistry* 43:1113–1121, 2006.
2. Lopatin VV, Askadskii AA, Peregudov AS, Vasilev VG, *J. Appl. Polym. Sci.* 96:1043–1058. 2005.
3. Durmaz S, Okay O, *Polym. Bull.* 46:409–418, 2001.
4. El-Sabbagh S, Mokhtar SM, Messieh SLA, *Journal of Applied Polymer Science* 70:2053–2059, 1998.
5. Ratner BD, Hoffman AS, Schoen JF, Lemons JE. *Biomaterials Science, an Introduction to Materials in Medicine.* Academic Press, New York, 1996.
6. Bajpai AK, Bhanu S, *J. Mater. Sci. Mater. Med.* 15:43-54, 2004.
7. Peppas NA, Langer R, New challenges in biomaterials. *Science* 263:1715-1720, 1994.
8. Aalaie J, Farahani EV, *Iranian Polymer Journal* 21(3):175-183, 2012.
9. Abdelhak M , Abdelkarim H, Barbara I, *J. Chem. Chem. Eng.* 6:7-17, 2012
10. Lee KE, Poh BT, Morad N, Teng, *Int. J. Polym. Anal. Charact.* 13:95-107, 2008.
11. Lee KE, Poh BT, Morad N, Teng TT, *J. Macromol. Sci. A* 46:240-249, 2009.
12. Rho T, Park J, Kim C, Yoon HK, Suh HK, *Polym. Degrad. Stab.* 51:287-293, 1996.
13. Yang MH, *Polym. Degrad. Stab.* 76:69-77, 2002.
14. Wallace A, Wallace GA, Abouzam AM, *Soil Sci.* 141:377-380, 1986.
15. Rosen J, Hellenas KE, *Analyst* 127:880-882, 2002
16. El-Kader FH, Gafer SA, Basha AF, Bannan SI, Basha MAF, *Journal of Applied Polymer Science* 118:413–420, 2010.

17. Cholakis C H, Zingg W, Sefton M V, *J Biomed Mater Res.* 23:417-441, 1989.
18. Horiike S, Matsuzawa S, *J. Appl. Polym. Sci.* 58:1335-1340, 1995.
19. Vargas R A, Garcia A, Vargas M A, 43:1271-1274, 1998.
20. Fritz H P, Breitsmer M, *Solid State Ionics* 45:255-260, 1991.
21. Peppas N A *Hydrogels in Medicine and Pharmacy. Polymers*, CRC Press, Boca Raton, vol. II, 1987.
22. Rajendran S, Mahendran O, *Ionics* 7:463-468, 2001.
23. Coleman M M, Painter P C, *Prog. Polym Sci.* 20:1-59, 1995.
24. Jahanshahi M, Rahimpour A, Mortazavian N, *Iranian Polymer Journal* 21(6):375-383, 2012.
25. Yeom CK, Lee KH, *J. Membr. Sci.* 109:257- 265, 1996.
26. Muhlebach A, Muller B, Pharira C, Hofmann M, Seiferling B, Guerry DJ, *Polym. Sci. Part A: Polym. Chem.* 35:3603-3611, 1997.
27. Kim KJ, Lee SB, Han NW, *Polym J.* 25:1295-1302, 1993.
28. Rafienia M, Zarinmehr B, Poursamar SA, Bonakdar S, Ghavami M, Janmaleki M, *Iranian Polymer Journal* 22(2):75-83, 2013.
29. Tanga Q, Huang K, Qianb G, Brian C, Benicewicz, *Journal of Power Sources* 229:36-41, 2013.
30. Zhang X, Burgar I, Lourbakos E, Beh H, *Polymer* 45:330S–3312, 2004.
31. El-din HMN, El-Naggar AWM, Faten IA, *Polym Int.* 52:225–234, 2003.
32. Xu N, Zhou D, Li L, He J, Chen W, Wan F, Xue G, *J Appl Polym Sci.* 88:79–87, 2003.
33. Barretta P, Bordi F, Rinaldi C, Paradossi G, *J Phys Chem B* 104(47):11019–11026, 2000.
34. Chan LW, Hao JS, Heng PWS, *Chem Pharm Bull.* 47(10):1412–1416, 1999.
35. Hassan CM, Peppas NA, *Adv Polym Sci.* 153:37–65, 2000.

36. Russo R, Macinconico M, Petti L, Romano G, J Polym Sci Part B: Polym Phys. 43(10):1205–1213, 2005.
37. Elashmawi IS, Hakeem NA, Abdelrazek EM, Physica B 403:3547– 3552, 2008.
38. Mohan S, Murugan R, Arabian J Sci Eng. Sect. A 22(2A):155–164, 1997.
39. Murugan R, Mohan S, Bigotto A, J Korean Phys Soc. 32(4):505–512, 1998.
40. Deng Y, Dixon JB, White GN, Loeppert RH, Anthony S, Juom R, Colloids and Surfaces A: Physicochem Eng Aspects 281:82–91, 2006.
41. Freddi G, Tsukada M, Beretta S, J Appl Polym Sci. 71:1563-1571, 1991.
42. Yan F, Zheng CR, Zhai XD, Zhao DJ, J Appl Polym Sci. 67:747-754, 1998.
43. Li X, Goh SH, Lai YH, Wee ATA, Polymer 41:6563-6571, 2000.
44. Abdelaziz M, Abdelrazek EM, Physica B 390:1-9, 2007.
45. Laot CM, Marand E, Oyama HT, Polymer 40:1095-1108, 1999.
46. Abdelrazek EM, Elashmawi IS, Labeeb S, Physica B 405:2021–2027, 2010.
47. Knudsen R, Sala O, Hase Y, J. Mol. Struct. 321(3):197-203, 1994.
48. Raaska T, Kunttu H, Räsänen M, Luppi J, Pajunen P, J. Mol. Struct. 221:195-208, 1990.
49. Patel G, Sureshkumar MB, Patel P, AIP Conf. proc. 1349:166-167, 2011.
50. Tauc J, Grigorovici R, Vanku A, Phys. Stat. Sol. (b) 15:627-637, 1966.
51. Shahada L, Kassem ME, Abdelkader HI, Hassan HM, J. Appl. Polym. Sci. 65:1653-1657, 1997.
52. Mott N F, Davis E A, Electronic processes in Non Crystalline materials. 2<sup>nd</sup> edn. Oxford university press, Oxford, 1973.
53. El-Samanoudy M M, Ammar A H, Status Solidi A 187(2):611-621, 2001.
54. Aggour YA, Polm. Degrade. Stab. 51:265-269, 1996.

55. Patel G, Sureshkumar MB, Singh NL, Bhattacharya SS, *Journal of International Academy of Physical Sciences* 14:91-100, 2010.
56. Chi SK, Seung MO, *Electrochim acta* 46:1323-1331, 2001.
57. Chen CH, Wang FY, Mao CF, Liao WT, Hsieh CD, *International Journal of Biological Macromolecules* 43(1):37-42, 2008.

## Chapter 5

# Characterization of PAM/PEO Blends

---

### *Abstract*

*This chapter gives an account of the characteristics of PAM/PEO blend in different weight proportion (70/30, 50/50 and 30/70) which is prepared by solution cast technique. These blends are investigated by spectroscopic techniques like FTIR, UV-Vis and RAMAN. Mechanical, Thermal and Morphological properties are also investigated. The results obtained from different characterization techniques show the blending effect on different properties. These properties of PAM/PEO blends are correlated with spectroscopic investigation.*

## 5.1. Introduction

Blending of polymers is an interesting as well as important route for providing new materials with desirable properties with economically low cost [1]. The properties of polymer blend can be controlled by blend morphology, blend composition and its processing condition [2]. The study of blend properties are very important to find its new applications in the field of biomedical and pharmacy [3, 4]. Polymer compatibility is an important criterion when dealing with blends. Polymer-polymer miscibility arises due to any specific interaction such as hydrogen bonding, dipole-dipole interaction or charge transfer process for pure polymer mixtures [5-8].

Due to increase in the applications of polymer in biomedical field, study of water soluble polymer like Poly (ethylene oxide) (PEO), poly (vinyl alcohol) (PVA), and polyacrylamide (PAM) have great interest [9, 10]. It is important to note that there are only very few studies on their blends. Polyacrylamide is used in multitude applications including water clarification, waste water treatment, oil recovery, agriculture and biomedical applications [11-13]. The high bio-adhesive property of acrylic polymers offers good prospects for using these polymers in controlled drug delivery systems for local applications [14, 15]. Structural and physical properties of elements doped PAM are far studied [16].

PEO is semi crystalline synthetic polymer. Because of its biocompatibility; it is used in many biomedical devices including drug delivery and tissue replacement [17-19]. PEO/Starch blends present great application in scaffolds for cell culture and tissue engineering [20, 21]. PEO has moderate tensile strength and it possesses good mechanical and electrical properties [22]. Some work is reported on optical and electrical properties of PEO based polymer electrolyte film [23-25]. Ferreiro et. al. reported that, when there is a change in blend ratio of PEO/PMMA, morphological transitions occurs [26, 27]. Chemical structure of PEO (presence of ether oxygen

and -OH end groups) makes some possibilities of hydrogen bonds formation, as it was already confirmed for e.g. PEO/poly (vinyl alcohol) and PEO/unsaturated polyester resin systems shows hydrogen bonding interaction [28, 29].

PAM and PEO individually blend with other polymers but to the best of our knowledge, there is no study of interaction of PAM and PEO polymer blends together. Only Vijayalakshmi et. al. has been studied thermal degradation characterization of blend of PEO and PAM [30, 31]. So the authors spot light on the preparation of solid films of PAM and PEO blends and also on the structural, thermal, optical, mechanical properties and morphological study of these blends. By means of FTIR and Raman spectroscopy, authors gives information regarding the intermolecular interaction between two polymer chains of PAM and PEO, which is quite helpful for the study of compatibility and miscibility of blends and the results were correlated with the results obtained from the other characterization techniques.

## **5.2. Results and Discussion**

### **5.2.1. FTIR Analysis**

FTIR spectroscopy of blend films were carried out to detect peak shifts, which may be due to interaction like hydrogen bonding between two polymers. Infrared spectroscopy is a fundamental technique to find out the presence of hydrogen bond which is characterized by changes in absorption bands of functional groups, which involved in the formation of hydrogen bond [32]. As absorption of the functional groups changes, it changes the force constant of donor and acceptor groups and due to this, frequencies of stretching and deformation of these groups are changing [32].

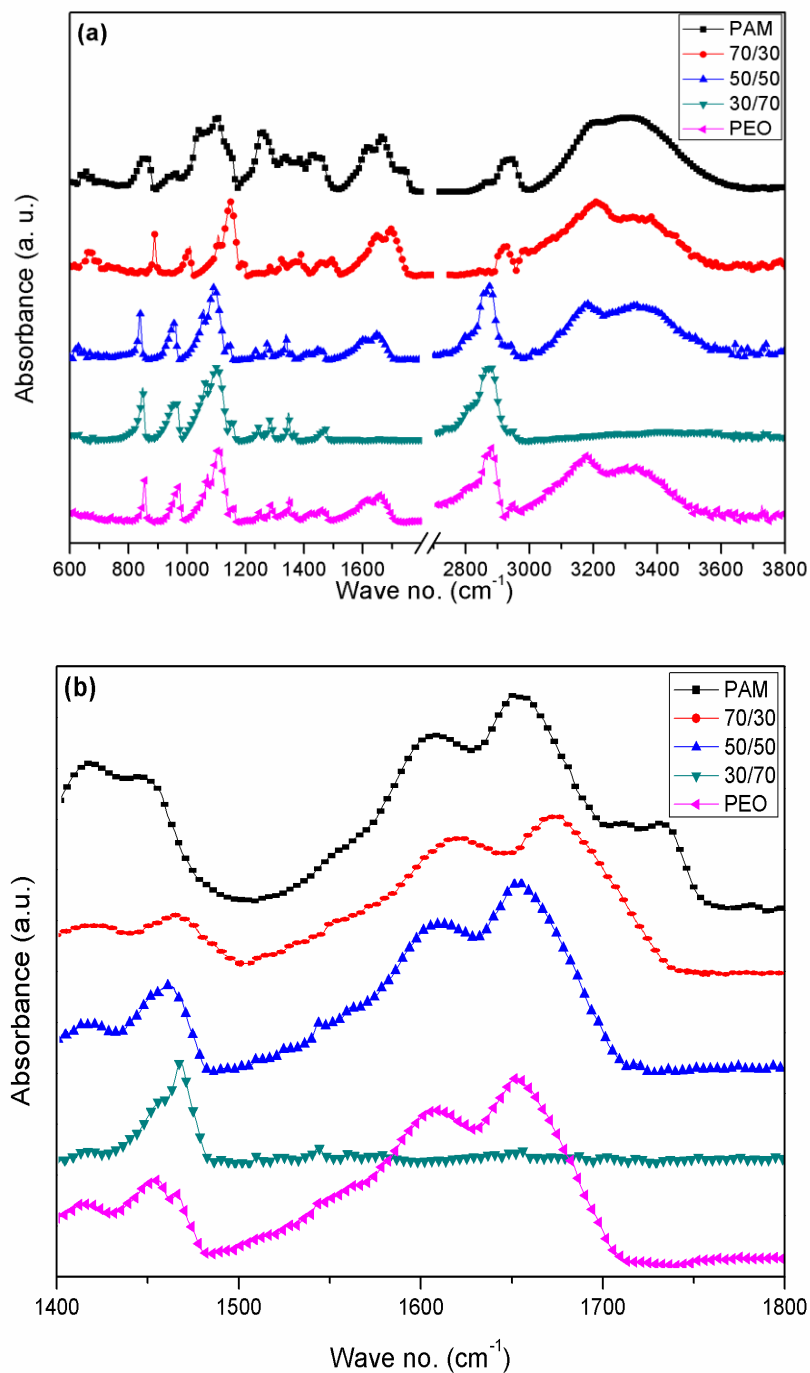


**Figure 5.1** FTIR Spectra of Pure and blend polymers (a) in the region of 600-3800 cm<sup>-1</sup> (b) in the region of 1400-1800 cm<sup>-1</sup>

**Figure 5.1** shows the spectra of pure polymers and blend films. Peak values for pure and blend polymers are shown in **Table 5.1**. PAM has two bands at  $3315\text{ cm}^{-1}$  and  $3212\text{ cm}^{-1}$  indicates N-H stretching vibrations and absorption peak at  $1651\text{ cm}^{-1}$  is due to C = O stretching, a peak at  $1607\text{ cm}^{-1}$  is attributed to N-H bending and at  $1447\text{ cm}^{-1}$  is due to C-N stretching vibrations [33, 34]. Poly Ethylene Oxide has two strong absorption bands at  $3332\text{ cm}^{-1}$  and  $3177\text{ cm}^{-1}$  which indicates -OH stretching vibrations and absorption band at  $2881\text{ cm}^{-1}$  is for asymmetric stretching of  $-\text{CH}_2$  group. Peaks at  $1610\text{ cm}^{-1}$  and  $1655\text{ cm}^{-1}$  indicate bound  $\text{H}_2\text{O}$  solvent in PEO polymer matrix in crystal form [34].

Compared with the pure polymers, for PAM/PEO blends, the absorption bands at  $3000\text{-}3600\text{ cm}^{-1}$  corresponding to  $-\text{OH}$  and  $-\text{NH}$  stretching vibrations, the intensity of peaks decreases and clearly shifted peaks indicates the formation of strong intermolecular hydrogen bonding between the  $-\text{CONH}_2$  group of Polyacrylamide and  $-\text{OH}$  group of Poly Ethylene Oxide. For 70/30 wt% of PAM/PEO blend, this shift is maximum on higher wave number side, so it has strong tendency for the formation of strong hydrogen bond [32, 35]. As we increase content of PEO in the blend, the above peak intensity starts decreasing and becomes very weak for 30/70 wt%. In the region  $1400 - 1800\text{ cm}^{-1}$  we observed four important peaks. The C-N stretching vibration of PAM shifted to higher wave number ( $1447$  to  $1469\text{ cm}^{-1}$ ) and the  $-\text{CH}_2$  scissoring vibration of  $-\text{CH}_2\text{OH}$  group of PEO also tends to shift towards higher wave number ( $1454$  to  $1469\text{ cm}^{-1}$ ). The N-H bending vibration of PAM is observed at  $1607\text{ cm}^{-1}$ . For blends it also shifts towards higher wave number ( $1607$  to  $1620\text{ cm}^{-1}$ ). Peak at  $1651\text{ cm}^{-1}$ , due to C=O stretching vibration of  $-\text{CONH}_2$  group of PAM is also shifted to higher wave number side to  $1678\text{ cm}^{-1}$ . These peak shifting observations support the formation of hydrogen bonding between  $-\text{CONH}_2$  group of

**Table 5.1** Assignments of the FT-IR characterization of bands of the pure PAM, pure PEO and PAM/PEO blend [16, 18, 36-38].

Wave no. (cm <sup>-1</sup> )	Peak Assignment (PAM)	Wave no. (cm <sup>-1</sup> )	Peak Assignment (PEO)	70/30 (wt %)	50/50 (wt %)	30/70 (wt %)
857	C-C Symmetric stretching	852	C-C Symmetric stretching	855	858	852
956	C-C Asymmetric stretching	966	-CH <sub>2</sub> rocking	974	974	956
1107	C-O-C stretching	1106	C-O-C stretching	1119	1107	1095
1447	C-N stretching	1454	-CH <sub>2</sub> scissoring	1469	1457	1469
1607	N-H bending	1610	Bound H <sub>2</sub> O in PEO	1620	1609	weak
1651	C=O Stretching	1655	matrix as solvent	1678	1654	weak
2938	C-H Asymmetric stretching	2881	C-H Asymmetric stretching	2950	2893	2875
3212	N-H Symmetric stretching	3177	-OH stretching	3229	3195	weak
3315	N-H Asymmetric stretching	3332	-OH stretching	3371	3354	weak

PAM and -CH<sub>2</sub>OH group of PEO. In this region maximum peak shift is observed for 70/30 wt% on higher wave number side. From all the blend spectra, peaks shift are observed for all blends, indicating that the intermolecular interaction occurs between two polymer chains. But for 70/30 wt% of PAM/PEO blend, maximum peak shift on higher wave number side are observed due to maximum intermolecular interaction. This indicates that the bond strength for 70/30 wt% is increased.

Final conclusion from all FTIR spectra can be drawn is that intermolecular interactions of hydrogen bonding with increasing bond strength between -CONH<sub>2</sub> group of PAM and -CH<sub>2</sub>OH group of PEO were confirmed by FTIR spectra and it is maximum for 70/30 wt%. Due to which we are getting higher mechanical and thermal properties of blend films.

### 5.2.2. UV-Vis Analysis

The absorption of light energy by polymeric materials in the UV-Vis region involves transition of electrons in  $\sigma$ ,  $\pi$  and n-orbital from the ground state to higher energy states [43-45]. The optical absorption method can be used for the investigation of the optically induced transitions and can provide information about the band structure and energy gap in crystalline and non-crystalline materials [46].

The absorbance process plays an important role in the optical properties of the polymers. The absorption coefficient was determined from the UV-VIS spectra using the formula:

$$\alpha = A/d \quad (1)$$

Where A is the absorbance and d is the thickness of the film. The Tauc relation for dependence of absorbance on photon energy is [47]:

$$\alpha(\nu) = B(h\nu - E_g)^x / h\nu \quad (2)$$

Where  $\alpha(\nu)$  is the absorption coefficient,  $E_g$  is the optical energy gap of the substance, h is plank's constant,  $\nu$  is the corresponding frequency, x is the parameter that gives the type of electron transition. It was observed that two distinct linear relations were found for  $x = 1/2$  (Direct transition) and  $x = 2$  (Indirect transition), corresponding to different inter band absorption processes and factor B depends on the transition probability and can be assumed to be constant within the optical frequency range [48, 49]  $E_g$  is the optical energy gap. On the basis of equation 2, direct and indirect band gap and absorption edge were determined.

### *Absorbance and band edges*

**Figure 5.2 (a)** shows the absorption spectra of the Pure and blended polymer films. From the spectra, peak height increases, band edge increases and the absorption band is found to shift towards shorter wavelengths with increasing the weight percentage of PEO. The optical absorption coefficient ( $\alpha$ ) was determined from the absorption spectra using equation (1). The plot of absorption coefficients ( $\alpha$ ) versus photon energy ( $h\nu$ ) of the pure and blended polymer films are shown in **Figure 5.2 (b)**. The position of the absorption edge values were calculated by extrapolating the linear portions of this plots to zero absorption values as shown in **Table 5.2**.

### *Direct and indirect optical band gap*

The optical band gap of the Pure and blend samples was determined from the UV–Vis spectra. The value of the optical direct and indirect energy gap is determined from the intersection of the extrapolated line of the curves with the photon energy axis at zero absorption value. In an allowed direct transition the electron is simply transferred vertically from the top of the valence band to the bottom of the conduction band, without a change in momentum (wave vector) [50]. For the determination of the direct optical band gap,  $(\alpha h\nu)^2$  was plotted as a function of photon energy ( $h\nu$ ) as shown in **Figure 5.2 (c)**.

In indirect band gap, a transition from the valence to the conduction band should always be associated with a phonon of the right magnitude of crystal momentum [48]. For indirect transition photon assistance requires. Indirect band gaps are obtained from the plots of  $(\alpha h\nu)^{1/2}$  versus photon energy ( $h\nu$ ) as shown in **Figure 5.2 (d)**. The values of direct and indirect band gap for the pure and blended films are listed in **Table 5.2**. From the **Table 5.2**, it is seen that direct and indirect band gap increases with increasing PEO percentage.

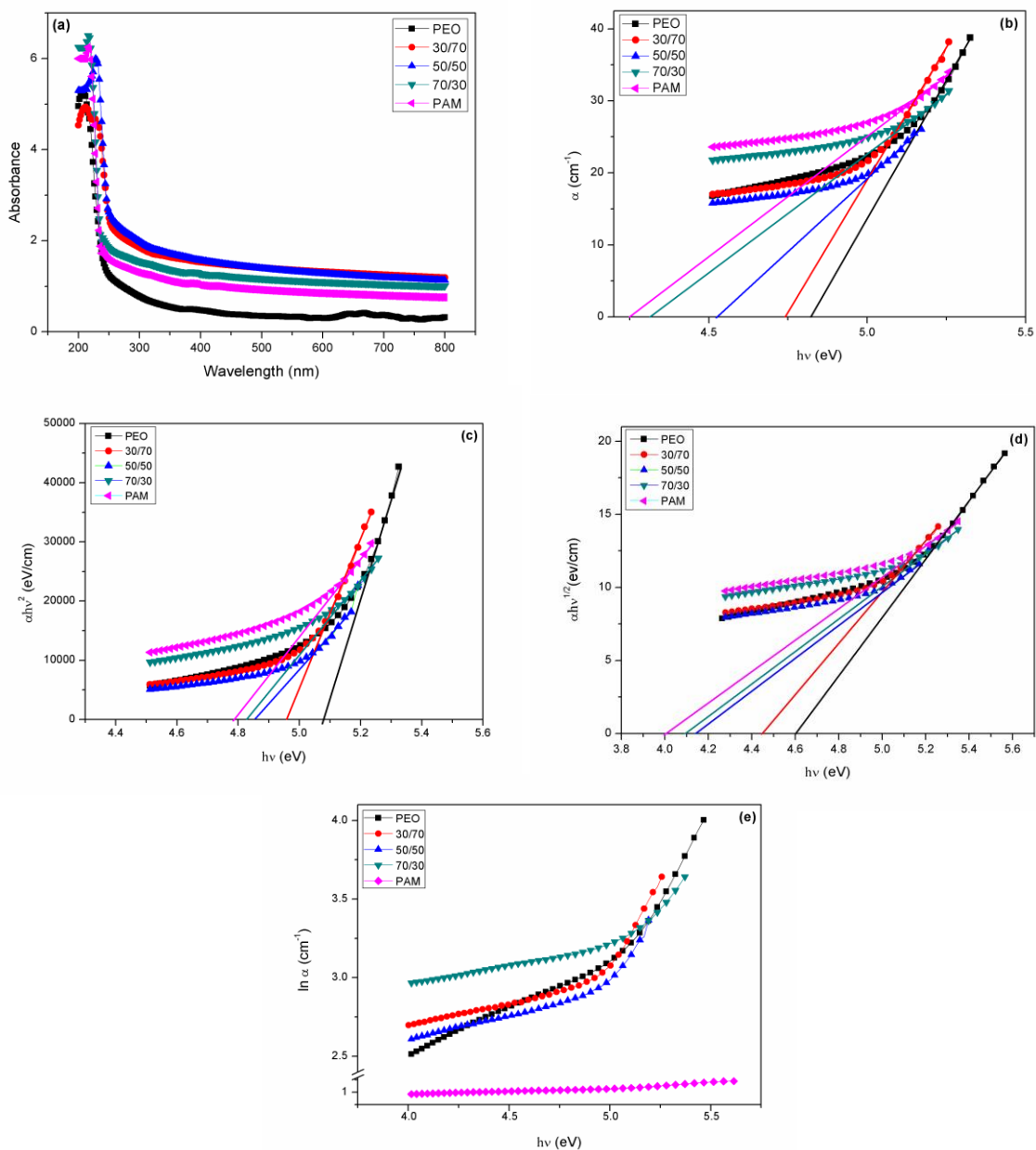


**Figure 5.2** Plot of (a) Absorption coefficient ( $\alpha$ ) vs Wavelength ( $\lambda$ ), (b) Absorption coefficient ( $\alpha$ ) vs Photon Energy ( $h\nu$ ), (c)  $(\alpha h\nu)^2$  vs  $h\nu$ , (d)  $(\alpha h\nu)^{1/2}$  vs  $h\nu$ , (e)  $\ln \alpha$  vs Photon Energy ( $h\nu$ )

This increase in the optical band gap values is due to the formation of defects due to the blending, and the interaction between the polymer chains [51-53] and the formation of some bonds [54]. As the crystalline nature of the films increases, the charge carrier cannot find a continuous chain to travel which causes the increase in the band gap, which in turn shows the effect of blending on the optical properties [48].

### ***Activation energy***

The optical activation energy can be determined using the Urbach rule [55] as

$$\alpha = B \exp(h\nu/E_a) \quad (3)$$

Where  $B$  is a constant and  $E_a$  is the activation energy, i.e. the inverse slopes of the exponential edge. The latter is interpreted as the width of the tail of localized states extending into the forbidden band gap from either the valence or conduction band [49].

The values of activation energy  $E_a$  is determined by taking the reciprocals of the slopes of the linear portions of plots of  $\ln \alpha$  versus photon energy ( $h\nu$ ) as shown in **Figure 5.2 (e)**. The values of  $E_a$  for the Pure and blended doped films are listed in **Table 5.2** and it increases with PEO wt%.

**Table 5.2** Absorption edge, optical band gap (both direct and indirect) and activation energy values of pure PAM, pure PEO and PAM/PEO polymer blend films.

<b>Composition (PAM/PEO)</b>	<b>Absorption edge (eV)</b>	<b>Direct Band gap (eV)</b>	<b>Indirect Band gap (eV)</b>	<b>Activation energy <math>E_a</math>(eV)</b>
100/0	4.26	4.79	4.01	0.59
70/30	4.34	4.83	4.09	0.88
50/50	4.55	4.86	4.15	1.96
30/70	4.74	4.96	4.45	2.11
0/100	4.83	5.07	4.59	2.38

### 5.2.3. RAMAN Analysis

The Raman spectroscopy is a suitable and efficient method for the structural analysis of polymers. It is possible to characterize molecular bonds in various phase and conformational states with the help of Raman spectroscopy. If two polymers are fully or partially miscible then, their Raman spectra have considerable difference in band position and shapes between the spectra of blend and each of the pure polymers [39].

Distinctive differences between PAM and PEO can be observed from their Raman spectra as shown in **Figure 5.3 (a, b)**. Raman peak values for pure and blend polymers are shown in **Table 5.3**. The bands near  $854\text{ cm}^{-1}$  corresponding to C-C stretching region of PAM. The bands at  $1107\text{ cm}^{-1}$  are attributed to the C-O-C stretching modes of PAM. The band near  $1400\text{ cm}^{-1}$  is assigned mainly to the C-N stretching vibration and a band near  $1711\text{ cm}^{-1}$  is attributed to C=O stretching mode of the PAM polymer chain.

For PEO, it is possible to observe the intense bands at  $847\text{ cm}^{-1}$  and  $1104\text{ cm}^{-1}$ , corresponding to the stretching modes of C-C and C-O respectively. The Raman band at  $1336\text{ cm}^{-1}$ ,  $1454\text{ cm}^{-1}$  and  $1633\text{ cm}^{-1}$  is correspondingly assigned to the  $-\text{CH}_2$  wagging,  $-\text{CH}_2$  deformation and  $-\text{CH}_2$  twisting.

Peak shift is observed for all blends, which indicates the intermolecular interaction between two polymer chains. Maximum peak shift are observed for 70/30 wt% of PAM/PEO blend due to maximum intermolecular interaction. In the range of the stretching vibrations of the  $-\text{CH}_2$  and  $-\text{CH}_3$  groups, an increase in the PEO content causes an increase in the intensity of the line assigned to the symmetrical vibration of the  $-\text{CH}_2$  group and a simultaneous monotonic shift of the peak position of this line from  $2919\text{ cm}^{-1}$  to  $2879\text{ cm}^{-1}$ .

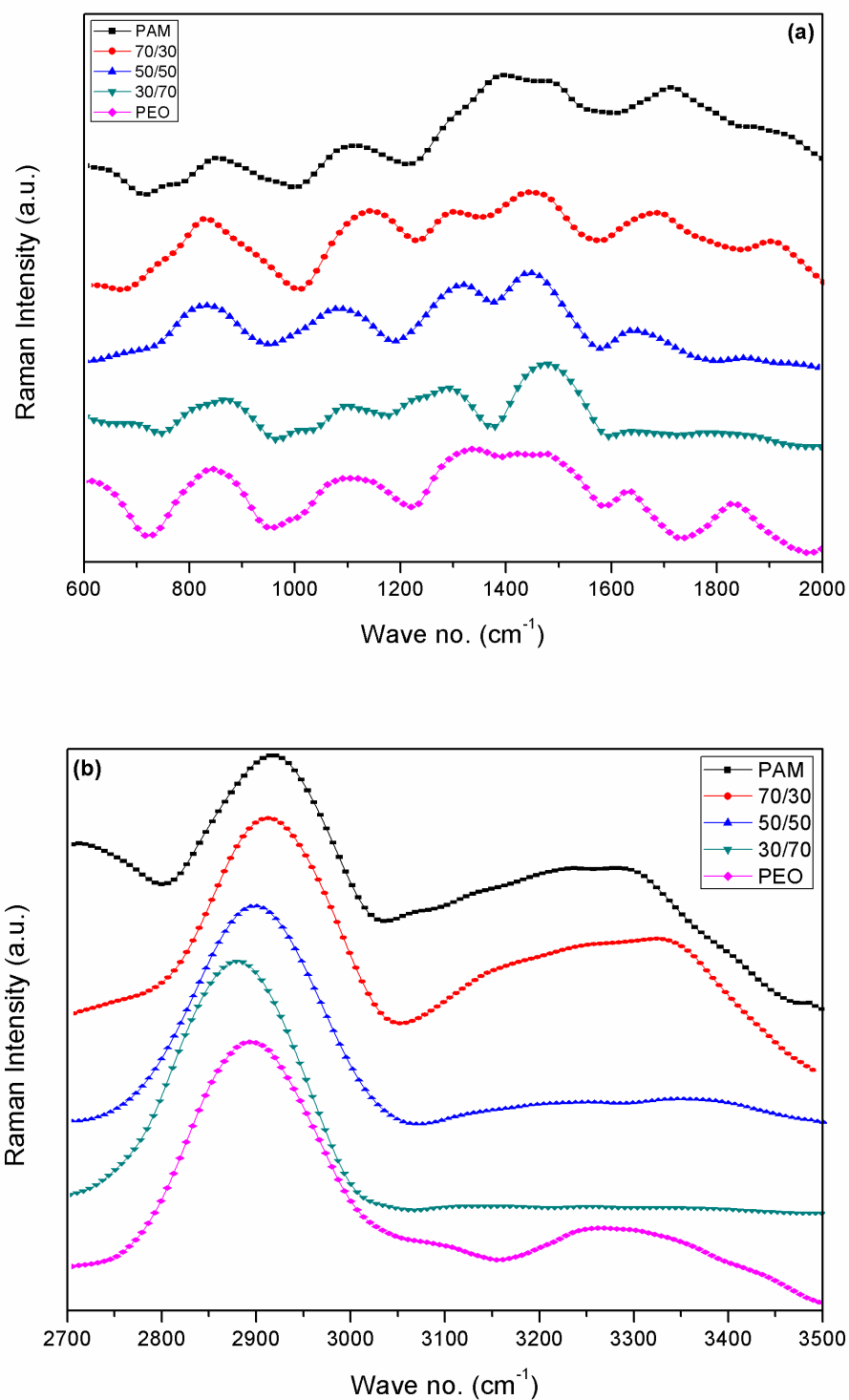


**Figure 5.3** Raman spectra of pure and blend films in the range (a) 600-2000 cm<sup>-1</sup> (b) 2700-3500 cm<sup>-1</sup>

Maximum peak shift is observed for 30/70 wt% on lower wave number side which indicates the decrease in bond strength. A simultaneous decrease in the intensities of the lines peaked at 3259  $\text{cm}^{-1}$  and 3270  $\text{cm}^{-1}$ , which is assigned to the  $-\text{NH}_2$  stretching of PAM and  $-\text{OH}$  stretching region of PEO respectively. Which is confirmed the interaction between  $-\text{CONH}_2$  group of PAM and  $-\text{CH}_2\text{OH}$  group of PEO. For these groups, maximum peak shift to higher wave number side is observed for 70/30 wt% (**Table 5.3**), which indicates the enhancement of bond strength.

We can see that for 30/70 blend ratio, peaks of  $-\text{NH}_2$  stretching of  $-\text{CONH}_2$  group of PAM and  $-\text{OH}$  stretching of  $-\text{CH}_2\text{OH}$  group of PEO is almost disappear, which reveals the interaction between these two group of pure polymers. A peak at 1479  $\text{cm}^{-1}$  becomes prominent and intense due to interaction, which means  $-\text{CONH}_2$  group of PAM convert into  $-\text{CH}_2\text{NH}_2$  group due to the interaction with  $-\text{CH}_2\text{OH}$  group of PEO [40]. Peaks of  $\text{C}=\text{O}$  stretching and  $-\text{NH}_2$  stretching are very weak, it also confirm our prediction. From all the Raman spectra, we concluded that hydrogen bonding interaction at molecular level occurs between  $-\text{CONH}_2$  group of PAM and  $-\text{CH}_2\text{OH}$  group of PEO which confirmed FTIR results.

**Table 5.3** Assignments of Raman bands of pure PAM, Pure PEO and PAM/PEO blends [37, 41-42].

PAM	Peak Assignment	PEO	Peak Assignment	70/30 (wt %)	50/50 (wt %)	30/70 (wt %)
854	C-C stretching	847	C-C stretching	833	829	865
1107	C-O-C stretching	1104	C-O stretching	1143	1086	1100
		1336	$-\text{CH}_2$ wagging	1300	1318	1290
1400	C-N stretching	1454	$-\text{CH}_2$ deformation	1460	1450	1479
1711	$\text{C}=\text{O}$ Stretching	1633	$-\text{CH}_2$ twist	1686	1650	weak
2919	$-\text{CH}_2$ stretching	2894	$\text{CH}_3$ stretching	2919	2898	2879
3259	$-\text{NH}_2$ stretching	3270	$-\text{OH}$ stretching	3323	weak	weak

#### 5.2.4. Mechanical Analysis

Mechanical properties of PAM/PEO were taken to study the Max load, Ultimate tensile strength (UTS), young's modulus (Y.M.), stress at break, stiffness and elongation at break for pure and blends films as shown in **Figure 5.4**. The mechanical properties in blends are changed, because pure polymer matrix provided different cross linking density with different weight% of blended polymer [56]. Those polymers, which have higher crystallinity, cross linking density or rigid chain, they gain a higher strength and lower extensions and therefore polymers with higher young's modulus and ultimate tensile strength value will have lower elongation value [56-58]. When we introduce PEO into PAM polymer matrix, mechanical properties of blends are greatly influenced. From the graph our results also agrees with the above conclusion. For 70/30 blend ratio the YM and UTS values are higher but have lower elongations value. Blend of PEO with PAM successfully improved the mechanical properties. When PEO is blended with PAM,

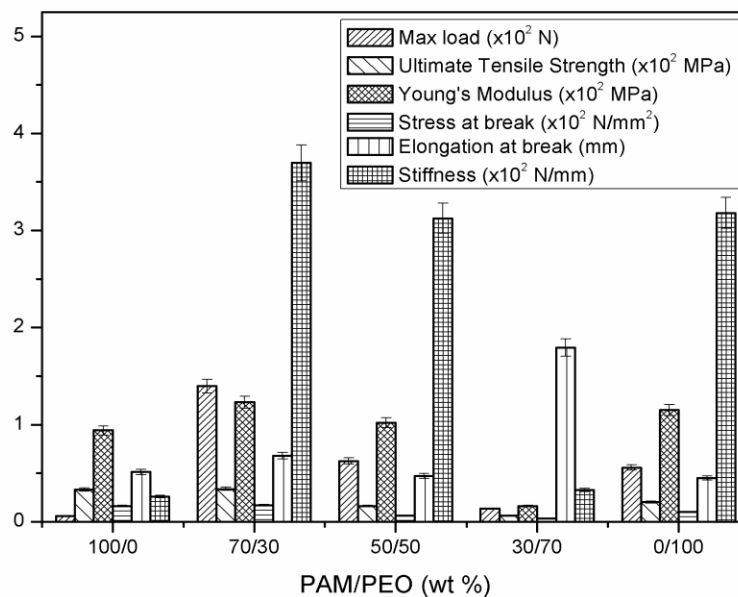


**Figure 5.4** Variation in Max load, Ultimate tensile strength, Young's Modulus, stress at break, Elongation at break, Stiffness as a function of PAM/PEO content

interaction at molecular level occurs, which causes the enhancement in mechanical properties. Enhancement in mechanical properties is due to the strong hydrogen bonding between  $-\text{CONH}_2$  groups in PAM and  $-\text{OH}$  group in PEO. This interaction becomes maximum for 70/30 wt%. Therefore we obtain maximum value of mechanical properties. This can also be correlated with IR analysis. As the maximum higher peak shift was observed for 70/30 wt% which indicates strong bond interaction and hence increase in mechanical properties.

### 5.2.5. Thermo gravimetric Analysis

Thermogravimetric analysis (TGA) is the most suitable methods for studying the thermal properties of polymers. The TGA and derivative TGA (DrTG) curve provides information about the nature and extent of degradation of the polymers. The effect of blend weight percentage on the TGA and DrTG of PAM/PEO blends are shown in **Figure 5.5 (a, b)**. Detailed information of thermograms is shown in **Table 5.4** and **Table 5.5**.

An important thermal property is the temperature corresponding to the maximum rate of weight loss ( $T_p$ ), which is defined as the peak value of the first derivative of the TGA curve.  $T_p$  was used as a measure of thermal stability. The first derivative curves for pure PAM, pure PEO and their blends are shown in **Figure 5.5 (b)** and their  $T_p$  values are listed in **Table 5.4**.

Thermal stability of blend is higher than the pure PAM because  $T_p$  shifted towards higher temperature.  $T_p$  was a maximum for 70/30 wt %, so this blend ratio is more thermally stable. This higher thermal stability was observed for 70/30 wt % blend sample by TGA and DrTG were due to the intermolecular cross linking reaction which gave highly compatible impact blend system [59, 60].

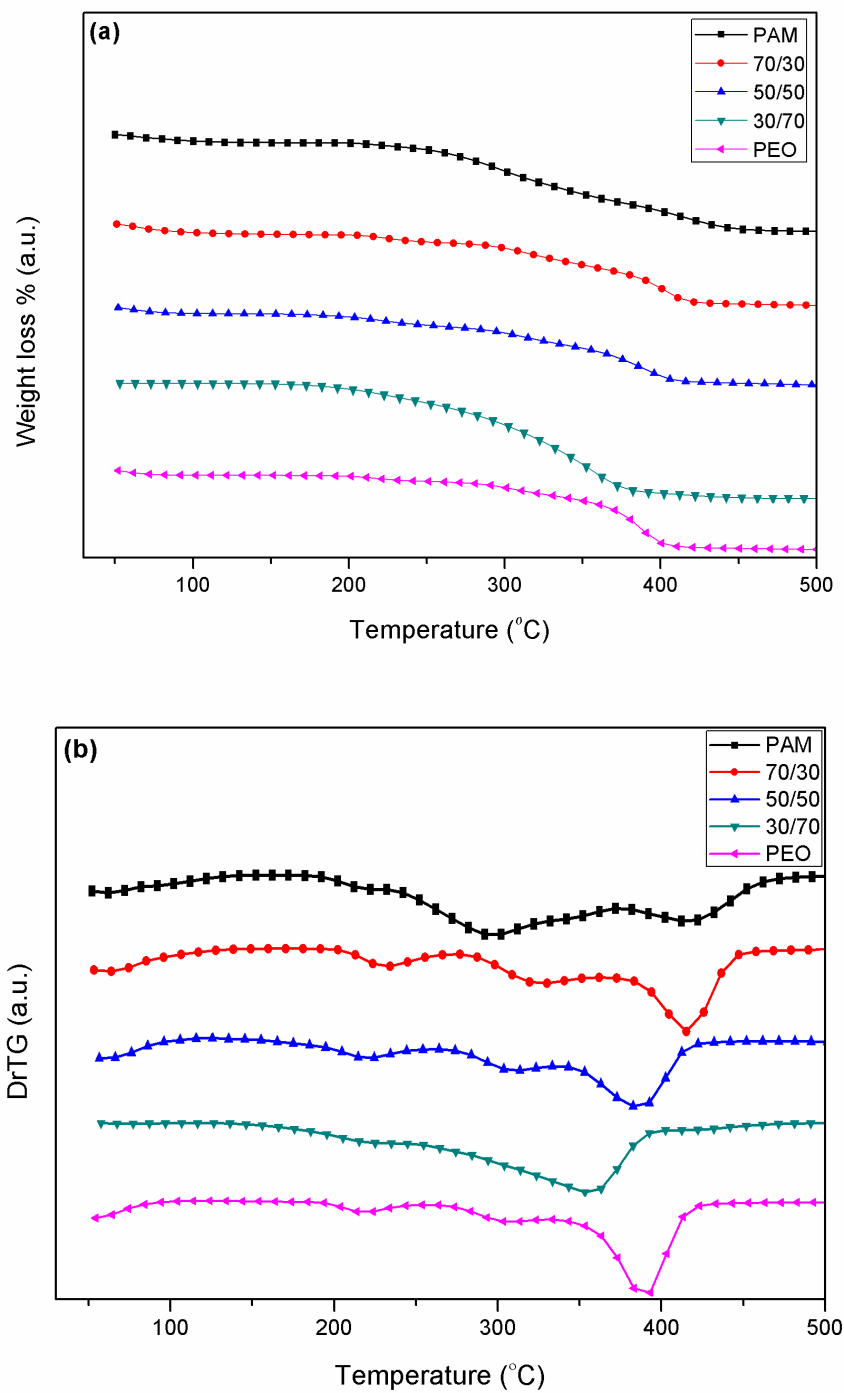


Figure 5.5 (a) TG of pure PAM, pure PEO and blends (b) Dr TG of pure PAM, pure PEO and blends

**Table 5.4 TG and DrTG data of Pure PAM, PEO and their blended samples**

PAM/PEO	Temperature(°C)		
	Starting	Ending	T <sub>p</sub>
100/0	184	220	203
	230	369	294
	377	489	415
70/30	190	254	218
	265	335	308
	350	503	391
50/50	150	253	214
	262	331	302
	341	457	385
30/70	130	238	214
	248	403	357
0/100	183	249	216
	260	328	305
	336	443	383

**Table 5.5 Effect of the Blend Ratio on the Temperatures Corresponding to Different Percentage Weight Losses in PAM/PEO Blends**

PAM/PEO Blend	T <sub>30</sub> (°C)	T <sub>40</sub> (°C)	T <sub>50</sub> (°C)	R <sub>500</sub> (%)
100/0	290	311	334	9.77
70/30	304	330	361	17.75
50/50	300	329	358	15.19
30/70	284	305	321	0.15
0/100	337	363	376	12.50

**Table 5.5** gives an idea about the effect of the blend ratio on the temperature corresponding to different weight losses (viz.  $T_{30}$  = temperature corresponding to 30 wt % degradation, and so on). It is observed from the table 5 that the 70/30 wt% had maximum temperature value for different weight losses. So we can conclude that the 70/30 wt% have greater thermal stability as compared to pure component.  $R_{500}$  indicate the residue value of polymer content at 500 °C. This value was also higher for the blend ratio of 70/30 wt%. From TGA, we conclude that the thermal stability regions of the blended samples were higher than the PAM and stability enhanced by increasing PEO content in PAM polymer matrix and it becomes more stable for 70/30 wt%. The thermal stability regions of the blended samples were higher than the PAM and stability enhanced by increasing PEO content in PAM polymer matrix and it becomes more stable for 70/30 wt%. This indicates the possibility of a strong bonding between PAM and PEO due to  $-\text{CONH}_2$  groups in PAM and  $-\text{OH}$  group in PEO, which is also confirmed by our FTIR study.

#### 5.2.6. Differential Scanning Calorimeter Analysis

To get the information regarding the different phase transitions temperature, DSC measurements have been carried out on the prepared samples. The DSC plot of the investigated (PAM/PEO) polymer blend is shown in **Figure 5.6 (a)**. The melting temperature  $T_m$  of the polymer blends depends on the PEO concentration. The melting temperature ( $T_m$ ) for pure PEO is observed around 67.65 °C where as it is shifted to 64.88, 67.20 and 72.09 °C in 70/30, 50/50 and 30/70 wt% of PAM/PEO blend films, respectively. DSC provides a quick method for determining polymer crystallinity. PAM does not showed melting peak in the DSC operation range, so heat of fusion values calculated from the melting peaks were considered for PEO portions.

The crystallinity ( $\chi_c$ ) of PEO in blend films was calculated from DSC data according to the following equation  $\chi_c = \Delta H / f_w \Delta H_0$  [61]. Where,  $\Delta H_0$  is heat of fusion or melting enthalpy for

per gram of 100% crystalline PEO(=213.7 J/g) [62].  $f_w$  is the weight fraction of PEO and  $\Delta H$  is heat of fusion or melting enthalpy of blend sample. The calculated melting enthalpy and the value of degree of crystallinity  $\chi_c$  (%) is shown in **Table 5.6**. In the present investigation, the degree of crystallinity of (PAM/PEO blend) polymers increases with concentration of PEO increases. The increment of crystallinity of polymer blends show that the PEO interacts strongly with the PAM.

**Table 5.6**  $T_m$  (°C),  $\Delta H$  (J/g),  $\chi_c$  (%), of PAM/PEO Blends

PAM/PEO blend (wt%)	$T_m$ (°C)	$\Delta H$ (J/g)	$\chi_c$ (%)
100/0	-	-	-
70/30	64.88	86.58	12.16
50/50	67.20	113.2	26.49
30/70	72.09	89.59	29.35
0/100	67.65	124.2	58.12

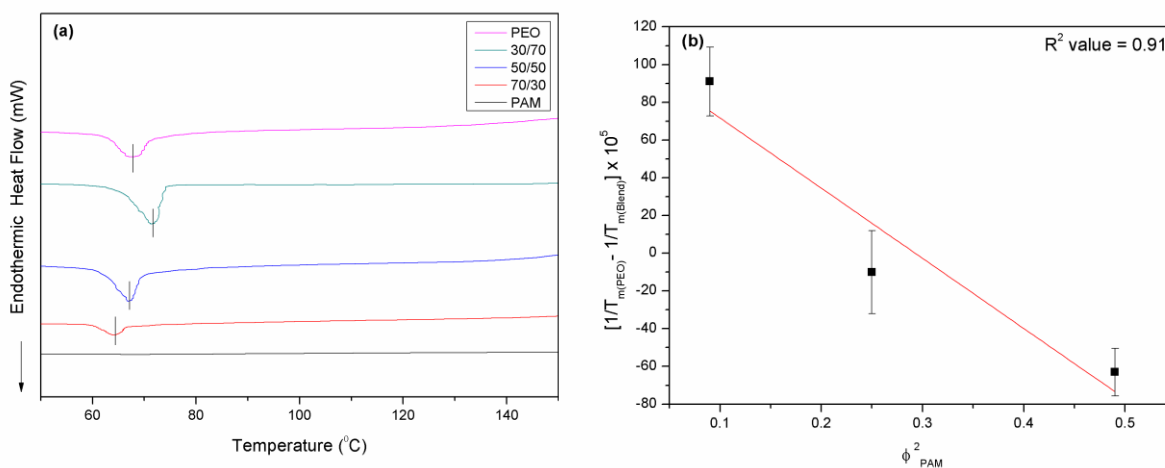


**Figure 5.6** (a) DSC curve of pure PAM, pure PEO and blends (b) Dependence of  $\frac{1}{T_{m(PEO)}} - \frac{1}{T_{m(Blend)}}$  with  $\phi_{PAM}^2$  for PAM/PEO blends

From the Flory-Huggins theory, Polymer-polymer interaction parameter can be calculated with the help of below Nishi-Wang equation [63]:

$$\frac{1}{T_{m(PEO)}} - \frac{1}{T_{m(blend)}} = \left[ \frac{R V_{PEO}}{V_{PAM} \Delta H_{PEO}} \right] \chi_{12} \phi_{PAM}^2$$

Where  $V_{PEO}$  and  $V_{PAM}$  is the molar volume of the repeating unit of the polymer;  $\Delta H_{PEO}$  is the melting enthalpy of fully crystalline PEO;  $\phi$  is the volume fraction;  $\chi_{12}$  is the polymer-polymer interaction parameter, R is the universal gas constant. From the above parameter for the blends and the evaluation of polymer -polymer interaction and hence miscibility of the system were performed. It can be shown that negatives values for the  $\chi_{12}$  are correlated to existence of interactions between the polymers, thus resulting in the miscibility of the system.

**Figure 5.6(b)** shows the curve of  $\frac{1}{T_{m(PEO)}} - \frac{1}{T_{m(blend)}}$  vs  $\phi_{PAM}^2$ . The slope of the line is related to the value of  $\chi_{12}$ . If the negative slope is obtained then value of  $\chi_{12}$  is negative which reveals the system is miscible. For PAM/PEO blend the interaction parameter  $\chi_{12}$  was calculated using below parameter.

$$R = 8.314 \text{ J}\cdot\text{K}^{-1}\cdot\text{mol}^{-1},$$

$$\Delta H_{PEO} = 7.6 \text{ J}\cdot\text{K}^{-1}\cdot\text{mol}^{-1},$$

$$V_{PEO} = 40.3 \times 10^{-6} \text{ m}^3\cdot\text{mol}^{-1},$$

$$V_{PAM} = 24.09 \times 10^{-6} \text{ m}^3\cdot\text{mol}^{-1}$$

The value of  $\chi_{12}$  is equal to  $-203.7$  so the negative value for  $\chi_{12}$  indicated miscibility of polymers.

### 5.2.7. Scanning Electron Microscopy

**Figure 5.7 (a-e)** shows scanning electron micrographs of the fracture surfaces of PAM and PEO and PAM/PEO blend with different composition. SEM micrographs clearly show the changed surface morphologies of the different blends as compared to pure polymers. As shown in **Figure 5.7 (a, e)**, surface of PAM and PEO are very smooth, showing only a limited number of small particles dispersed along the micrograph. As we increase the fraction of PEO in the PAM polymer matrix, surface appears heterogeneous due to enhanced volume fraction of polymer. From the blend's micrographs, (**Figure 5.7 (b-d)**), we concluded that as we added PEO in PAM polymer matrix, polymer chains form irregular shaped clusters. But for 70/30 wt% quite homogeneous surface obtained with good dispersion of PEO. This may be attributed to the formation of hydrogen bonding between two polymers [64]. This also confirmed our FTIR results. From **Figure 5.7 (c, d)** surface appears packed in, separated domains and porous for 50/50 wt % and 30/70 wt %. While from **Figure 5.7 (b)** surfaces are quite homogeneously dense and much reduced domains with good dispersed PEO particle in PAM polymer matrix, which show the maximum strong intermolecular interaction between PAM and PEO for 70/30wt%, which is also correlated with DSC result. Crystallinity is increases as percentage of PEO increases, so we get rougher surface for 50/50 and 30/70 wt% other than 70/30 wt%. From SEM micrograph 70/30 wt% blend is miscible so hydrogen bond taking place[64]. Hence 70/30 wt% had more thermally stable and have higher mechanical properties. These results also correlated with FTIR conclusion.

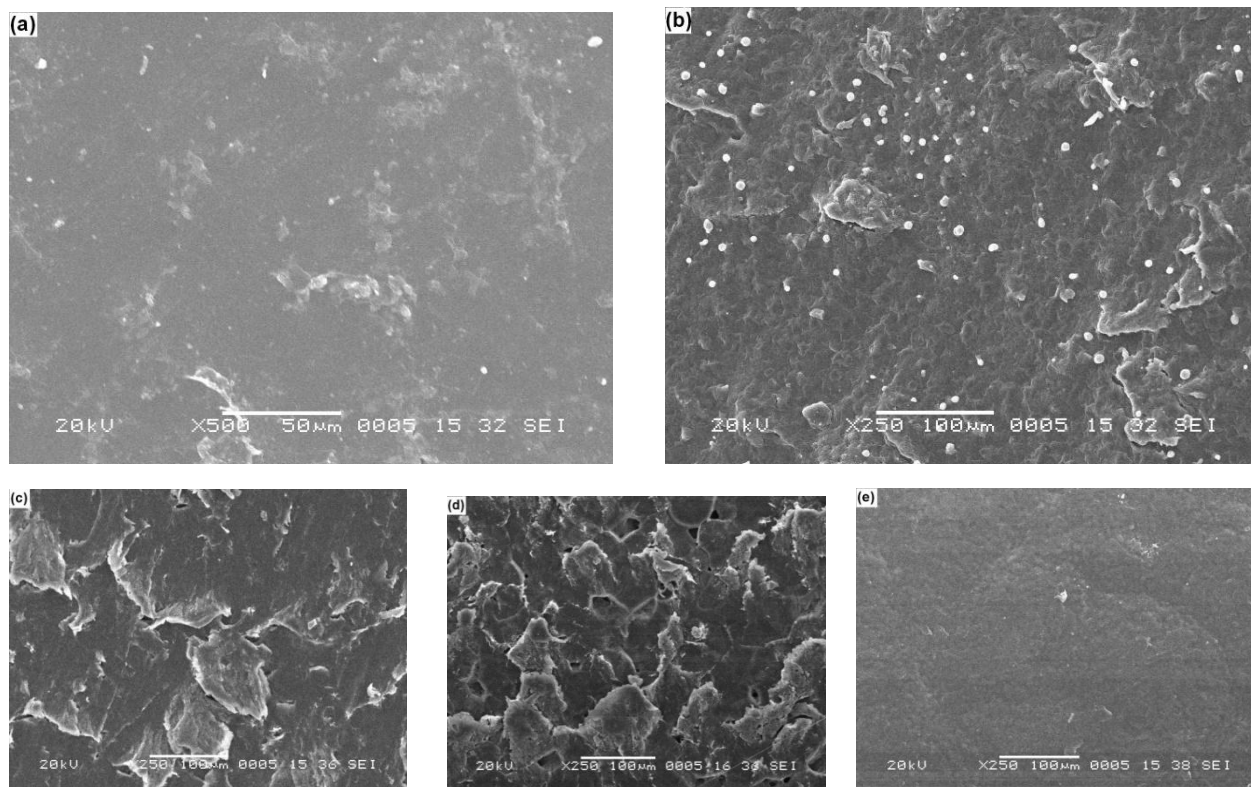


**Figure 5.7** Scanning Electron Micrograph of (a) Pure PAM (b) 70/30 (c) 50/50 (d) 30/70 (e) Pure PEO

### 5.3. Conclusions

FTIR and Raman analysis showed that when PEO blend with PAM, blend components exhibited significant interaction with each other via hydrogen bonding between  $-\text{CONH}_2$  groups in PAM and  $-\text{CH}_2\text{OH}$  group in PEO. This intermolecular interaction is maximum for 70/30 wt% which exhibited the strong bond interaction and due to this it has maximum thermal and mechanical properties. Optical spectra provide proof for interaction between PAM and PEO. The shift of the absorption edge in the blends reflects the variation in the energy gap which arises due to the intermolecular interaction between PAM and PEO. DSC analysis showed the increment of crystallinity as increases PEO wt% and also the negative value for polymer-polymer interaction parameter  $\chi_{12}$  indicated miscibility of polymers. SEM micrograph also showed the good dispersion and homogeneity for 70/30 wt% of PAM/PEO blend. Miscibility of the polymer is

---

also confirmed by SEM micrograph. So from this study we concluded that blend of PAM/PEO with 70/30 wt% is most suitable and compatible with most enhancing properties.

## 5.4. References

1. Sauchez IC. Bulk and Interface-thermodynamics of polymer alloys. *Annual review of material science*, 13; 387-412, 1983. [DOI: 10.1146/annurev.ms.13.080183.002131]
2. Utracki LA. *Polymer blends handbook*. Kluwer Academic Publishers; Vol. 2; ISBN-13: 9781402011146, 2003.
3. Florence Croisier, Christine Jérôme. *European Polymer Journal*; 49(4); 780–792, 2013. [DOI: <http://dx.doi.org/10.1016/j.eurpolymj.2012.12.009>]
4. Caykara T, Demirci S. *Polym Plast Tech & Engg*; 2007; 46(7); 737–741, 2007. [DOI:10.1080/03602550701273971]
5. Yuk SH, Cho SH, Lee HB. *J Controlled Release*; 37; 69–74, 1995. [[http://dx.doi.org/10.1016/0168-3659\(95\)00065-G](http://dx.doi.org/10.1016/0168-3659(95)00065-G)]
6. Araya-Hermosilla R, Broekhuis AA, Picchioni F. *European Polymer Journal*; 50; 127–134, 2014. [<http://dx.doi.org/10.1016/j.eurpolymj.2013.10.014>]
7. Dean K, Yu L, Bateman S, Dong YW. *J Appl Polym Sci*; 103(2), 802–811, 2007. [DOI: 10.1002/app.25149]
8. Mruthyunjaya S, Swamy TM. *J Macro Sci*; 44(3); 321–327. [DOI:10.1080/10601320601077492]
9. Imre B, Pukánszky B. *European Polymer Journal*; 49; 1215–1233, 2013; [<http://dx.doi.org/10.1016/j.eurpolymj.2013.01.019>]
10. Caulfield MJ, Qiao GG, Solomon DH. *Chem Rev*; 102(9); 3067-3084, 2002. [DOI: 10.1021/cr010439p]
11. Lopatin VV, Askadskii AA, Peregudov AS, Vasilev VG. *J Appl Polym Sci*; 96(4); 1043–1058, 2005. [DOI: 10.1002/app.21477]
12. Abdelhak M, Abdelkarim H, Barbara I. *J Chem Chem Eng*; 6; 7-17, 2012. [ISSN: 1934-7375]
13. Wever DA, Picchioni F, Broekhuis AA. *European Polymer Journal*; 49; 3289–3301, 2013. [<http://dx.doi.org/10.1016/j.eurpolymj.2013.06.036>]
14. Gavrilin MV. *Pharm Chem J*; 35(1); 35–39, 2001. [DOI: 10.1023/A:1010402826818]

15. Suzuki H, Miyemoto N, Masad T, Hayakawa E, Ito K. *Chem Pharm Bull (Tokyo)*; 44(2); 364–371, 1996. [DOI: <http://dx.doi.org/10.1248/cpb.44.364>]
16. Abderlrazek EM, Ibrahim HS. *Physica B*; 405; 4339-4343, 2010. [Doi:10.1016/j.physb.2010.07.038]
17. Lee K Y, Yuk SH. *Progress in Polymer Science*; 32(7); 669–697, 2007. [DOI: <http://dx.doi.org/10.1016/j.progpolymsci.2007.04.001>]
18. Parmar AV, Bahadur A, Kuperkar K, Bahadur P. *European Polymer Journal*; 49; 12–21, 2013. [DOI:10.1016/j.eurpolymj.2012.10.009]
19. Salmaso S, Semenzato A, Bersani S, Matricardi P, Rossi F, Caliceti P. *International Journal of Pharmaceutics*; 345; 42–50, 2007. [DOI: <http://dx.doi.org/10.1016/j.ijpharm.2007.05.035>]
20. Pereira AG , Paulino AT, Rubira AF, Muniz EC. *eXPRESS Polymer Letters*; 4(8); 488–499, 2010. [DOI: 10.3144/expresspolymlett.2010.62]
21. Pereira AG, Paulino AT, Nakamura CV, Britta EA, Rubira AF, Muniz EC. *Materials Science and Engineering C*; 31(2); 443–451, 2011. [DOI: <http://dx.doi.org/10.1016/j.msec.2010.11.004>]
22. Sim LH, Gan SN, Chan CH, Kammer HW, Yahya R. *Materials Research Innovations*; 13(3); 278-281, 2009. [DOI: 10.1179%2F143307509X440523]
23. Kiran Kumar K, Ravi M, Pavani Y, Bhavani S, Sharma AK, Narasimha Rao VV. *Physica B*; 406; 1706–1712, 2011. [doi:10.1016/j.physb.2011.02.010.]
24. Reddeppa N, Sharma AK, Narsimha Rao VV, Chen W. *Microelectronic Engineering*; 112; 57-62, 2013. [<http://dx.doi.org/10.1016/j.mee.2013.05.015>]
25. Elashmawi IS, Abdelrazek EM, Hezma AM, Rajeh A. *Physica B*; 434; 57–6, 2014.. [<http://dx.doi.org/10.1016/j.physb.2013.10.038>.]
26. Ferreira V, Douglas JF, Warren J, Karim A. *Phys Rev E*; 65; 042802-[1-4], 2002. [DOI: 10.1103/PhysRevE.65.042802]
27. Ferreira V, Douglas JF, Warren J, Karim A. *Phys Rev E*; 65; 051606-[1-16], 2002. [DOI: 10.1103/PhysRevE.65.051606]

28. Sawatari Ch, Kondo T. *Macromolecules*; 32; 1949-1955, 1999. [DOI: 10.1021/ma980900o]
29. Zheng H, Zheng S, Guo Q. *J Polym Sci A Polym Chem*; 35; 3169–3179, 1997. [DOI: 10.1002/(SICI)1099-0518(19971115)35:15<3169::AID-POLA10>3.0.CO;2-9]
30. Vijayalakshmi SP, Madras G. *J Appl Polym Sci*; 101; 233–240, 2006. [DOI 10.1002/app.23246.]
31. Vijayalakshmi SP, Raichar A, Madras G. *J Appl Poly Scie*; 101; 3067–3072, 2006. [DOI 10.1002/app.24115]
32. Pielichowska K, Głowinkowski S, Lekki J, Binias D, Pielichowski K, Jency J. *European Polymer Journal*; 44(10); 3344–3360, 2008. [DOI: <http://dx.doi.org/10.1016/j.eurpolymj.2008.07.047>]
33. Sowwan M, Faroun M, Musa I, Ibrahim I, Makharza S, Sultan W, Dweik H. *Int J Phy Sci*; 3(6); 144–147, 2008. [ISSN 1992–1950]
34. Colthup NB, Daly LH, Berley SE. *Introduction to Infrared and Raman Spectroscopy* (3<sup>rd</sup> edition); Academic press INC. Elsevier; 1990. [ISBN 0080917402, 9780080917405]
35. Chen N, Zhang J. *Chinese Journal of Polymer Science*; 28(6); 903-911, 2010. [DOI: 10.1007/s10118-010-9167-x]
36. Gaurang Patel, Mundan B Sureshkumar. *Iran Polym J*; 2013. [DOI: 10.1007/S 13726-013-0211-x.]
37. Guo C, Liu H, Wang J, Chen J. *Journal of Colloid and Interface Science*; 209; 368-373, 1999. [DOI: Jcis.1998.5897]
38. Bostan MS, Mutlu EC, Kazak H, Keskin SS, Oner ET, Eroglu MS. *Carbohydrate polymers*; 2013. [DOI: <http://dx.doi.org/10.1016/j.carbpol.2013.09.096>]
39. Dong J, Fredericks PM, George GA. *Polym Degrad Stab*; 58; 159-169, 1997. [DOI: [http://dx.doi.org/10.1016/S0141-3910\(97\)00040-2](http://dx.doi.org/10.1016/S0141-3910(97)00040-2)]
40. Lee JH, Jung HW, Kang IK, Lee HB. *Biomaterials*; 15(9); 705-711, 1994. [[http://dx.doi.org/10.1016/0142-9612\(94\)90169-4](http://dx.doi.org/10.1016/0142-9612(94)90169-4)]

41. Sundaraganesan N, Puviarasan N, Mohan S. *Talanta*; 54; 233-241, 2001. [http://dx.doi.org/10.1016/S0039-9140(00)00585-3]
42. A da costa AM, Amada AM. *Polymer*; 41(4); 5361-5365, 2000. [DOI: http://dx.doi.org/10.1016/S0032-3861(99)00732-6]
43. John RD. *Applications of Absorption Spectroscopy of Organic Compounds*. Prentice-Hall Inc.; 1965. [ISBN: 0130388025]
44. Srivastava AK, Virk HS. *Journal of Polymer Materials (Netherlands)*, 17(3), 325-328, 2000.
45. Rajesh Kumar, Asad Ali S, Mahur AK, Virk HS, Singh F, Khan SA, Avasthi DK, Rajendra Prasad. *Nucl Instr and Meth in Phys Res B*; 266(8); 1788-1792, 2008. [http://dx.doi.org/10.1016/j.nimb.2008.01.010]
46. Gaurang Patel, MB Sureshkumar, Purvi Patel. *AIP Conf Proc*; 1349; 166-167, 2011. [DOI: 10.1063/1.3605788]
47. Tauc J, Grigorovici R, Vanku A. *Phys Stat Sol (b)*; 15(2); 627-637, 1996. [DOI: 10.1002/pssb.19660150224]
48. Shahada L, Kassem ME, Abdelkader HI, Hassan HM. *J Appl Polym Sci*; 65(9); 1653-1657, 1997. [DOI: 10.1002/(SICI)1097-4628(19970829)65:9<1653::AID-APP1>3.0.CO;2-E].
49. Mott NF, Davis EA. *Electronic processes in Non Crystalline materials*. 2<sup>nd</sup> edition; Oxford university press; USA; 1979. [ISBN: 0198512880]
50. S Kilarkaje, Manjunatha V, Raghu S, Ambika Prasad MV, Devendrappa H. *J. Phys. D: Appl. Phys.*, 44, 105403, 2011. [DOI: doi:10.1088/0022-3727/44/10/105403]
51. Nouh SA, *Radiation Measurement*; 38(2); 167-172, 2004. [DOI: http://dx.doi.org/10.1016/j.radmeas.2003.11.004]
52. Singh NL, Sharma A, Avasthi DK. *Nucl Instrum Methods B*; 206; 1120-1123, 2003. [DOI: http://dx.doi.org/10.1016/S0168-583X(03)00935-2]
53. Buttafava A, Consolati G, Di Landro L, Mariani M. *Polymer*; 43(26); 7477-7481, 2002. [DOI: http://dx.doi.org/10.1016/S0032-3861(02)00708-5]

54. Mishra R, Tripathy SP, Sinha D, Dwivedi KK, Ghosh S , Khathing DT, Muller M, Fink D, Chung WH. Nucl Instrum Methods B; 168(1); 59-64, 2000. [DOI: [http://dx.doi.org/10.1016/S0168-583X\(99\)00829-0](http://dx.doi.org/10.1016/S0168-583X(99)00829-0)]
55. Lakshmi GB VS, Ali V, Siddiqui A M, Kulriyac PK, Zulfequar M. Radiat Eff Defects in Solid; 164(3); 162–169, 2009. [DOI: 10.1080/10420150902764186]
56. Patel G, Sureshkumar MB, Singh NL, Bhattacharya SS. Journal of International Academy of Physical Sciences. 14; 91-100, 2010. [ISSN 0974 - 9373]
57. Chi SK, Seung MO.. Electrochim acta; 46; 1323-1331, 2001. [DOI: [http://dx.doi.org/10.1016/S0013-4686\(00\)00727-1](http://dx.doi.org/10.1016/S0013-4686(00)00727-1)]
58. Gaurang Patel, M B Sureshkumar, Purvi Patel. AIP Conf Proc; 1391; 645-648, 2011. [DOI: 10.1063/1.3643636]
59. El-Kader FH, Gafer SA, Basha AF, Bannan SI, Basha MAF. J Appl Polym Sci; 118(1); 413–420, 2010. [DOI: 10.1002/app.30841]
60. Aggour YA. Polm. Degrade. Stab; 51(3); 265-269, 1996. [DOI: [http://dx.doi.org/10.1016/0141-3910\(95\)00205-7](http://dx.doi.org/10.1016/0141-3910(95)00205-7)]
61. Jurkin, T., & Pucic, I. Radiation Physics and Chemistry, 81, 1303–1308, 2012.
62. Shin JH, KimKW, Ahn HJ, Ahn JH, JMater Sci Eng, B 95:148, 2002.
63. A. G. B. Pereira, A. T. Paulino, A. F. Rubira, E. C. Muniz, eXPRESS Polymer Letters Vol.4, No.8, 488–499, 2010.
64. Shefali Mishra, Bajpai R, Katare R, Bajpai AK. J Mater Sci: Mater Med; 17(12); 1305–1313, 2006. [DOI: 10.1007/s10856-006-0605-9]

## Chapter 6

# Characterization of PMMA/TiO<sub>2</sub> composites

---

### *Abstract*

*This chapter gives an account of the characteristics of PMMA/TiO<sub>2</sub> composites in different weight proportion (0.03%, 0.1% and 0.5% of TiO<sub>2</sub>) which is prepared by solution cast technique. These blends are investigated by spectroscopic techniques like FTIR and UV-Vis. Mechanical, Thermal and Morphological properties are also investigated. The results obtained from different characterization techniques show the doping effect on different properties. These properties of composites are correlated with spectroscopic investigation.*

## 6.1. Introduction

Polymeric materials are cheaper and easier to process as well as they are convenient to assemble. The benefits of lightweight polymeric materials over metallic materials are well known. Polymers are of deep interest to society and are replacing metals in diverse fields of life, which can be further modified according to modern applications. As we know, incorporating inorganic particles into polymer matrix is a practicable way to obtain advanced materials of composite [1]. In recent years, organic/inorganic composite materials have attracted considerable attention in both scientific and industrial circles, because they offer attractive potential for diversification and application of traditional polymeric materials [2, 3]. Organic– inorganic hybrid materials are hi-tech because they can present simultaneously both the properties of an inorganic molecule besides the usual properties of polymer. These hybrid materials sometimes lead to unexpected new properties, which are often not exhibited by individual compounds and thus open a new avenue for chemists, physicists and materials scientists [4]. These hybrid materials are new, versatile class of materials, exhibiting a vast application potential, due to their tailorable mechanical, optical and electrical properties [5-7].

When two different kinds of materials are used in combination to improve one or more properties of the component material is called composites. Composites materials are generally consist of a continuous phase which is surrounded by dispersed phase. Changes in size of dispersed phase (macroscopic to nano) reflect changes in physical properties. Homogeneity improves for smaller dispersed phase. Composite materials can be classified by the chemical interactions between the two phases. Kickelbick [8] used the strength of the intermolecular forces to classify the types of hybrid materials formed, contrasting those with chemical bonding between phases, weaker intermolecular forces between phases, or those with little or no

interaction between the phases. Interaction between the inorganic and the organic phase by hydrogen bonding in hybrid materials exists. The structure of the different classes varies widely and includes a dispersion of the inorganic in the continuous phase, an interpenetrating network of inorganic component and polymer, pendant inorganic groups attached to the polymer backbone, and true hybrids, described as structures where covalent bonds exist between inorganic and organic phase [9]. These differences in structure can affect the pyrolysis behavior of the hybrid material. The mechanical properties of particulates-filled polymers are significantly influenced by interfacial interactions, which depend on the interfacial compatibility and interfacial adhesion between the particulates and the matrix [10]. In recent years, studies on optical and electrical characteristics of polymers have fascinated much consideration in their application in optical and electronic devices [11]. The optical properties of the polymers can be correctly customized by the addition of dopant depending on their reactivity with host matrix. Optical parameters (e.g. refractive index, optical band gap, etc.) of poly methyl methacrylate (PMMA) depend on its molecular structure and they can be modified. Titanium dioxide or Titania ( $\text{TiO}_2$ ) is a harmless white material widely used in photo electrochemical solar energy conversion and environmental photo catalysis (treatment of polluted water and air) including self cleaning and anti fogging surfaces [12, 13]. It is also commonly used as a high refractive index material in optical filter applications and sensors [14, 15]. Nano structured  $\text{TiO}_2$  is used in solar cell research and displays [16].  $\text{TiO}_2$  thin films are valued for their good durability, high dielectric constant, high refractive index, excellent transparency in the visible range and biocompatibility. In polymer light emitting diode devices, mixing  $\text{TiO}_2$  nanoparticles into poly [2-methoxy-5-(20-ethyl-hexyloxy) - para-phenylenevinylene] MEH-PPV results in increased current densities, radiances and power efficiencies [17, 18]. Electrical and optical properties of polyvinyl alcohol thin films doped with metal salts have been investigated by Abd et al.[19]. Refractive index is an important optical

parameter for the design of prisms, windows and optical fibers [20]. The absorbance process plays an important role in the optical properties of polymers. From the absorption spectra, it is possible to understand variation of molecular formation of polymer structures.

The study of the optical absorption spectra in solids provides necessary information about the band structure and the energy gap in the crystalline and non-crystalline materials. Analysis of the absorption spectra in the lower energy part gives information about atomic vibration while the higher energy part of the spectrum gives knowledge about the electronic states in the atom [19].

A. Qureshi et al. studied optical and electrical properties of polypropylene/TiO<sub>2</sub> composites [21]. The band gap width ( $E_g$ ) depends on many parameters, e.g. on crystallinity of materials, on their anisotropy, temperature, pressure, on effect of external electric and magnetic forces [22]. A similar change of optical energy band gap in polymers was published under doping PMMA with metal halogenides [23], after ions implantation in polyimide [24], and after implanting electrons or protons in PP, PTFE, PET, PI [25].

Here PMMA/TiO<sub>2</sub> system was chosen as a model to prepare inorganic/ polymer composites. Preparation and characterization of the PMMA/TiO<sub>2</sub> composites is described in this chapter. The structural, optical, mechanical, thermal and morphological properties are studied. The analyses confirmed the good dispersion of TiO<sub>2</sub> particles in PMMA polymer matrix and making successfully composites films with good properties.

## 6.2. Results and Discussion

### 6.2.1. FTIR Analysis

FTIR (Fourier transform infrared) spectroscopic techniques are used to quantitatively assess polymer interactions for many years. Infrared spectroscopy is a tool to find out the possible interaction between the polymer and inorganic dopant. In addition to FTIR's simplicity and

universal use, the frequencies of bands and the band shape are directly related to microscopic physical quantities and hence from the spectra we can correlate the other properties. The interaction can be studied by noting the shift of the peaks, developments of new peaks, changes in shapes like changes in peak intensity, development of shoulders in the existing peaks in the FTIR spectrum [26-28].

**Table 6.1** Assignment of different vibrational modes of PMMA and its various composites.

Vibrational Modes ↓	Wave number (cm <sup>-1</sup> )			
	TiO <sub>2</sub> % in PMMA polymer →	0%	0.03%	0.1%
-CH <sub>2</sub> rocking	733	732	733	732
-CH <sub>2</sub> rocking with skeleton stretching	750	750	750	750
Ti-O-C vibration		809	810	810
C-C stretching	841	841	840	841
C-O stretching	1140	1140	1140	1140
-CH <sub>3</sub> symmetric stretching	1387	1384	1387	1388
-COO <sup>-</sup> stretching	1435	1434	1434	1434
-CH <sub>3</sub> bending	weak	1441	1446	1446
-CH <sub>2</sub> bending coupled with -CH <sub>3</sub> bending	1487	1482	1480	1480
C=O stretching	1719	1722	1721	1721
-CH <sub>2</sub> symmetric stretching		weak	2925	2922
O-CH <sub>3</sub> symmetric stretching	2948	2950	2950	2950
-CH <sub>2</sub> asymmetric stretching	2993	2995	2993	2990

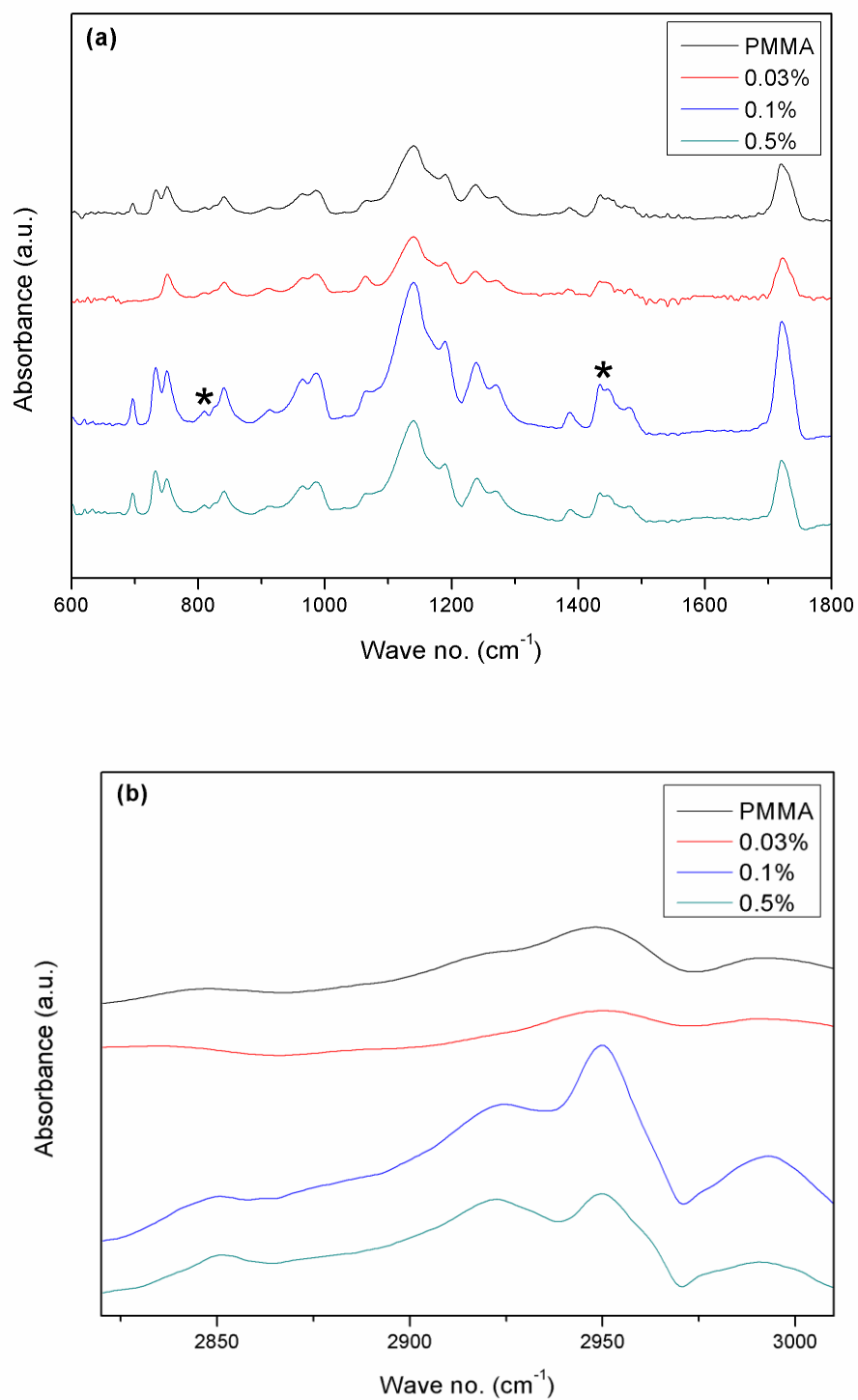


**Figure 6.1** FTIR Spectra of pure PMMA and Their composites (a) in the range 600 – 1800  $\text{cm}^{-1}$  (b) in the range 2800 – 3000  $\text{cm}^{-1}$

In this section, FTIR spectra were employed to identify the chemical interaction of PMMA/TiO<sub>2</sub> composite films of various composition ratios. FTIR spectra are presented in **Figure 6.1**. The vibrational mode assignment with their values for pure PMMA and their composites are shown in **Table 6.1**. The band at 809 cm<sup>-1</sup> (marked as \* in **Figure 6.1**) appears for composites only, which is due to Ti–O–C vibration. The peak around at 1443 cm<sup>-1</sup> and 1487 cm<sup>-1</sup> for PMMA attributed to -CH<sub>3</sub> bending and -CH<sub>2</sub> bending coupled with CH<sub>3</sub>-O bending respectively, whereas the -CH<sub>3</sub> stretching vibration is centered at 1387 cm<sup>-1</sup>[29]. Peak at 1435 cm<sup>-1</sup> (marked as \* in **Figure 6.1**) become prominent in composites sample which is due to carboxylate (-COO<sup>-</sup>) stretching. This clearly indicates the interaction between PMMA and TiO<sub>2</sub> which confirmed the results obtained by Annalisa Convertino et. al.[30]. Characteristic absorptions due to the stretching of ether (C-O) carbon and carbonyl (C=O) of the ester group are observed at 1140 cm<sup>-1</sup> and 1719 cm<sup>-1</sup> for all the composites with changes in absorption intensity. Carbonyl peak's shape and intensity are changed for composites. This is due to the coordination of Ti<sup>+4</sup> with carbonyl oxygen on the ester side of PMMA that is acting as a transient crosslink [29]. Two bands 2925 cm<sup>-1</sup> and 2993 cm<sup>-1</sup> are appearing due to -CH<sub>2</sub> stretching modes of PMMA, Figure 5. The asymmetric stretching mode at 2993 cm<sup>-1</sup> and symmetric stretching mode at 2925 cm<sup>-1</sup> of -CH<sub>2</sub> group exhibits noticeable changes in intensity for the composites with TiO<sub>2</sub> filler. Intensity of the absorption of these peaks increases (as compare to pure PMMA) with TiO<sub>2</sub> addition and maximum for 0.1% of TiO<sub>2</sub>. The peak at 2925 cm<sup>-1</sup> is lacking in pure PMMA and almost disappears for 0.03% as seen in **Figure 6.1 (b)**. The 2950 cm<sup>-1</sup> peak's intensity and shape for the PMMA/TiO<sub>2</sub> composite become maximum and sharp respectively for 0.1wt% TiO<sub>2</sub> content and the 2925 cm<sup>-1</sup> peak's intensity become less intense with addition of TiO<sub>2</sub>. These changes in these peaks are the indication of the PMMA's interactive role with TiO<sub>2</sub> [31].

There are noticeable changes in above peaks in intensity as shown in **Figure 6.1 (a)**. Noticeable peaks sharpening and shape changing is indicating the bonding like interaction between PMMA and TiO<sub>2</sub> particles. These changes are observed maximum for 0.1wt% of TiO<sub>2</sub>, that provide a proof for the strong bond (increasing bond strength) interaction and there for the mechanical and thermal properties are prominent for 0.1wt% of TiO<sub>2</sub>.

### 6.2.2. UV-Vis Analysis

The absorption spectra of most organic composites in the visible and near-UV region are broadband and contain one or several maxima depending upon the electron transition as suggested by KrasovitskiI and Bolotin [32]. The various optical properties obtained for different samples are listed in **Table 6.2**. Absorption coefficient ( $\alpha$ ) vs wavelength ( $\lambda$ ), plot is shown in **Figure 6.2 (a)**. From **Figure 6.2 (a)** we can see a sharp increase of light absorption below 250 nm, which corresponds to  $\pi \rightarrow \pi^*$  transitions of carbonyl groups in macromolecules [33]. And the presence of a weak absorption peak at near 276 nm, is considered to be a positive identification of carbonyl group which is corresponds to  $n \rightarrow \pi^*$  transition of aldehydic carbonyl group of PMMA polymer. But the intensity of this peak decreases with increase in the doping percentage and at higher doping percentage it disappears. Light absorption increases as TiO<sub>2</sub> percentage increases, in comparison to pure PMMA. These spectra show the transitions of the electrons from a fundamental level to the excited levels. In absorption spectra, small peaks can be observed beside the fundamental maxima, showing the vibrational transitions in the structure of materials. Optical absorption studies on pure and doped films were carried out to determine the optical constants such as optical band gap ( $E_g$ ) and the position of the fundamental band edge. According to Shahada et al. [34], it was observed that two distinct linear relations were found, corresponding to different inter band absorption processes. The lower energy range of  $x = 2$  is

typical of an indirect allowed transition. The indirect optical energy gap can be obtained from the plot of  $(\alpha hv)^{1/2}$  versus  $hv$ , while the direct energy gap,  $x = 1/2$ , can be obtained from the plot of  $(\alpha hv)^2$  versus  $hv$ , is believed to be appropriate for the higher energy absorption. The position of the absorption edge was calculated by extrapolating the linear portions of  $\alpha$  vs  $hv$  plots (**Figure 6.2 (b)**) to zero absorption value. For pure film, the absorption edge lies at 4.50 eV and for doped films, the values are found to increase from 4.50 to 4.92 eV. Values of its absorption edge for 0.1 % of  $TiO_2$  lies at 4.85eV above pure PMMA. The plots of  $(\alpha hv)^2$  versus  $hv$  for different dopant percentage in polymer are shown in **Figure 6.2 (c)**. The intercept on the energy axis on extrapolating the linear portion of the curves to zero absorption value may be interpreted as the value of the band gap. The values obtained for direct band gap,  $E_g$  for the different percentage of  $TiO_2$  samples are found to be nonlinear. For pure PMMA, the direct band gap lies at 4.53 eV while for doped films, the values are found to vary with doping percentage as shown in **Table 6.2**. Its values are found to increase from 4.53 eV to 5.01 eV. The indirect band gap were obtained from the plot of  $(\alpha hv)^{1/2}$  vs  $hv$  (photon energy), as shown in **Figure 6.2 (d)**, should be linear. For pure PMMA, the indirect band gap lies at 4.44 eV while for doped films, the values are found to increase from 4.44 eV to 4.84 eV.

**Table 6.2** Various of absorption edge and direct/indirect band gap with different blend percentage

TiO <sub>2</sub> Percentage (%)	Absorption edge ( $\Delta E$ ) (eV)	Direct band gap ( $E_{g(Dir)}$ )	Indirect band gap ( $E_{g(Indir)}$ )
0%	4.50	4.53	4.44
0.03%	4.91	5.01	4.84
0.1%	4.85	4.97	4.78
0.5%	4.92	4.99	4.72

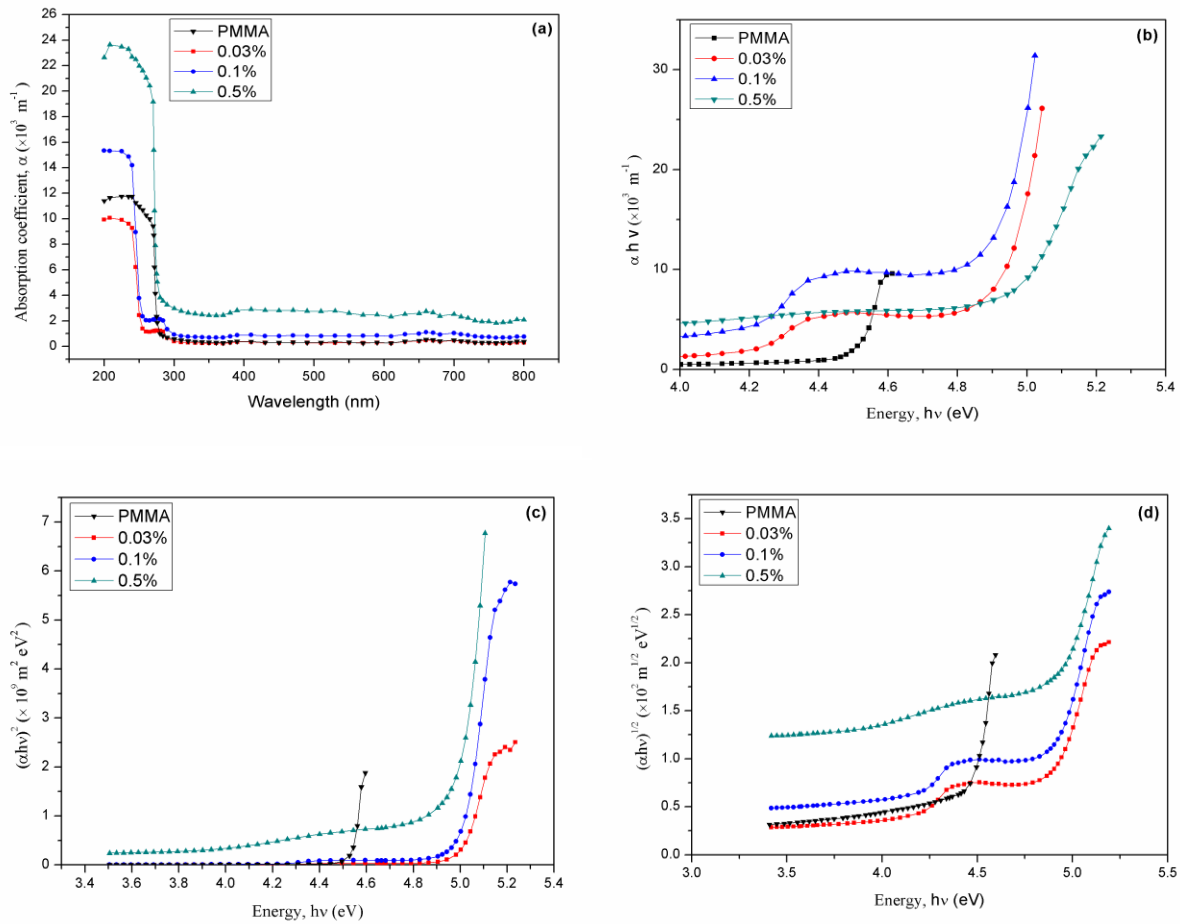


**Figure 6.2** Plot of (a) Absorption coefficient ( $\alpha$ ) vs Wavelength ( $\lambda$ ), (b) Absorption coefficient ( $\alpha$ ) vs Photon Energy ( $h\nu$ ), (c)  $(\alpha h\nu)^2$  vs  $h\nu$ , (d)  $(\alpha h\nu)^{1/2}$  vs  $h\nu$

### 6.2.3. Mechanical Analysis

The mechanical properties of the composite films such as elongation at break, Young's modulus, stress at break and ultimate tensile strength as a function of weight fraction of TiO<sub>2</sub> are displayed in **Figure 6.3 (a, b)**. The mechanical properties of the composite films such as ultimate tensile strength, elongation at break, etc. as a function of weight fraction of TiO<sub>2</sub> are displayed as graph (**Figure 6.3 (a, b)**). Due to introduction of TiO<sub>2</sub> particles into PMMA matrix, the values of mechanical properties such as ultimate tensile strength, Young's modulus and stress at break of composites exhibit increase up to the extent 0.1% of TiO<sub>2</sub>, beyond which it tends to decrease.

The difference in these values, in PMMA/TiO<sub>2</sub> composites are due to the difference in cross linking density provided by PMMA with different weight fraction values of TiO<sub>2</sub>. In general polymers having either a high degree of crystallinity, cross linking or rigid chain exhibit a high strength and low extendibility, thereby giving a high Young's Modulus (YM) values, high stress at peak value and low elongation value [35]. This is also true in this case. Maximum value of the mechanical properties obtained for the 0.1% TiO<sub>2</sub> composites due to the strong bond interaction between PMMA matrix and TiO<sub>2</sub>, while in other cases this interaction may be weak. Beyond 0.1%, mechanical properties value decreases because, increasing amount of TiO<sub>2</sub> particles makes it more difficult for dispersion and easier for particles agglomeration. Since agglomerated particles makes possible to generate defects in the composites, so stress concentration occur within PMMA matrix, resulting in a decreased tensile strength and other properties.

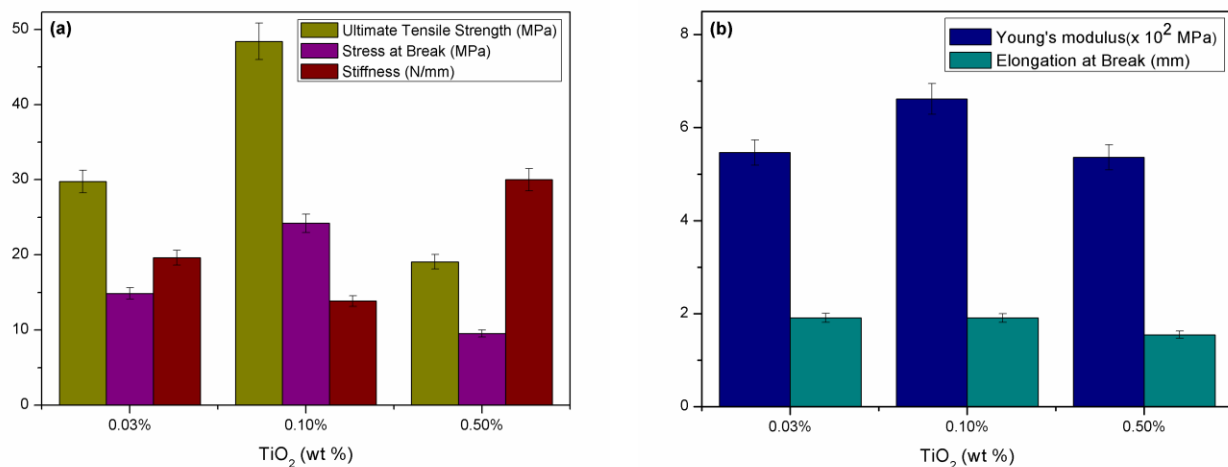


**Figure 6.3** Variation in Ultimate tensile strength, stress at break, Stiffness, Young's Modulus, Elongation at break as a function of TiO<sub>2</sub> content

#### 6.2.4. Differential Scanning Calorimeter Analysis

The glass transition behavior of the synthesized PMMA/TiO<sub>2</sub> samples was investigated by DSC. The obtained DSC thermograms are shown in **Figure 6.4 (a)**. The values of glass transition temperature were taken as the midpoint of the glass transition event. The obtained results are collected in **Table 6.3**. At the glass transition temperature, the bonds between TiO<sub>2</sub> and the polymer chains are broken, and the macromolecule starts to move. In **Figure 6.4**, shifting of T<sub>g</sub> implies that PMMA and TiO<sub>2</sub> have miscibility in amorphous state. T<sub>g</sub> of the pure PMMA sample is observed at 65.5 °C and it is maximum for 0.1% TiO<sub>2</sub> at 67.2°C. This implies that there is a strong bond interaction and good dispersibility between PMMA and TiO<sub>2</sub> in this composition.

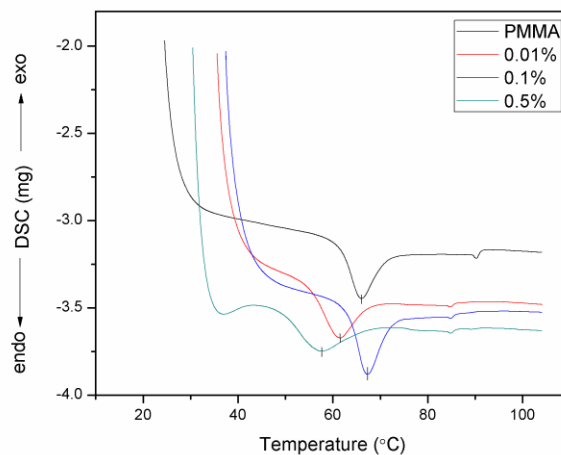


**Figure 6.4** DSC curve for PMMA and its composites.

**Table 6.3** Glass Transition temperature (T<sub>g</sub>) °C of different PMMA/ TiO<sub>2</sub> Composites.

TiO <sub>2</sub> % in PMMA	T <sub>g</sub> (°C)
0 %	65.6
0.03 %	61.2
0.1 %	67.2
0.5 %	57.5

### 6.2.5. Thermal gravimetric Analysis

The thermal stability of the synthesized composite samples was studied by non-isothermal thermogravimetry. The Thermo gravimetric (TG) and derivative thermo gravimetric (DTG) curves obtained for the pure PMMA and PMMA/TiO<sub>2</sub> samples in nitrogen atmosphere are shown in **Figure 6.5 (a, b)**. The difference in the thermal decomposition was observed clearly from derivative TG (DrTG) curve as shown in **Figure 6.5 (b)**. The initial weight loss was observed for all samples due to moisture evaporation. The major weight losses occurred in the range of 260 – 430 °C for all the composite samples. It can be noticed from the TG curves in **Figure 6.5 (a)** that the composite samples start losing mass at lower temperature (at about 260 °C) than the pure PMMA sample. The onset of mass loss of composite samples is shown in **Table 6.4**. Also, the onset of mass loss is maximum for 0.1% of TiO<sub>2</sub> in composite samples. In comparison to composites samples 0.1 % of TiO<sub>2</sub> is also more stable than other composites, which clearly proved by peak temperature (Tp) value of degradation peak as shown **Table 6.4**. It is well studied by Kashiwagi et. al.[36] that PMMA thermally decomposes in steps, first degraded scissions at chain end initiation from unsaturated end groups and then most stable step degraded by random scission with in the mail polymer chain. [37]. The DTG curve of pure PMMA (**Figure 6.5 (b)**) has a peak at 378 °C, which corresponds to depolymerization initiated by random main chain scission and a peak at 308 °C which corresponds to depolymerization initiated by unsaturated end group.[38]. The DTG curves of 0.03% of TiO<sub>2</sub> composites also contain one small hump like peak at 280 °C while for 0.1% and 0.5 % composites shows one peak at 353 °C and 342 °C respectively, originating from the depolymerization initiated by random main chain scission. These results show that amount of PMMA chains with double bond at the end are larger in the pure PMMA than in the composites samples. So TiO<sub>2</sub> particles may

be react with unsaturated end groups of PMMA. As a result of it the number of unsaturated end groups is reduced.

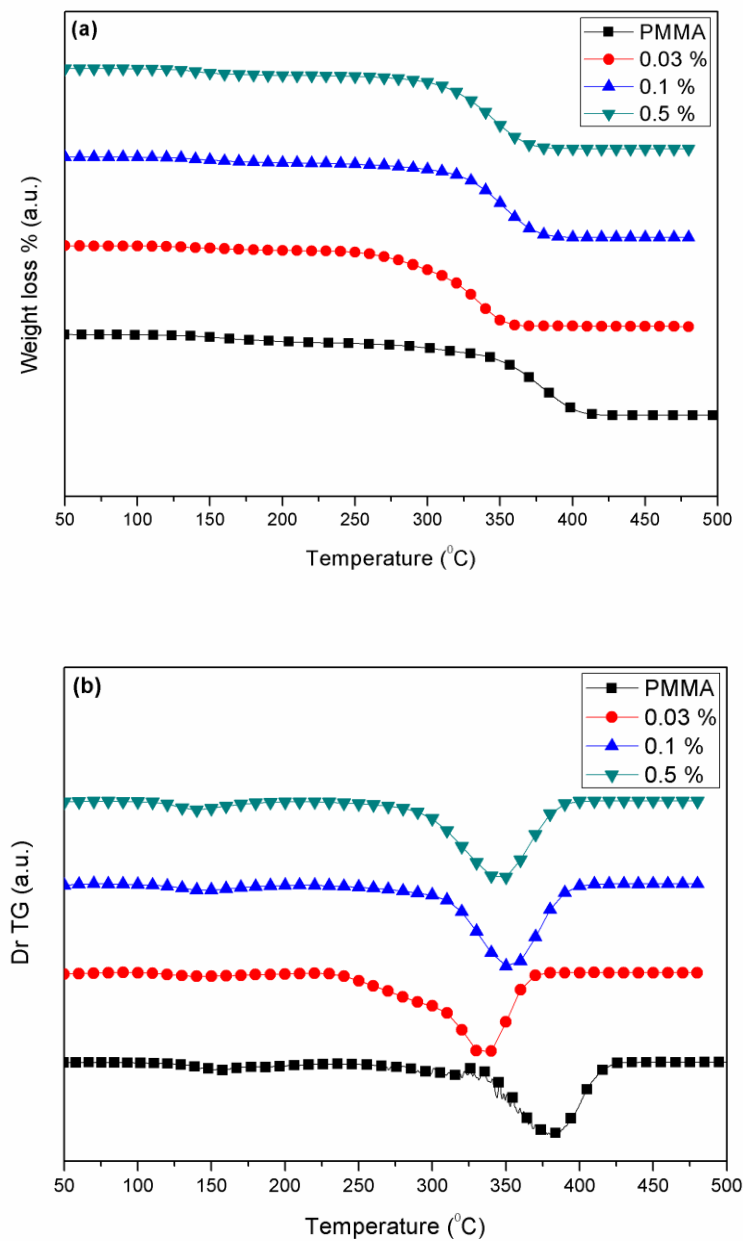


Figure 6.5 (a) TG of pure PMMA and their composites (b) Derivative TG of pure PMMA and their composites

**Table 6.4** TG and DrTG data of Pure PMMA and their composites

TiO <sub>2</sub> wt % in PMMA	Temperature(°C)		
	Starting	Ending	T <sub>p</sub>
0/100	325	426	378
0.03%	260	369	336
0.1%	300	400	353
0.5%	289	389	342

### 6.2.6. Scanning Electron Microscopy

For organic/inorganic hybrid materials, dispersion of inorganic dopant in organic materials is very important to study the properties of composites materials. So, microscopic study on cross section of composite samples was conducted using SEM. **Figure 6.6** shows SEM micrographs of PMMA (**Figure 6.6 (a)**) and its composites with different TiO<sub>2</sub> weight contents (**Figure 6.6 (b-d)**). From SEM image for PMMA (**Figure 6.6 (a)**), smooth and homogeneous surface with some straps obtained. TiO<sub>2</sub> particles disperse differently in the polymer matrix with different percentage filler as shown in **Figure 6.6 (b-d)**. PMMA polymer and the TiO<sub>2</sub> fillers proved homogeneous and compatible without any phase separation occurring when a 0.1% of TiO<sub>2</sub> fillers was added in PMMA polymer matrix. While for 0.5% of TiO<sub>2</sub>, the surface morphology of the composite polymer sample shows many clusters or chunks randomly distributed. That's why 0.1 % of TiO<sub>2</sub> have good mechanical and thermal properties compared to others.

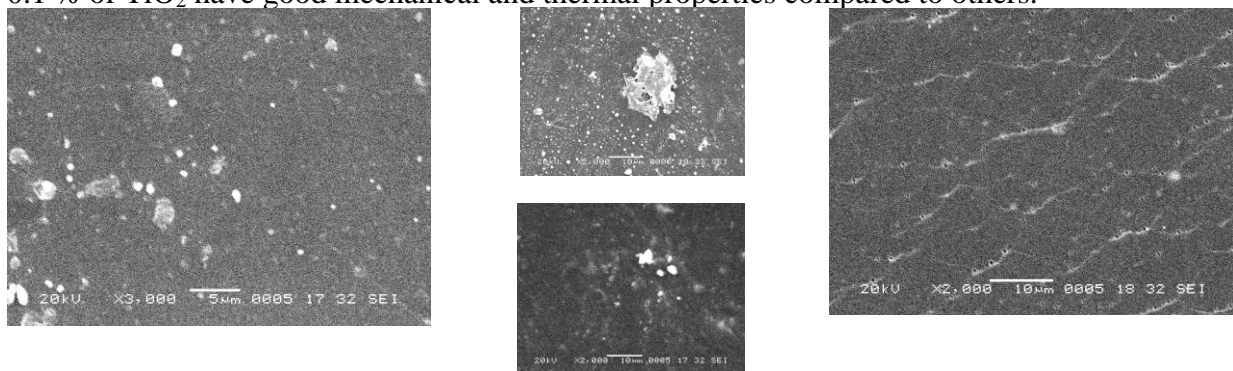


**Figure 6.6** Scanning Electron Micrograph of (a) Pure PMMA (b) 0.03% (c) 0.1% (d) 0.5% of TiO<sub>2</sub>

### 6.3. Conclusions

Mechanical, Thermal and Structural studies have been carried out to characterize PMMA/TiO<sub>2</sub> polymer composites. The FTIR analysis clearly shows that -COOCH<sub>3</sub> group of PMMA bonding with the TiO<sub>2</sub>. When 0.1 wt% TiO<sub>2</sub> is added to PMMA polymer system, strong interaction is formed between PMMA and TiO<sub>2</sub>. Which results in maximum values of mechanical properties such as young's modulus, Ultimate tensile Strength etc. and thermal properties of PMMA/TiO<sub>2</sub> composites. From DSC study, miscibility behavior of PMMA/TiO<sub>2</sub> composites is proved. Glass transition temperature is also maximum for 0.1 wt% of TiO<sub>2</sub>. From UV-Vis spectra, the optical band gap ( $E_g$ ) (Direct and Indirect) is found to be compositional dependence. The optical energy gap is less for 0.5% TiO<sub>2</sub> composition. From SEM micrograph, homogeneous and compatible without any phase separation occurring when a 0.1% of TiO<sub>2</sub> fillers was added in PMMA polymer matrix. From above conclusion for just 0.1% of TiO<sub>2</sub> cause changes in PMMA polymer matrix and enhancing thermal and mechanical properties.

## 6.4. References

1. Sun YP, Hao EC, Zhang X et al, *Langmuir* 13:5168–5174, 1997.
2. Pinnavaia TJ, Beall GW *Polymerclay nanocomposites*. John Wiley and Sons, New York, 2001.
3. Wei Li, Hong Li, Yong-Ming Zhang, *J Mater Sci* 44:2977–2984, 2009.
4. Mingjiao Yang, Yi Dan, *Colloid Polym Sci* 284: 243–250, 2005.
5. Meneghetti P and Qutubuddin S *Langmuir* 20 3424, 2004.
6. Mark J E *Polym. Eng. Sci.* 36 2905, 1996.
7. Qiang X, Chunfang Z, Zun Y J and Yuan C S *J. Appl. Polym. Sci.* 91 2739, 2004.
8. Kickelbick G. *Prog Polym Sci* ;28(1):83–114, 2003.
9. Rohan L. Holmes, Jonathan A. Campbell, Robert P. Burford, Inna Karatchevtseva, *Polymer Degradation and Stability*, 94. 1882–1889, 2009.
10. Demjén, Z., Pukánszky, B. & Nagy, J. *Compos. Part A*, 29, 323–329, 1998.
11. Acosta JL, Morales E *Solid State Ion* 85:85. 1996. [2] Kim JY, Kim SH *Solid State Ion* 124(1–2):91, 1999.
12. C.A. Linkous, *Environ. Sci. Technol.* 34, 44754, 2000.
13. A. Fujishima, T.N. Rao, D.A. Tryk, *J. Photochem. Photobiol. C1*, 1, 2000.
14. P. Loebel, M. Huppertz, D. Mergel, *Thin Solid Films* 251, 72, 1994.
15. I. Hayakawa, Y. Iwamoto, K. Kikuta, *Sens. Actuators B* 62 , 55, 2000.
16. A. Hagfeld, B. Didriksson, *Sol. Energy Mater. Sci. Cells* 31,481, 1994.
17. S.A. Carter, J.C. Scott, P.J. Brock, *Appl. Phys. Lett.* 31, 1145, 1997.
18. J. Zhang, X. Ju, B. Wang, Q. Li, T. Liu, T. Hu, *Synth. Metals* 118, 181, 2001.
19. Abd E l, Kader F H, Osman W H, Ragab H S, Sheap A M, Rizk M S & Basha M A F, *J polym Matter*, 21, 49, 2004.

20. Ma H L, Zhang X H & Lucas J, *J Non-cryst solids*, 101, 128, 1993.
21. A. Qureshi, Dolly Singh, N.L. Singh, S. Ataoglu, Arif N. Gulluoglu, Ambuj Tripathi, D.K. Avasthi *Nuclear Instruments and Methods in Physics Research B* 267 3456–34, 2009.
22. J.M. Ziman, in *Principles of the Theory of Solids* (Cambridge University Press, Cambridge, 1979).
23. H.M. Zidan, M. Abu-Elnader, *Physica B*. 355, 308, 2005.
24. V. Švorčík, I. Miček, V. Rybka, V. Hnatowicz, *J. Mater. Res.* 12, 1661, 1997.
25. R. Mishra, S.P. Tripathy, D. Sinha, K.K. Dwivedi, S. Ghosh, D.T. Khathing, M. Muller, D. Fink, W.H. Chung, *Nucl. Instrum. Meth. B*. 168, 59, 2000.
26. Vijay V. Soman and Deeplai S. Kelkar, *Macromol. Symp.*, 277, 152-161, 2009.
27. S. York, R. Frech, A. Snow, D. Glatzhofer, *Electrochim Acta*, 46, 1533, 2001.
28. A. P. Rhode, R. Frech, *Solid State Ionics*, 121, 91, 1999.
29. Jiao Wang, Xiuyuan Ni, *Journal of Applied Polymer Science*, Vol. 108, 3552–3558, 2008.
30. Annalisa Convertino, A.; Gabriella Leo, A., Marinella Striccoli, B.; Gaetano Di Marco, C.; Lucia Currib, M. *Polymer*, 49, 5526-5532, 2008.
31. Ahmad S, Saxena TK, Ahmad S et al , *J Power Sources* 159:205–209, 2006.
32. B. M. Krasovitskiĭ and B. M. Bolotin, *Organic Luminescent Materials*, 2nd ed. (Khimiya, Moscow, 1984; VCH, Weinheim, 1988).
33. M. Hammama, M.K. El-Mansy, S.M. El-Bashir, M.G. El-Shaarawy, *Desalination* 209, 244, 2007.
34. L. Shahada, M. E. Kassem, H. I. Abdelkader, and H. M. Hassan, *J. Appl. Polym. Sci.* 65, 1653, 1997.

35. Kim Chi S and Oh Seung M, *Electrochim Acta.*, 46,1323-31, 2001.
36. T. Kashiwagi, A. Inaba, J.E. Brown, K. Hatada, T. Kitayama, and E. Masuda, *Macromolecules*, 19, 2160-2168, 1986.
37. L. Katsikas, J.S. Velickovic, H. Weller, and I.G. Popovic, *J. Therm. Anal.*, 49, 317, 1997.
38. E. Dz' unuzovic' , M. Marinovic' -Cincovic', J. Vukovic', K. Jeremic', J.M. Nedeljkovic' *POLYMER COMPOSITES*—737-742, 2009.

---

## Chapter 7

# Conclusion and Future Work

---

### *Abstract*

*This chapter gives the details of correlations of the spectroscopic investigation results with those available from other studies and also summarizes the results obtained by various above mentioned experiments along with the future plan of work.*

## 7.1. Conclusion

### 7.1.1. PVC/PMMA Blends

By the careful study of the FTIR and Raman spectra, hydrogen bond interaction between CH-Cl group of PVC and C=O group of PMMA occurs. It is clearly seen that there is a trend in these peaks to shift to the higher wave number side. For 80/20 wt% has maximum peak shifting on higher wave number side. This increase in wave numbers is due to the increase in the vibrational frequency. This increase in frequency is due to the increase in the strength of the bond and hence increases the mechanical and thermal properties of the polymer blend. Therefore we can conclude that by noting shift of the peaks in the FTIR and Raman spectrum we can draw conclusion about the mechanical and thermal properties of the polymer blend. Thus we are correlated mechanical and thermal properties with spectroscopic investigation by FTIR-ATR spectral studies.

UV-VIS spectra have been studied by the Tauc model. The optical band gap ( $E_g$ ) (Direct and Indirect) is found to be compositional dependent. Sharp increase of light absorption occurs in all the samples below 220 nm which corresponds to  $\pi \rightarrow \pi^*$  transitions of carbonyl group. It is clear that the indirect optical energy band gap increases with increasing PMMA content. The existence and variation of optical energy gap may be explained by invoking the occurrence of local crosslinking within the amorphous phase of PMMA and PVC.

When PMMA is blended with PVC these interaction are weakened by the presence of PMMA up to 10% of PVC. Beyond 10% of PMMA, we observed reversal behavior of PMMA affecting on PVC. So the mechanical properties increase beyond 10% of PMMA and exhibit higher values at

20% of PMMA. Because at 20% of PMMA, the interaction between PVC and PMMA molecules is higher and the dipole-dipole attraction is also reaches at maximum value.

Peak temperature ( $T_p$ ) was maximum for 80/20 wt%, so this blend was more stable. This higher thermal stability was observed for 80/20 wt% blend sample by TGA and DrTG which was due to the intermolecular cross-linking reaction giving highly compatible impact blend system.

In phase mixing homogeneity occurs at the lower level of PMMA (for 20% of PMMA), however, it is absent in higher concentration of PMMA in PVC polymer matrix. This may probably be recognized by the increased mechanical and thermal properties as it shows the regularity in stiff chain structure of PVC.

### 7.1.2. PAM/PVA Blends

The results reported here in this study showed that compatible PAM/PVA blends were prepared successfully using solution cast technique. FTIR and Raman analysis cleared the conclusion about the specific hydrogen bonding interaction between  $-\text{CONH}_2$  groups in PAM and  $-\text{OH}$  group in PVA, these results in the higher thermal stability and improved mechanical properties. But the maximum shift on higher wave number side of IR and Raman peaks observed for 50/50 wt%, which implies that bond strength is increased. Therefore thermal stability and mechanical properties are also increased maximum for 50/50 wt%. It is noticeable that the blend with 50/50 wt% showed the most increased thermal stability and improved mechanical properties among the other blends.

From UV-Vis studies, intermolecular interaction was confirmed by noticeable changes in absorption spectra. The position of absorption edge was slightly shifted towards higher side.

Direct and indirect band gap also vary between 5.35 eV to 5.47 eV and 4.57 eV to 4.87 eV respectively.

Blend of PVA with PAM effectively improved the mechanical properties. When PVA is blend with PAM, interaction at molecular level occurs, which reveals the enhancement of mechanical properties. Enhancement in mechanical properties is due to a strong hydrogen bonding between –CONH<sub>2</sub> groups in PAM and –OH group in PVA. This interaction becomes maximum for 50/50 wt% therefore we obtain maximum value of mechanical properties for this blend.

From TGA, we conclude that the thermal stability regions of the blend samples were higher than the PAM and stability enhanced by increasing PVA content in PAM polymer matrix and it become more stable for 50/50 wt%.

From SEM micrograph, interaction between PAM and PVA is much greater than others (smaller domains of dispersed PVA) and surface of 50/50 blend ratio is rougher than the other blends. Morphological changes in the blend samples were also explained and results also correlated with the other studies.

### 7.1.3. PAM/PEO Blends

Blends of PAM and PEO were obtained as semi-transparent, flexible and free standing films with good thermal, optical and mechanical properties. FTIR and Raman analysis showed hydrogen bonding between –CONH<sub>2</sub> groups in PAM and –CH<sub>2</sub>OH group in PEO. This intermolecular interaction is maximum for 70/30 wt% which exhibited the strong bond interaction.

Optical spectra provide proof for interaction between PAM and PEO. The shift of the absorption edge in the blends reflects the variation in the energy gap which arises due to the intermolecular

interaction between PAM and PEO. This structural variation increases with increase in the concentration of PEO, which is reflected in the form of decrease in the energy gap of the blends. Direct gap decreases from 5.07 eV to 4.83 eV and indirect band also decreases from 4.59 eV to 4.09 eV.

Enhancement in mechanical properties is due to the strong hydrogen bonding between  $-\text{CONH}_2$  groups in PAM and  $-\text{OH}$  group in PEO. This interaction becomes maximum for 70/30 wt% which reveals in the form of higher mechanical properties like tensile strength and young's modulus.

From TGA and DrTGA, 70/30 wt% had maximum temperature value for different weight losses. So we can conclude that the 70/30 wt% have greater thermal stability as compared to pure component.

From SEM micrograph of 70/30 wt%, surfaces are quite homogenously dense and reduced domains with good dispersed PEO particle in PAM polymer matrix, which show the maximum strong intermolecular interaction between PAM and PEO for 70/30wt%.

So from this study we concluded that blend of PAM/PEO with 70/30 wt% is most suitable and compatible blend ratio with most enhancing properties.

#### 7.1.4. PMMA/TiO<sub>2</sub> Composites

From FTIR spectral studies, we concluded that due to the interaction between PMMA and TiO<sub>2</sub>, the mechanical and Thermal properties were enhanced greatly. The FTIR analysis clearly shows that  $-\text{COOCH}_3$  group of PMMA bonding with the TiO<sub>2</sub> and it is maximum for 0.1 wt% of TiO<sub>2</sub>. This indicates strong interaction occurred between PMMA and TiO<sub>2</sub>, which results maximum values of mechanical and thermal properties.

UV-VIS spectra have been studied by the Tauc model. The optical band gap ( $E_{\text{gopt}}$ ) (Direct and Indirect) is found to have compositional dependence. Sharp increase of light absorption occurs in PMMA below 220 nm which corresponds to  $\pi \rightarrow \pi^*$  transitions of  $-\text{COOCH}_3$  structures. In the absorption spectra, weak absorption peak near to 276 nm corresponds to  $n \rightarrow \pi^*$  transition of aldehydic carbonyl group.

From DSC study miscibility behavior of PMMA/TiO<sub>2</sub> composites is proven. Glass transition temperature is also maximum for 0.1 wt% of TiO<sub>2</sub> which is directly correlate with the FTIR spectra.

From TGA analysis, there is no much difference observed between pure PMMA and 0.1% of TiO<sub>2</sub> doped polymer. But other than 0.1% of TiO<sub>2</sub> degraded TGA data were obtained.

We can conclude that by noting shift of the peaks in the FTIR and Raman spectrum we can draw conclusion about the mechanical and thermal properties of the polymer blend. Thus from the study of the spectra of the polymer blends we can draw some conclusion regarding the mechanical and thermal properties without performing the actual mechanical or thermal studies. The enhancement of these properties is related to the blue shift of the prominent peaks in FTIR and Raman spectrum and the red shift indicates decline in the properties. Thus we are correlated mechanical and thermal properties of polymer blends with spectroscopic investigation by FTIR and Raman spectral studies.

From UV-VIS absorption spectra, weak absorption peaks corresponds to  $\pi \rightarrow \pi^*$ ,  $n \rightarrow \pi^*$  transition of different carbonyl group are considered as interaction peak marker. So we can predict the carbonyl group interaction by noticing this peak. And also correlate it with FTIR and

Raman spectroscopy. By noting down blue shift or red shift of carbonyl peak we will be able to conclude about bond interaction in two or more polymers.

## 7.2. Future Work

In conclusion, the present work has clearly shown that a careful combination of results from different experimental methods and theoretical calculations can help to explain interfacial phenomena and to give valuable information concerning the inter-phase properties like intermolecular interaction of polymer blends.

Bio-based polymers are attracting increased attention due to environmental concerns. Bio-based polymers not only replace existing polymers in a number of applications but also provide new combinations of properties for new applications. Polymer blending offers time and cost effective method to develop materials with desirable properties like polymer membrane. Therefore preparation of polymer membrane and effect of blending of polymer (polyacrylamide) with other bio-polymer (chitosan, Sodium Alginate, guar gum etc.) in different concentration will be studied. Main objective of study is to improve the Sorption, diffusion, and pervaporation separation ability of the membrane. The membrane has the capability to separate out water from water mixture. Membranes have improved flexibility, reduced cost, improved process ability, and enhanced selectivity and/or permeability compared to a single polymer.

Objectives to identify the blending behavior of polymer membrane with bio-polymer are as follows:

- To characterize the developed membrane in order to find its Structural, chemical, mechanical and thermal properties using spectroscopic techniques.

- To evaluate the performance of the developed membrane in terms of selectivity and permeability for the separation of water and chemical mixture.
- In the future work we also add the inorganic fillers in blend, which further enhances the different properties of the polymeric blend membrane.

Generalized two-dimensional (2D) correlation spectroscopy, proposed by Noda in 1986, has lately attracted considerable attention for its wide application compared with conventional one-dimensional spectra. Vibrational spectroscopic studies on polymer blends usually require hydrogen bonds as miscibility enhancers in blends, and IR and Raman spectroscopy to investigate hydrogen bonds. Generalized 2D IR correlation spectroscopy may identify various intra- and intermolecular interactions between polymer and its surrounding, either organic or inorganic, through specific correlation of bands.

Generalized 2D FTIR and Raman correlation spectroscopy will be applied to the study:

- The conformational changes and specific interactions in blends of any polymers.
- Simplification of complex spectra consisting of many overlapped peaks, and enhancement of spectral resolution by spreading peaks over the second dimension
- Establishment of explicit assignments through correlation of bands
- Measure the specific sequential order of spectral intensity of the polymer peaks which changes with different concentration of blend sand composites.
- Direct correlation between FTIR and Raman bands
- It may utilize with a number of different spectroscopy, e.g., FTIR, Raman, NIR, fluorescence, UV, and X-ray, and combining this spectroscopic measurement with

---

various physical perturbations, e.g., mechanical, thermal, chemical, optical, and electrical stimuli, to investigate a very wide area of applications.

Bio based polymer membrane will be characterized in order to find its structural, chemical, mechanical and thermal properties which may correlate with 2D FTIR and Raman spectroscopic results by measuring the various peak shifting.

# Publications

---

1. Spectroscopic correlation of Mechanical properties of PVC/PMMA polymer blends  
**Gaurang Patel**, M. B. Sureshkumar, N. L. Singh, S. S. Bhattacharya  
**Journal of International Academy of Physical Sciences** Vol. 14 No.1 (2010) 91-100.  
[ISSN 0974 - 9373]
2. Optical Characterization of PVC, PMMA and PVC/PMMA polymer blends  
**Gaurang Patel**, M. B. Sureshkumar, Purvi Patel  
Proceedings of International Conference on Recent Trends in Material Science and Technology, 2010, 3.61-3.64.
3. Improvement in Mechanical Properties of PMMA Polymer due to the Doping of TiO<sub>2</sub>  
**Gaurang Patel**, M. B. Sureshkumar, N. L. Singh  
Proceedings of DAE-BRNS 3rd International Symposium on Materials Chemistry 2010  
ISBN No.: 81-88513-40-7, 527.
4. An Optical Characterization of PVA/PAM Polymer Blend  
**Gaurang Patel**, M. B. Sureshkumar  
**AIP Conf. Proc.** 1349, 166-167 (2011). [doi: 10.1063/1.3605788]
5. Structural, Optical and Mechanical properties of PVC/PMMA Polymer Blend by Spectroscopic Techniques  
**Gaurang Patel**, M. B. Sureshkumar  
**AIP Conf. Proc.** 1391 (2011), 645-648. [doi: 10.1063/1.3643636]
6. Effect of TiO<sub>2</sub> on Optical Properties of PMMA: An Optical Characterization  
**Gaurang Patel**, M. B. Sureshkumar, Purvi Patel  
**Advanced Materials Research**, Vols. 383-390 (2012), 3249-3256.  
[doi:10.4028/www.scientific.net/AMR.383-390.3249]

7. Investigation of Structural, Thermal and Mechanical properties of PMMA/TiO<sub>2</sub> composites: A Comparative study  
**Gaurang Patel, M. B. Sureshkumar**  
**National Journal of Applied Sciences and Engineering**, Vol. 1/Issue 2/July-Sept. 2012, 50-59. [ISSN 2278-0734]
  
8. Study of Blends of Poly acrylamide(PAM) and Poly Ethylene Oxide(PEO) by FTIR Spectroscopy  
**Gaurang Patel, M. B. Sureshkumar, Purvi Patel**  
Proceedings of 4th International Conference on Perspective in Vibrational spectroscopy (ICOPVS-2013), August 2013, 291-292. ISBN No: 978-93-82880-54-7.
  
9. Preparation of PAM/PVA blending films by solution-cast technique and its characterization: a spectroscopic study  
**Gaurang Patel, M. B. Sureshkumar**  
**Iranian Polymer Journal**, 2013, DOI 10.1007/s13726-013-0211-x
  
10. Preparation Of Pam/Peo Blends Films And Its Characterizations: A Spectroscopic Investigation  
**Gaurang Patel, M. B. Sureshkumar**  
Under review **Polymer Express Journal**

### *Presented Paper*

1. Spectroscopic correlation of Mechanical properties of PVC/PMMA polymer blends  
**Gaurang Patel, M. B. Sureshkumar, N. L. Singh, S. S. Bhattacharya**  
11<sup>th</sup> International Conference of the International Academy of Physical Sciences (CONIAPS XI)  
University of Allahabad, Allahabad, India, Feb 2010
  
2. Effect of TiO<sub>2</sub> on Optical Properties of PMMA: An Optical Characterization

**Gaurang Patel, M. B. Sureshkumar, Purvi Patel**

International conference on Manufacturing of Science and Technology (ICMST-2010)

Kuala Lumpur, Malaysia, Nov 2010

3. Optical Characterization of PVC, PMMA and PVC/PMMA polymer blends

**Gaurang Patel, M. B. Sureshkumar, Purvi Patel**

International conference on Recent Trends in Material Science and Technology (ICMST-2010), Indian Institute of Space Science and Technology, Thiruvananthapuram, India, Oct 2010.

4. An Optical Characterization of PVA/PAM Polymer Blend

**Gaurang Patel, M. B. Sureshkumar**

55<sup>th</sup> DAE Solid State Physics Symposium-2010 (SSPS-10)

By BRNS and DAE of Govt. of INDIA, Manipal University, Manipal, Dec 2010

5. Improvement in Mechanical Properties of PMMA Polymer due to the Doping of TiO<sub>2</sub>

**Gaurang Patel, M. B. Sureshkumar, N. L. Singh**

International Symposium of Material Chemistry (ISMC-2010)

Bhabha Atomic Research Centre (BARC), Mumbai, India, Dec 2010

6. Interaction between Polyacrylamide (PAM) and Polyvinyl alcohol (PVA) in Blends system: An FTIR Study

**Gaurang Patel, M. B. Sureshkumar, Purvi Patel**

Presented in ICMAT-2011 Symposium on Membrane Materials And Technologies for Emerging Applications at Singapore in June 2011.

7. Investigation of Structural, Thermal and Mechanical Properties of PMMA/TiO<sub>2</sub>

Composites: A Comparative Study

**Gaurang Patel, M. B. Sureshkumar, Purvi Patel**

Presented in ICMAT-2011 Symposium on Solution Processing Technology for Inorganic Films, Nanostructures and Functional Materials at Singapore in June 2011.

8. Estimation of Optical Band Gap Energy and carbonaceous Cluster in Polymer Blend of Poly Acrylamide (PAM) and Poly Ethylene Oxide (PEO)

**Gaurang Patel**, M. B. Sureshkumar

3<sup>rd</sup> International Multi-component Polymer Conference (IMPC-2012)

M G University, Kottayam, Kerala, India, March 2012

9. A Study of Photoluminescence Spectra of PMMA/TiO<sub>2</sub> Polymer Composites

**Gaurang Patel**, M. B. Sureshkumar

Seminar on Preparation and Characterization of Crystalline and Non-Crystalline Solids

Organized at Department of Physics, The M. S. University of Baroda, Vadodara,

Nov. 2012.

10. Study of Blends of Poly acrylamide(PAM) and Poly Ethylene Oxide(PEO) by FTIR Spectroscopy

**Gaurang Patel**, M. B. Sureshkumar, Purvi Patel

Presented at 4<sup>th</sup> International Conference on Perspective in Vibrational spectroscopy

(ICOPVS- 2013), Bishop Moore College, Mavelikara, Kerala, India, August 2013